STUDIES ON REMOVAL OF HEAVY METALS FROM AQUEOUS SOLUTION USING MELANIN COATED MATRIX

Thesis

Submitted in partial fulfilment of the requirements for the degree of

DOCTOR OF PHILOSOPHY

by

VISHNU M

(Register No: 158021CH15F14)

DEPARTMENT OF CHEMICAL ENGINEERING

NATIONAL INSTITUTE OF TECHNOLOGY KARNATAKA

SURATHKAL, MANGALORE - 575 025

August 2019

STUDIES ON REMOVAL OF HEAVY METALS FROM AQUEOUS SOLUTION USING MELANIN COATED MATRIX

Thesis

Submitted in partial fulfilment of the requirements for the degree of

DOCTOR OF PHILOSOPHY

by

VISHNU M

(Register No: 158021CH15F14)

Under the Guidance of

Dr KEYUR RAVAL

Dr RAJ MOHAN B

DEPARTMENT OF CHEMICAL ENGINEERING

NATIONAL INSTITUTE OF TECHNOLOGY KARNATAKA

SURATHKAL, MANGALORE - 575 025

August 2019

D E C L A R A T I O N

I hereby *declare* that the Research Thesis entitled "**Studies on Removal of Heavy Metals from Aqueous Solution Using Melanin Coated Matrix**" which is being submitted to the **National Institute of Technology Karnataka, Surathkal** in partial fulfilment of the requirements for the award of the Degree of **Doctor of Philosophy** in Chemical Engineering is a *bonafide report* of the research work carried out by me. The material contained in this Research Thesis has not been submitted to any University or Institution for the award of any degree.

Place: Surathkal

Date: 30 August 2019

Vishnu M

Reg No.: 158021CH15F14

Department of Chemical Engineering

National Institute of Technology

Karnataka, Surathkal- 575 025

C E R T I F I C A T E

This is to *certify* that the Research Thesis entitled "**Studies on Removal of Heavy Metals from Aqueous Solution Using Melanin Coated Matrix**" submitted by **Mr. Vishnu M** (Register Number: 158021CH15F14) as the record of the research work carried out by him, is *accepted as the Research Thesis submission* in partial fulfillment of the requirements for the award of degree of **Doctor of Philosophy**.

Research Guides:

Dr Keyur Raval
Assistant Professor

Dr Raj Mohan B
Professor

Dr Prasanna B D
HOD and Chairman, DRPC

ACKNOWLEDGEMENTS

It brings a sense of pride and joy to be the part of one of the most prestigious and beautiful campuses in India, NITK! The journey of both M. Tech and PhD were the best days of my life. A lot of people and factors have been synergistic with me to achieve this goal. I can remember all those only with courtesy and gratitude.

As the Principal Investigator and later as Research Supervisor, the kind of support, help and confidence extended by Dr Keyur Raval is priceless. He has taught me many skills for life and has always advised me to be happy. I would like to acknowledge the physical, mental and financial support extended by him during the course of our work.

I am deeply indebted to Prof Raj Mohan B, my other Research Supervisor for being the *Guru* and the guidance that he has given from his experience of life, which made the best impacts in our work. He has inspired us to aim high, work to achieve big and have always reminded that success comes to the faithful and down to earth. The confidence and inspiration bestowed from him will be of use for life.

I would like to thank Prof B C Meikap of IIT Kharagpur who was my external examiner and Prof Kannan Pakshirajan of IIT Guwahati for the thesis reviews which helped to improve the quality of the content.

I would like to thank my Doctoral Thesis Assessment Committee (DTAC) and Research Progress Assessment Committee (RPAC) members Dr Jagadeesh Babu P. E., Associate Professor, Chemical Engineering Department Dr Vishwanath K P Assistant Professor, Department of MACS and Dr Darshak R Trivedi, Associate Professor, Chemistry Department for their encouragement, insightful, valuable and constructive comments which helped in fruitful progress of my work.

I express my sincere thanks and gratitude towards the Head of the Department of Chemical Engineering Dr Hari Mahalingham and DTAC chairman Dr Prasanna B D. I would also like to express my whole-hearted gratitude towards Prof Karnam Umamaheshwara Rao, Director of NITK for aid given throughout my work. The Department of Science of Technology (DST), Govt of India, is deeply acknowledged for the financial grant given for this project

I am deeply grateful to Prof Vidya Shetty K for the ICP-OES facility, Dr Jagadeesh Babu P. E. for the particle size analysis, Dr Hari Prasad Dasari for the TGA facility, Dr Shib Sankar Mal, Assistant Professor, Department of Chemistry for FTIR facility, Prof K Udaya Bhat of Department of Metallurgical and Materials Engineering for the DSC,

TEM facilities, and Prof Anandhan Srinivasan of Department of Metallurgical and Materials Engineering for FTIR facility.

The analysis centres Amrita Institute of nanosciences and molecular medicine, Kochi for XPS analysis; Manipal Institute of Pharmacy for zeta potential analysis; University of Mangalore for the FESEM and EDS analysis, Centre for Nano Science and Engineering (CeNSE), IISc Bangalore for the SEM, EDS and XPS analysis, STIC Kochi for the XRD analysis are thankfully acknowledged.

I am deeply obliged to Mr Sadashiva, Mrs Shashikala, Mrs Thrithila Shetty, Mrs Bhavyashree, Ms Vijetha Kotian, Mrs Sandhya, Mr Mahadeva, Mr Harish, Mr Suresh, Mr Ramesh and all other non-teaching staff for the help they have rendered to me.

I am courtly and indebted to my senior and brother Harsha Thaira for teaching me, for helping me in every possible way. I am thankful to My M. Tech colleagues Mrs Reju Rajan and Miss. Niharika Guptha for their support, hard work, enthusiasm and wisdom. I would like to thank my dearest friends Priyanka Uddandarao, Pragadeesh, Smruthi Prabhu, Dr Gopinath Kalaiarasan, Dr Abhinav K Nair, Akhil Vijay, Dr Anjana Anantharaman, Dr Shivanand M, Irfana Shajahan, Deekshtiha Kulal, Minimol, Dr Sushma, Atmuri Shourya of Chemical Engineering Department for the help they have extended to me in times of need.

I wish to extend my thanks to Mr Prasanth Huligol of MME department for the TEM images, Dr Jayalakshmi of MME department for DSC analysis, Dr Sunil Kumar, Ms Rajalekshmi, Ms Nithya, Mr Praveen Mishra, Mr Aranganathan of Chemistry Department for the FTIR analysis.

From the bottom of my heart, I would like to thank Dr Arun Augustine, Nimith, Sterin, Sibeesh, Nandu V, Nithya Bhaskar, Anjali, Mansoor, Asif, Khasim, Ansab who made my NITK life a colourful one.

I would like to dedicate all the achievements what I gained in life to my Father Mr Manirethan Nair T K, who dreamt for me, who always took care of me and who is always my advisor. I am deeply indebted to my Mother Mrs P N Indira Bhai, Sisters Veena and Revathy together with their husbands Prasanth and Hari Krishnan for the support and love they gave during my hardships.

Vishnu Manirethan

ABSTRACT

The biopolymer/biopigment Melanin is known for its free radical scavenging property. Melanin obtained from the marine bacteria Pseudomonas stutzeri is used for the removal of Hg (II), As (III), As (V), Pb (II), Cr (VI) and Cu (II) from aqueous medium. The melanin produced by the bacterium is confirmed to be nanoparticle (32 ± 0.98 nm) using TEM and particle size analysis. Different characterisations such as SEM, TGA, DSC, FTIR, BET surface analysis, zeta potential analysis, XRD were conducted to understand the physio-chemical properties of melanin. The kinetic, thermodynamic and equilibrium studies were conducted to achieve the removal of 85%, 87% 92% and 95% Hg (II), Cr (VI), Pb (II) and Cu (II) respectively from water having 10 mg/L adsorbate concentration and 0.2 g/L of adsorbent loading. Trivalent and pentavalent arsenic showed ineffective binding to melanin which was resolved by functionalising melanin using iron and copper. On functionalisation, melanin could remove more than 99 % of As (III) and As (V) from aqueous medium having arsenic concentration of 10 mg/L and loading of 0.8g/L and 2g/L of Fe-melanin and Cu-melanin respectively. For effective heavy metal adsorption and effortless removal of adsorbent from the aqueous medium, melanin nanoparticles were coated on to different matrices and batch removal studies were performed. Adsorption studies using melanin immobilised N, N-diethylacrylamide hydrogel, melanin coated PVDF membrane, melanin impregnated activated carbon were conducted and found that efficient removal of heavy metals was achieved by melanin impregnated activated carbon. Continuous adsorption studies using melanin impregnated activated carbon as a fixed bed column was performed by varying the parameters such as influent flow rate, heavy metal concentration and adsorbent loading in the column. The flow rate of 0.5 mL/min, the heavy metal concentration of 1 mg/L and adsorbent loading of 100 mg were the optimised parameters for efficient heavy metal removal. Thomas model fitted well with the experimental data compared to the Adam-Bohart's model. Efficient desorption of Hg (II), Pb (II) and Cu (II) were obtained using 3N HCl and Cr (VI) using 1N citric acid. Melanin was re-functionalised after treatment with 5N HCl, and effective reuse of melanin for removal of all heavy metals was achieved until four cycles of study.

Keywords: *Adsorption; Biosynthesised melanin; Heavy metal remediation; Desorption.*

TABLE OF CONTENTS

INDEX OF FIGURES

INDEX OF TABLES

LIST OF ABBREVIATIONS

Abbreviations	Full form
AAS	Atomic Absorption Spectrophotometer
BET	Brunauer-Emmett-Teller
DSC	Differential Scanning Calorimetry
EDS	Energy Dispersive Spectroscopy
FT-IR	Fourier Transform Infrared Spectroscopy
ICP-OES	Inductively Coupled Plasma- Optical Emission Spectroscopy
OD	Optical Density
RT	Room Temperature
RPM	Rotations Per Minute
SEM	Scanning Electron Microscopy
TEM	Transmission Electron Microscopy
TGA	Thermo Gravimetric Analysis
XRD	X-Ray Diffraction

NOMENCLATURE

Notation	Description (units)
C	Concentration of heavy metals (mg/L)
h	Hours (h)
q	Amount adsorbed per gram of adsorbent (mg/g)
t	Time (min)
T	Temperature (ºC)
V	Volume (L)
V	Flow rate (m^3/hr)
w	Weight of the adsorbent (mg)
z	Bed height (cm)
μ	Micron (m)

1. INTRODUCTION

Water is one of the prime natural resources upon which survival of all life forms is reliant on. Only 2.5% of the world's total water is non-saline fresh water and fit for consumption. Rapid industrialisation and increase in population have paced up groundwater contamination, mainly because of the industrial and domestic discharges mainly consisting of heavy metals. Heavy metals are high-density metallic chemicals which are found on earth's crust and most of which impart toxic effects to life forms and its habitat. They have a relatively high specific density (more than $5g/cm^3$) and are noxious or lethal even at minor concentrations. At lower concentrations, some of these metals are essential in maintaining various biochemical and physiological functions of biota but noxious when they exceed a certain threshold level. Most common heavy metals found in groundwater are arsenic, lead, chromium, cadmium, copper, and zinc (Huang et al. 2018; Vinodh et al. 2011; Xu et al. 2018).

The heavy metal contamination of groundwater across the globe are either result of industrial anthropogenic activities or due to natural factors like mineral deposits in the earth's crust. Heavy metals cannot be disintegrated to a nontoxic form, unlike the organic pollutants (Sun et al. 2019). Heavy metals found in earth's crust have turned out to be an environmental hazard and is exposed to different life forms due to various anthropogenic activities such as industrial processing, smelting operations, mining etc. Heavy metal contamination of groundwater sources can even occur naturally due to metal corrosion, soil erosion, leaching of metals to the deep soil, weathering of mineral-rich rocks, volcanic eruption etc. (Burakov et al. 2018; Derkowski and Marynowski 2018; Tchounwou et al. 2012). Metal processing in various industries, refinery processes, petroleum and coal combustions, nuclear power plants, paper processing plants, textiles, wood processing factories, plastics, electronic production centres, etc. contribute to the heavy metal contamination of natural water bodies (Gul and Nasreen 2018; Power et al. 2018; Sherlala et al. 2018).

Our investigation aims at removing divalent mercury, trivalent arsenic, pentavalent arsenic, hexavalent chromium, divalent lead and divalent copper from groundwater. Copper, chromium and lead forms inseparable precipitates at pH near to or higher than neutral in solution at lower concentrations. Mercury precipitates above 6.5, copper

precipitates above pH 7 (Hosseinzadeh et al. 2018), lead above 5.5 (Bradl 2004) and chromium at around 8.5 (Sulaymon et al. 2013). Usually, the heavy metal contaminated groundwater has slightly acidic to near neutral pH, and therefore, the treatment has to be in this pH range to remove the heavy metals (Callura et al. 2018). The properties, occurrence, permissible limits and health impacts of heavy metals of study are briefed as follows.

Groundwater analysis at various parts in the Indian states of Orissa, Haryana, Gujarat, Jharkhand, Andhra Pradesh, Orissa and West Bengal was reported to have mercuric concentrations above the permissible limit of 0.001 mg/L (Srivastava 2003). Mercury is the only metal in earth's crust that exists in the liquid form, and it exists in -2, 0 and +2 oxidation states which are all pernicious to life forms. The toxic effects and severity changes with the oxidation states. Right from inhalation to ingestion, it causes severe threat to health and finally can be fatal (Bernhoft 2012; Bhatt and P 2019). It exists mainly in the environment as in metallic, organic and inorganic forms and present in different kinds of rocks and coal (Yard et al. 2012). WHO and the Bureau of Indian Standards (BIS) has set the maximum permissible limit of mercury in drinking water as 0.001 mg/L of mercury (Vikrant and Kim 2019).

Natural existence of mercury is found as mineral deposits of Cinnabar (HgS) in the earth's crust. Even though abundant deposits are at very few locations, it is found in smaller concentrations in different parts of the world which when weathered gets mixed with the groundwater. Major contribution of mercuric poisoning of environment are through human anthropogenic activities which includes fossil fuel combustion, incineration of municipal as well as hospital solid wastes (González-Fernández et al. 2014). As per the United Nations Environment Program (UNEP), 35% of mercury emissions to the environment are contributed by the gold extraction and purification sector (Arias et al. 2017). Mercury reaches the human body mainly through the food chain; even inhalation can be the route. Lung and eye irritation, skin rashes, diarrhoea are the primary symptoms of its poisoning. It can give impact on nerve, brain, and kidney leading to its damage and can even impair the genetic material which leads to the development of mongolism and affect the reproductive system by damaging the sperms, causing congenital disabilities and miscarriages. The decadence of learning and

understanding abilities, personality changes, tremors, vision fluctuation, deafness, destabilisation of muscle coordination, memory loss are the few very critical impacts of mercury on human life (Bernhoft 2012; Carocci et al. 2014).

42.7 million people in nine districts of West Bengal are exposed to water contaminated with arsenic concentration above the permissible limit (WHO) of 0.01 mg/L (Soni and Shukla 2019). Some tube wells in West Bengal have an arsenic concentration of 3400 $\mu g/L^9$, where the source of arsenic is geologic in origin (Ratnaike 2003). Arsenic is a group 16 metalloid in the periodic table with atomic number 33 and density of 5.72 g/cm^3 and is mostly present in groundwater as arsenic trioxide (As_2O_3). Arsenic exists in different oxidation states -3, 0, 3 and 5 where it is dominantly present in surface water as +5 in protonated forms of H_3AsO_4, $H_2AsO_4^-$, $HAsO_4^{2-}$and AsO_4^{3-} and has a high metal ion chelating and precipitating property (Wei et al. 2019). Arsenic exists as arsenic (III) under reducing conditions and predominantly in the protonated form of H_3AsO_3, $H_2AsO_3^-$, and $HAsO_3^{2-}$ which can chelate with the metal sulphides (Wuana and Okieimen 2011). The toxicity of inorganic arsenic changes with the oxidation state it possesses, i.e., trivalent arsenic is 60 times more toxic than that of the pentavalent form (Xie et al. 2018).

Arsenic enters the human body mainly through inhalation, absorption through skin and ingestion. Once it enters the body, arsenic gets accumulated in liver, kidneys, heart, lungs and smaller amounts in the muscles, nervous system, gastrointestinal tract, and spleen (Benramdane et al. 1999). Arsenic interferes with the enzyme functioning; energy pathway; DNA functioning, replication, and repair. It can even replace phosphate groups in energy molecules like ATP. It can interfere with cellular mechanisms leading to lipid peroxidation and DNA impairment (Cobo and Castiñeira 1997). Acute arsenic toxicity can invite nausea, vomiting, abdominal pain and diarrhoea (Mueller and Benowitz 1989). On a bigger scale, acute psychosis, skin rashes which can later diffuse, cardiomyopathy (Greenberg et al. 1979), seizures, renal failure, respiratory failure, several neurological manifestations etc. Chronic effects of arsenic toxicity include Mee's lines in nails, hyperpigmentation, palmar and solar keratosis (Lien et al. 1999), increased risk of cardiovascular, peripheral vascular, respiratory diseases, diabetes mellitus, and neutropenia. A dose of 100 mg to 300 mg can be fatal

(Ratnaike 2003). Chronic arsenic toxicity cannot be cured (Campbell and Alvarez 1989; Ratnaike 2003).

Lead is abundantly used worldwide for its physiochemical properties such as resistance to corrosion, non-conductance, softness etc. Lead has been used in various industries like batteries, paints, weapons, pipes, paper, pigments, shipping etc. (Basu et al. 2019). According to WHO, lead is a cumulative toxicant which affects almost all organs in the body. It is extremely harmful to children. It directly affects brain, liver, kidney and bones. Lead gets accumulated in tooth and bones and are subsequently released to the bloodstream and makes life at risk (Bardestani et al. 2019). The permissible limit for lead in drinking water should not exceed 0.01 mg/L as per the WHO (Mahar et al. 2019).

Several locations in India are reported to have hexavalent chromium in groundwater, the majority of which are caused by the improper industrial effluent expulsion (Ahamed et al. 2018; Kanagaraj and Elango 2019; Pavithra et al. 2019). Tanneries are the prime chromium contaminator of groundwater and other drinking water sources. Kanpur in Uttar Pradesh, as reported by the Central Pollution Control Board of India (CPCB), have groundwater with Cr (VI) concentration up to 250 times than that of the WHO standard limit of 0.05 mg/L (Sharma et al. 2012). Vellore district in Tamil Nadu is reported to have remarkably higher chromium concentration in the soil as well as the groundwater due to the tannery effluents (Mahimairaja et al. 2014).

Chromium exists in different oxidation states of -2, 0, 3, 6; out of which hexavalent chromium or Cr (VI) is the most inimical one based on toxicity (Guertin 2005). 0.05 mg/L is the maximum permissible concentration of chromium in drinking water as per the Indian Standards (IS) stipulated by the CPCB and the Central Ground Water Commission (CGWC) and WHO (Giagnorio et al. 2018). Pulmonary fibrosis, chronic bronchitis emphysema, bronchial asthma owing to hypersensitivity, pneumoconiosis etc. are some of the pulmonary impacts of chromium poisoning. Inhalation of chromium fumes or aerosols is reported to develop cancer due to the direct mixing of Cr (VI) with blood (Services 1999). Cr (III) above specific concentrations has an inhibitory effect on cell growth and multiplication, while Cr (VI) imparts chromosomal

aberrations leading to mutagenicity (Baruthio 1992; Wilbur et al. 2012). The lethal dose is 300 mg, and the target organ is the kidney.

Copper industries are one of the flourished sectors in India. Different processes are followed to extract pure copper from ore, which leads to the production of waste and effluent consisting of copper, which is either discharged to the landfills or the aquifers. Different scenarios of copper processing industries expelling copper waste and tainting the environment had been reported (Gossuin and Vuong 2018; Wang et al. 2019). Copper exists mainly in oxidation states of +1 and +2, out of which cuprous form of copper shows higher toxicity compared to the cupric form. Even though the cupric form has lesser toxicity, it may transform into cuprous form in cells which impart toxic effects (Lee et al. 2016).

Copper as a mineral is a non-substitutable trace element in the human body. Deficiency of it can cause a wide stretch of diseases and syndromes while the long-term vulnerability can invite a series of health defects. Exposure to copper can cause irritation in eyes, nose, and mouth, but higher intake can damage liver and kidney, and to a greater extent, it can even be fatal. Chronic exposure can deplete intelligence in adolescents and can also result in Wilsons Syndrome, which is featured by corneal copper deposition, hepatic cirrhosis, demyelination and brain damage, renal diseases etc.

Numerous technologies are in practice to remediate heavy metals from drinking water as well as wastewaters such as chemical precipitation, ion exchange, membrane filtration, electrochemical treatment methodologies, coagulation, floatation etc. (Fu and Wang 2011; Kobielska et al. 2018). Several limitations are also associated with these methods which primely are the reduced removal efficiencies at lower concentrations, inadequate selectivity, sludge disposal issues and higher costs associated with the operation (Othman et al. 2012; Gan et al. 2018; Sun et al. 2019)

The adsorption process is an effective and versatile method for the removal of heavy metals, and the combined desorption process helps to solve sludge disposal problems (Gupta et al. 2010). During the recent years, various adsorbents have been developed for heavy metal removal with higher removal efficiencies and lower costs. Various adsorbents available for heavy metal removal include activated carbon (Kyzas et al.

2019), activated alumina (Hojamberdiev et al. 2018), iron hydroxide(Abdullah et al. 2019), hydrous zirconium oxide (He et al. 2019), iron oxide coated polymeric materials (Ma et al. 2019), zero-valent iron (Dongsheng et al. 2019), titanium dioxide (Vajedi and Dehghani 2019), chitosan (Jiang et al. 2019), sawdust activated carbon (Burakov et al. 2018), sulfonated lignite (Robles et al. 2016).

Literature has reported the use of a wide variety of adsorbents; synthetic, natural and functionalised; to remove heavy metals in the range of 50 to 100 mg/L. Studies on removal of heavy metals at lower concentrations from aqueous medium are employed with a very high quantity of adsorbent. This led to the study for the need of an efficient adsorbent required in minimum quantity and maximum removal of heavy metal at very low concentrations from aqueous solutions since heavy metals' concentration in ground waters are mostly in the range less than 5 mg/L (Chaturvedi et al. 2018; Nath et al. 2018; Sen and Sarkar 2019). Hence, to overcome the problems associated with conventional adsorbents like the inability to remove heavy metals at lower concentrations, prolonged equilibrium time and adsorbent toxicity; a novel biosorbent Melanin which is a biopolymer and biopigment derived biologically from a marine bacterium is used.

The term 'Melanin' came from the Greek word *Melanos,* meaning dark. It was extracted from human eye membrane in 1840 by a Swedish Chemist Berzelius. Melanin is a biopigment which gives a brown to black colouration to the widely distributed animal kingdom and even give grey colouration to human beings. It is a polymer formed from the monomeric units of 5, 6-dihydroxyindole and 5,6-dihydroxy indole-2-carboxylic acid (Solano, 2014). Apart from its function of photoprotection and thermoregulation, it is an excellent free radical scavenger, cations chelator and has antimicrobial property. There are different types of Melanin, mainly eumelanin, pheomelanin, neuromelanin, allomelanins, and so on. Eumelanin is dark or brown coloured, pheomelanin is usually red coloured, and allomelanin is a devoid nitrogen form of Melanin with dark to totally black colouration. Neuromelanin is mainly found in the brain (Butler and Day 1998; Hung et al. 2003; Liu 2005). The molecular structure of eumelanin is represented in Figure 1.1 (Nordlund et al. 1998).

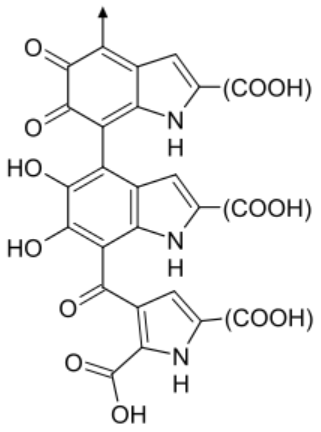

Figure 1.1. The molecular structure of Melanin

Melanin synthesised by the bacterium *Pseudomonas stutzeri*, obtained from the marine sediment is used as the adsorbent for this study. It is structurally similar to eumelanin (Thaira et al. 2016).

Melanin has got a great deal of attention due to its various biological features like metal ion chelation, anti-oxidant activity, free radical scavenging behaviour and photoprotection. It has a considerable affinity towards metal ions. Possible functional groups responsible for metal binding are carboxyl (COOH), amine groups (NH) and phenolic hydroxyl (OH) (Chen et al. 2009). Melanin is a chemically and thermally stable biopolymer which can resist acid as well as moderately high temperatures thereby making it a promising adsorbent for water purification and later for its reuse. It can resist concentrated acids and is stable till temperatures up to 60°C. It can be produced and extracted from various sources such as bacteria, fungus, human hair, by enzymatic methods or synthetic methods. Biological and enzymatic processes are more specific and safer from harmful chemicals. Melanin being a natural polymer is eco-friendly and does not add up to the contamination level of the aqueous medium. Metal ions can easily bind to the functional group due to the charge as well as a high surface area of the melanin nanoparticles. The transfer of metal ions from bulk to the solid phase is hence simplified (Solano 2014).

1.1. Scope and objectives of the study

This work aims to use Melanin for heavy metal removal and to optimise the adsorption conditions for effective and efficient removal of heavy metals from the aqueous medium. A Melanin coated polymer matrix is used for this research.

This research work has the following objectives,

1. To biologically synthesise Melanin and study the physicochemical properties
2. To conduct laboratory scale studies for adsorption of heavy metals on to Melanin coated matrix.
3. To conduct kinetic, equilibrium and thermodynamic adsorption studies of heavy metals on Melanin.
4. To investigate desorption kinetics of heavy metals from Melanin coated matrix.
5. To develop a continuous adsorption system for heavy metal removal by Melanin coated matrix.

1.2. Organisation of the thesis

The research work is organised and annotated as five chapters and is as follows:

Chapter 1 introduces the hazards caused by heavy metals in drinking water and the causes for it. Further, the need for drinking water treatment followed by the existing remediation methods to achieve it is discussed. The effectiveness and importance of adsorption are later reviewed, followed by the employability of Melanin for the remediation of heavy metals from water.

Chapter 2 covers the literature survey on adsorption of different heavy metals of interest using various adsorbents mainly naturally derived ones — the study comprised of both batch and continuous mode of adsorption. The use of Melanin from other sources on heavy metal removal and its characteristics are also illustrated in the section.

Chapter 3 describes the materials and methods employed for the study as per the objectives of the work. This section comprises of synthesis and characterisation of Melanin from the bacteria followed by the kinetic, thermodynamic and equilibrium batch adsorption studies. Coating and impregnation of Melanin to matrices to perform

batch and continuous adsorption studies and finally desorption, regeneration and reuse methodologies are discussed further.

Chapter 4 comprises the results pertinent to the adsorption of heavy metals to Melanin. The chemical and morphological study of both Melanin and heavy metals are annotated before and after adsorption. Effect of various parameters on the batch as well as continuous adsorption is demonstrated, which is followed by adsorption-desorption cycles for the efficient reuse of the adsorbent.

Chapter 5 summarises the overall work outcomes and scope for future dissertations. The Melanin nanoparticle's binding properties, optimised parameters for adsorption and binding efficiencies are summarised here.

2. LITERATURE REVIEW

2.1. Heavy metal removal by batch adsorption

Different adsorbents which are reported to have removed chromium from the aqueous medium, their operating conditions, efficiency and modelling parameters are catalogued in Table 1. The binding of chromium to different adsorbents are reported to be between pH 2 and 3 and at room temperature. It binds to adsorbents in an anionic form and hence the equilibrium time is comparatively higher than that of other metals. Removal of lead from aqueous solutions by adsorption had been reported using a variety of materials, both natural and synthetic. Some of the adsorbents and the experimental technicalities are assorted in Table 2. Adsorption of lead to different adsorbents was favoured in pH range between 5 to 6 and at temperature ranges 25 to 35ºC. The initial adsorbate concentration of study was from 50 mg/L in most of the literature, and studies on removal of lead at lower concentration did not show much higher removal efficiencies. Copper is a toxic heavy metal that had undergone several studies on removal from the aqueous medium by adsorption using various adsorbents. The adsorbent, parameters of adsorption, nature of adsorption and efficiency is briefly tabulated in Table 3. Copper removal from aqueous solutions is majorly reported at pH ranging from 5 to 6. Table 4 summaries the adsorbents reported for the removal of mercury from aqueous solutions. Mercury is adsorbed as divalent cationic form, and the pH corresponding to maximum binding varies according to the adsorbent. Adsorbents for removal of mercury are less reported compared to other heavy metals, and the reported ones have very low removal efficiencies with very high equilibrium time for removal or higher adsorbent loading. Organic and functionally modified adsorbents are used to remove As (III) and As (V) from aqueous solutions and are listed in Table 5. There are very few literature reported to have removed arsenic from an aqueous medium using organic adsorbents. Arsenic being a metalloid, does not easily bind based on the charge attractions to various materials. Inorganic compounds like zeolite, silica and compounds with iron, copper and manganese content are reported to have higher arsenic removal abilities. Many of the naturally derived materials are functionalised using iron to achieve inexpensive methods of arsenic removal.

2.2. Heavy metal removal by continuous adsorption

Different adsorbents are employed for the removal of heavy metals in a fixed column mode and the effect of different parameters like flow rate, adsorbate concentration; mass loading is studied. The experimental data is used to model different standard models and theoretically validated. The model parameters obtained using the characteristic equations gives an insight into the column behaviour on the heavy metal binding, the liquid flow regime and can be employed for the scaling up of adsorption process together with the optimised parameters obtained from the batch adsorption studies. Different adsorbents used as fixed bed columns, the operating conditions and nature of heavy metal removal are detailed in Table 6.

Table 1. Overview of chromium adsorbents, adsorption capacity, parameters, and properties.

Sl. No.	Adsorbent	Adsorption capacity	Optimum parameters for adsorption	Isotherm and nature of adsorption	Remarks	Reference
1.	Novel crosslinked chitosan	325.2 mg/g	pH = 2, T= 30 ºC, C_o= 20 mg/L	Freundlich	Modification protected chitosan from acid and basic conditions	Vakili et al. 2018
2.	Bone char	4.8 mg/g	pH = 1, t = 2 h	Langmuir, endothermic	Fitted well with second-order kinetic model	Hyder et al. 2015
3.	Carbon slurry	15.24 mg/g	pH = 2, t = 70 min, T = 303 K	Langmuir and Freundlich. Feasible, Spontaneous and endothermic	Fitted to pseudo-second order rate kinetics.	Gupta et al. 2010
4.	Fermentation waste of *Corynebacterium glutamicum*	0.236 mmol/g	pH = 2, t = 4 h, C_o = 10 mg/L, T = 25 ± 2 °C	Langmuir	Equations to predict adsorption of Cr (VI) at different concentrations were developed.	Park et al. 2008
5.	Lignin	60.4 mg/g	pH = 2, t = 24 h	Freundlich	70% desorption using NaOH	Albadarin et al. 2011
6.	Lignocellulosic substrate from wheat bran	35 mg/g	t = 24 h, pH = between 2 and 3,	Langmuir	Different characterisations were done for adsorption confirmation and adsorbent.	Dupont and Guillon 2003

Table 2. Overview of lead adsorbents, adsorption capacity, parameters and properties

Sl. No.	Adsorbent	Adsorption capacity	Optimum parameters for adsorption	Isotherm and nature of adsorption	Reference
1.	Saw dust	3.19	C_o = 5 mg/L, w=20 mg, pH 5 and RT	Langmuir	Yu et al. 2001
2.	Activated carbon prepared from Algerian dates stones of *Phoenix dactylifera. L*	9.91	C_o = 50 mg/L, w = 0.1 g, pH 6 and T=25 ºC	Freundlich, exothermic adsorption	Chaouch et al. 2014
3.	Activated carbon from *Eichhornia*	16.61	C_o = 20 mg/L, w = 15 g, pH 3 and RT	Freundlich	Shekinah et al. 2002
4.	*Mucorrouxii* biomass	17.13	C_o= 100 mg/L, w = 0.25 g, pH 5-6, T= 30 ºC	-	Yan and Viraraghavan 2000
5.	Pinecone activated carbon	27.53	Co = 100 mg/L, w = 0.1 g, pH 6 T = 25 ºC	Langmuir, chemisorption	Momčilović et al. 2011
6.	Cashew nut shells activated carbon	28.90	Co = 40 mg/L, w = 0.6 g, pH 6.5, T = 30 ºC	Freundlich, physisorption	Udeye 2009
7.	Activated carbon prepared from biomass plant material of *Euphorbia rigida*	279.72	Co = 50 mg/L, w = 0.8 g, pH 5, T = 40 ºC	Langmuir, spontaneous, endothermic, chemisorption	Gerçel and Gerçel 2007

Table 3. Overview of copper adsorbents, adsorption capacity, parameters and properties

Sl. No.	Adsorbent	Adsorption capacity	Optimum parameters for adsorption	Isotherm and nature of adsorption	Remarks	Reference
1.	Activated carbon from *Elais guineensis* kernel	3.93 mg/g	pH = 5, 100 rpm, C_o = 50 mg/L, T = 30 ± 2 °C, t = 6 h..	Temkin adsorption isotherm.	*Elais guineensis* kernel is an agricultural waste product, hence economical.	Tumin et al. 2008
2.	Mycelium pellets of *Phanerochaete chrysosporium*	3.9 mmol Cu per gram of dry mycelium	t = 2 h, pH = 6, T= 25 °C.	Langmuir	A comparative study with synthetic exchange resin (1.04 mM Cu/g)	Sing and Yu 1998
3.	Banana peel	27.78 mg/g	pH = 6, t = 60 min, 120 rpm, T = 20 °C	Langmuir; spontaneous, exothermic	Particles size > 75 µm showed maximum adsorption	Hossain et al. 2012
4.	Jatropha Biomass (Bark, Endosperm and Endosperm + Seed Coat)	11.541, 20.475 and 22.910 mg/g respectively	pH = 5, t = 60 min, T = 25 °C, 200 rpm	Langmuir; Chemisorption	Adsorption followed pseudo-first order model.	Nacke et al. 2016
5.	Activated carbon prepared from grape bagasse	43.47 mg/g	T = 45 °C, pH = 5.	Langmuir and Dubinine Radushkevich; chemisorption	Follows pseudo-second order and rate-limiting step is chemisorption.	Demiral and Güngör 2016
6.	Activated carbon	93% removal per gram of charcoal	pH = 4, t = 2 h.	--	The effect of interfering ions like lead and cobalt was studied.	Netzer and Hughes 1984
7.	Shells of lentil (LS), wheat (WS), and rice (RS)	7.391, 16.077, and 17.422 mg/g	t = 3 h, pH = 6, 150 rpm, T = 333K	Langmuir and Freundlich; endothermic and spontaneous	The removal efficiency was WS>LS>RS	Aydın et al. 2008

Table 4. Overview of mercury adsorbents, adsorption capacity, parameters and properties

Sl. No.	Adsorbent	Adsorption capacity	Optimum parameters for adsorption	Isotherm and nature of adsorption	Remarks	Reference
1.	*Phragmites karka* (Trin)	1.79 mg/g for natural and 2.27 mg/g for treated	pH = 4, 100 rpm, T = 40°C, t = 40 min	Langmuir and Freundlich. Spontaneous, feasible, and endothermic	Treated showed better efficiency than natural.	Raza et al. 2015
2.	Powdered activated carbon (PAC) and granular activated carbon (GAC)	91.4% removal, 0.151 mg Hg/g carbon	w(PAC)= 0.25 to 4.50 g/L, w(GAC)=0.2 to 20 g/l.	Freundlich	2 mg/L was the initial concentration of study.	Abdel-Shafy et al. 1998
3.	Exhausted coffee waste (ECW)	31.75 mg g^{-1}	w = 0.4 g/L, Co = 77.98 mg/L, pH =7, t = 192.40 min, T= 33 °C and 375 rpm.	Langmuir, endothermic	Chemisorption, poor desorption and reusability.	Mora Alvarez et al. 2018
4.	FS-400 granular activated carbon (GAC)	93% Hg removal	pH = 7, w = 100 mg/L, t = 1 h, Co = 10 ng/L	Freundlich,	Chemisorption, Particle size of 0.2 mm had adsorption efficiency of 100%	Ma et al. 1992
5.	Thioether-functionalized corn oil biosorbent	8.150 mg/g	T= 20, t = 23h,	Freundlich	Chemisorption	Dunn et al. 2018
6.	Dry biomass of *Chlorella vulgaris*	32.6 mg/g	w= 0.5g/L, Co = 11.0 to 90.6 mg/L pH=5,	Langmuir	Physisorption	Solisio et al. 2019

Table 5. Overview of arsenic adsorbents, adsorption capacity, parameters and properties

Sl. No.	Adsorbent	Adsorption capacity	Optimum parameters for adsorption	Isotherm and nature of adsorption	Reference
1.	Chitosan coated with Fe-Mn binary oxide	3.91 and 3.89 mg g-1 for As (III) and As (V)	pH=3 to 8, w=0.5 g/L, 180 rpm, T= 22 ± 1 °C, Co=0.5 mg/L	Freundlich, chemisorption	Nikić et al. 2018
2.	Natural orange peel (NOP) and charred orange peel (COP)	60.9 mg/g for COP, 32.7 mg/g for NOP	pH 6.5, w = 4g/L, T=20±2 °C, t =120 min, Co = 200 mg/L	Langmuir, chemisorption	Abid et al. 2016
3.	Iron impregnated biochar	2.16 mg/g	T = 20 ± 2 °C, w = 0.1 g, Co = 5 mg/L, pH= 5.8 ± 0.2,	Freundlich, chemisorption	Hu et al. 2015
4.	Iron coated rice husk	2.5 mg/g	t = 6h, pH = 4, Co = 5 mg/L, w = 4 g/L, T = 23 °C	Langmuir	Pehlivan et al. 2013
5.	Zeolite modified with copper oxide and iron oxide	Zeolite/CuO NCs = 44.8, Zeolite/Fe_3O_4 NCs= 47.4	Co=100 mg/L, t = 40 minutes, w = 0.15 g, pH = 4 to 6, RT.	Langmuir, chemisorption	Alswat et al. 2016
6.	Iron hydroxide/ manganese dioxide doped straw activated carbon	75.82 mg g^{-1}	pH=3, T = 30°C, w = 10 mg, Co = 20 mg/L, t= 8h	Langmuir, chemisorption	Xiong et al. 2017
7.	*Staphylococcus xylosus* biomass pre-treated with Fe(III)	54.35 and 61.34 $mg \cdot g^{-1}$ for As (III) and As (V) respectively	pH=7, Co=1 g/L and t=30 min for As (III) pH= 3, Co=2 g/L and t=2.5 h for As (V)	Langmuir, physisorption	Aryal et al. 2010

Table 6. Overview of continuous adsorption studies, parameters and operating conditions using different adsorbents

Sl. No.	Metals	Adsorbent	Capacity	Operating conditions	Nature of adsorption and models	Reference
1.	Pb (II), Cu (II), Zn (II)	Agricultural wastes (groundnut shell, orange and banana peel, rice husk, coconut husk and Wawa tree saw dust)	75% (pH 5.0 - 7.0), 98 % (pH 5.0) and 86% (pH 3.0)	Cu (w= 2.5 g, Co= 40.7 mg/L, pH = 4.4 and t = 64 min), Pb (w= 2.5 g, Co = 196.1 mg/L pH= 5.6, t= 60 min) Zn (w = 3.1 g, Co= 70.2 mg/L, pH = 4.3, t = 50 min)	Response surface methodology was used to find the effect of different parameters and their combination on adsorption	Janyasuthiwong et al. 2015
2.	Cr (VI)	Modified corn stalk (MCS)	Efficiency= 93.78 %, q = 138 mg/g, t_b = 188.32 min	Co=200 mg/L, v=10 mL/min z= 2.9 cm, pH= 4.91, t= 288 min w= 576 mg,	Thomas and Yoon-Nelson models.	Chen et al. 2012
3.	Hg (II)	Rice husk ash	122.88 mg/g	Co= 100 mg/L; pH = 5.5, w= 50 g, v= 30 mL/min.	bed-depth service time (BDST) model	Tiwari et al. 1995
4.	As (III)	Activated alumina and iron oxide impregnated activated alumina (IOIAA)	AA = 0.310 and IOIAA = 0.380 g/kg	z= 18 cm, v= 0.016 cm^3/sec, Co= 0.1 mg/L, pH= 7.6	BDST model for initial zone of breakthrough and pore diffusion model	Singh and Pant 2006b

The use of inorganic and synthetic adsorbents for the removal of heavy metals from water can make it unfit for drinking by secondary pollution due to the presence of adsorbent particles itself. For example, agents like zeolites in aqueous medium exchanges metals ions to adsorb the heavy already present in water. These ions will be present in the water after the heavy metal removal. This has led to the use of biosorbents or naturally occurring nontoxic materials for heavy metal removal. Our survey of literature has found that natural adsorbents do not have better capability to remove heavy metals at lower concentrations and also the efficiency of removal is less at lower adsorbent loading (Tables 1, 2, 3, 4, 5 and 6). In this study, the potential of biosynthesised Melanin for the removal of heavy metals from water at lower concentrations is explored. The use of Melanin from other sources for the removal of different metals are discussed below.

2.3. Heavy metal adsorption using Melanin

Saini and Melo (2013) synthesised Melanin using tyrosinase enzyme. This Melanin was used for the adsorption of uranium. It showed good uptake capacity over a broad range of pH and also equilibrium was reached within 2 hours of contact. Kinetic data fitted well into Lagergren's pseudo-second-order kinetic model. The maximum loading capacity of 588.24 mg/g was calculated from Langmuir plot studied in the initial uranium concentration from 50 mg/L to 800 mg/L. Thermodynamic studies revealed that the sorption process was favourable understudied conditions. Binding of uranium to the surface of Melanin was confirmed by Energy Dispersive Spectroscopy (EDS) and FTIR.

Chen et al. (2010) have done a study on the removal of Pb (II) and Cd (II) ions using squid Melanin. Results showed that maximum content of bound ions on the surface of Melanin is 0.93 mM/g for Cd (II) and 0.65mM/g for Pb (II). Adsorption yield was high in the pH range of 4.0 – 7.0. Temperature and macro salts like NaCl, $MgCl_2$, and $CaCl_2$ do not affect the binding of Pb (II), but adsorption of Cd (II) decreased. Possible functional groups responsible for adsorption are phenolic/hydroxyl (OH), carboxyl (COOH), and amine groups (NH). Desorption of adsorbed metal ions was done using HCl and EDTA.

Sono et al. (2012) described the use of hydrophobic polymer PVDF coated with synthetic and hair Melanin for the adsorption of Pb (II). Synthetic eumelanin coated polymer shows a higher adsorption rate towards Pb (II) than other metal ions like Cu^{2+}, Zn^{2+}, Cd^{2+}. The maximum adsorption capacity was about 138 µg Pb (II) per disc for synthetic Melanin and in the case of hair Melanin, 126 µg Pb (II) per disc.

Sajjan et al. (2013) have done adsorption of Cu^{2+} and Pb^{2+} using Melanin extracted from *Klebsiella* sp. GSK after immobilising the Melanin in sodium alginate beads. The adsorption capacity reported was about 169 mg/g for Cu^{2+} and 280 mg/g for Pb^{2+}.

The comparative study of adsorption by Melanin with other adsorbents for copper, lead and uranium are briefed in Table 5. Melanin from different sources is used as the adsorbent, which showed a remarkably higher level of adsorption capacity when compared with the activated carbon (Tables 1, 2 and 4).

Table 7. Comparison of adsorption capacity of Melanin with other adsorbents

Sl. No.	Metal adsorbed	Adsorption capacity range (mg/g)	Reference
1	Copper	3.92 to 43.47	Table 3
2	Lead	2.89 to 240.06	Goel et al. (2005), Gerçel and Gerçel (2007)
3	Uranium	3.54 to 98	Shuibo et al. (2009) Tsunashima et al. (1981)
4	Lead by Squid Melanin	134	Chen et al. (2010)
5	Copper and Lead by *Klebsiella* Melanin alginate bead	169 (Cu^{2+}) 280 (Pb^{2+})	Sajjan et al. (2013)
6	Uranium by Synthetic Melanin	588.24	Saini and Melo (2013)

From Table 7, it is evident that the heavy metal adsorption capacity of Melanin is much higher than the conventional adsorbents. The adsorption efficiency of Melanin is higher at lower heavy metal concentrations, which can exalt it as an excellent adsorbent and replace charcoal, which is commonly used hitherto. Tables 1, 2, 3, 4, 5 and 6 depict the use of different adsorbents for the removal of heavy metals in which higher adsorption efficiency is shown at a higher initial heavy metal concentration which generally does not prevail in real life groundwater scenarios. At lower initial heavy metal concentration, the adsorption rate of standard adsorbents is very less. Melanin has high metal scavenging property at very low heavy metal concentration, which makes it a better adsorbent for commercial use in the future.

3. MATERIALS AND METHODS

3.1. Materials

Heavy metals solutions of concentration 1000 mg/L are prepared from the respective salts and used as stock from which the working concentration of the solution is prepared by dilution. Mercury nitrate monohydrate (≥98%), potassium dichromate (≥99%), lead nitrate (≥99%), anhydrous copper sulphate (≥98%), sodium arsenite (≥98.5%, CDH, India) and sodium arsenate (≥99%, CDH, India) are used for the preparation of stock solutions of Hg (II), Cr (VI), Pb (II), Cu (II), As (III) and As (V) in distilled water. The working concentration ranged from 1 to 25 mg/L produced from the stock. The heavy metal solution pH was confined using 1N HCl and 1N NaOH solutions and monitored using pH meter (HI98115 GroLine pH tester, Hanna Instruments, Romania). The adsorption experiments were conducted with 50 mL working volume unless otherwise specified.

3.2. Methodology

3.2.1. Biosynthesis of Melanin pigment

The bacterial culture of *Pseudomonas stutzeri* HMGM-7 was procured from MTCC culture collection, Chandigarh, India. Tryptic Soy broth dissolved in seawater as medium stoppered in an Erlenmeyer flask was sterilised and inoculated with the bacteria. *P. stutzeri* starts producing Melanin to the medium as extracellular black pigment within 8 hours of inoculation and will be complete by 48 hours. The extraction procedure of Melanin was initiated after removing the suspended particles and cells from the medium by centrifugation at 5000 rpm (6930 series, Kubota, Japan) for 5 minutes. The medium was alkalinised to pH 12 and then autoclaved, which was followed by centrifugation at 5000 rpm for 10 minutes to remove all the undissolved components in the medium. The medium containing dissolved Melanin was then acidified to pH 2 and kept overnight at 4ºC for Melanin precipitation. The medium was then centrifuged at 12000 rpm for 20 minutes to yield the precipitated Melanin. The obtained Melanin was washed with ethanol, acetone and again distilled water and then dried at room temperature and stored at -20ºC (Ganesh Kumar et al. 2013).

3.2.2. Functionalization of Melanin for arsenic adsorption

Melanin was functionalized by a method of oxidation using potassium permanganate after copper adsorption and another method of heat treatment after iron adsorption for arsenic removal from aqueous solutions.

A required quantity of purified and dried Melanin was added to 0.5 mol/L of copper solution derived from copper nitrate trihydrate (Loba Chemicals, 95%) maintained at pH 4 and 35°C. After 5 hours of orbital shaking at 150 rpm, Melanin was separated from the Cu (II) solution by centrifugation (12000 rpm, 20 min) and washed with distilled water. The separated Melanin was then added with 25 mL 0.1 N $KMnO_4$ (> 98.5%, Emplura, India) solution and was kept for shaking in an orbital shaker for 15 minutes. Melanin was separated from the solution by centrifugation, which was followed by its repeated washing using distilled water until the colour of $KMnO_4$ was not visible in the wash water. Melanin was then made to dry in an oven maintained at 37°C.

The required quantity of Melanin was added to 0.5 mol/L ferrous solution derived from ferrous sulphate heptahydrate (98%, HiMedia) maintained at native pH of 1.8 and was kept for shaking in an orbital shaker maintained at 35°C. Melanin was separated by centrifugation (12000 rpm, 20 min) after 5 hours of incubation and then washed with distilled water. The separated Melanin was then kept in a hot air oven at 100 ± 5 °C for 6 hours. Melanin functionalized by both means was used to conduct batch and continuous studies for the removal of As (III) and As (V) from the aqueous medium.

3.2.3. Characterisation of Melanin

3.2.3.1. Morphological characterisation and surface chemistry determination

The size and morphology of the Melanin were apprehended using Scanning Electron Microscope (SEM, JSM-6380, JOEL, Japan) and Transmission Electron Microscope (TEM, JEM-2100, JOEL, Japan). In the case of SEM imaging, the samples were sputter coated with a thin layer of gold before imaging for charge dissipation. For TEM imaging, the Melanin was dispersed in distilled water using a probe ultrasonicator (Tip diameter 1/8" stepped microtip, Sonics Vibra-cell Ultrasonic Processor, USA) and a small drop of the dispersed sample was placed on a TEM copper grid coated with thin

a layer of amorphous carbon. The surface chemistry of the biosynthesised Melanin was determined using Fourier-Transform Infrared Spectroscopy (FT-IR). All the spectra were documented in the range of 4000-400 cm^{-1} (Silicon carbide source, 16 number of scans and 4 cm^{-1} resolution, model Alpha, Bruker Germany make). Particle size analysis of the biosynthesised Melanin was done using Nanoparticle analyser ('Nanopartica' SZ–100, Horiba Scientific, Japan). Pure samples were dispersed in distilled water using ultrasonicator before introducing into the instrument. To understand the surface charge of Melanin at different pH, the zeta potential was analysed (Nano ZS - ZEN3600, Malvern Zeta Sizer, UK). The average surface area, average pore volume and pore diameter were analysed using a BET analyser (Novae 2200, Quanta chrome, USA). The TGA (Seiko Instruments TGA/DTA Exstar 6300, Japan) and DSC (Netzsch, DSC 404 F1, Germany) analysis were conducted to find the thermal stability of Melanin at higher temperatures. Powder X-ray Diffraction (XRD, Bruker AXS D8 Advance) was conducted to find the chemical form of iron and copper impregnated on melanin. The heavy metal adsorbed Melanin was dried and analysed using X-ray photon spectroscopy (XPS, aluminium kα monochrome X-ray source, Axis Ultra DLD, Kratos Analytics, UK) to find the speciation of heavy metals on adsorption.

3.2.4. Batch adsorption studies at different pH

Batch adsorption experiments were conducted by adding calculated quantity of dried Melanin to 10 mg/L individual sample solutions of Hg (II), As (III), As (V), Cr (VI), Pb (II) and Cu (II) and adjusting the pH to the desired value using 0.1N NaOH and 0.1N HNO_3. The solution was then agitated at 200 rpm in an orbital shaker maintained at 318 K. The samples were collected at specific time intervals and centrifuged at 12000 rpm for 10 min. The residual concentrations of Hg (II), As (III), As (V), Cr (VI), Pb (II), and Cu (II) were analyzed using Atomic Absorption Spectrophotometer (AAS, GBC 932 plus) and Inductively Coupled Plasma – Optical Emission Spectrometer (ICP-OES, Agilent 5100, USA) and the amount of metal ions adsorbed on to the Melanin was calculated by using the following equation:

$$q_t = (C_0 - C_t)\frac{V}{W} \quad (1)$$

Where, q_t (mg/g) is the amount of heavy metal ions adsorbed at a given time per unit mass of the adsorbent, C_o (mg/L) is the initial heavy metal concentration, C_t (mg/L) is the residual heavy metal concentration in solution at equilibrium, V (L) is the sample volume, and w (g) is the amount of adsorbent.

3.2.5. Adsorption kinetic and equilibrium studies

Melanin of concentration 0.2 g/L was agitated in individual heavy metal solutions of concentrations 5 mg/L, and 15 mg/L at 200 rpm and 318 K and the residual heavy metal concentration in solution is estimated for conducting the kinetic studies. Webber and Morris Intraparticle Diffusion Model, Lagergren's pseudo-first-order and pseudo-second-order equations were used to model the kinetics of Hg (II), As (III), As (V), Cr (VI), Pb (II) and Cu (II) adsorption on Melanin.

3.2.5.1. Intra-particle diffusion model

A mechanistic approach to explain the sorption kinetics is the Intra-particle diffusion model. Generally, adsorption is governed by either of external diffusion, pore diffusion, surface diffusion and adsorption on the surface of pores or in any combination of these. Intra-particle diffusion of heavy metals to Melanin was explored by modelling the kinetic adsorption data in the characteristic equation of Intraparticle Diffusion Model. It can be described as a function of adsorption capacity and time as described by Weber and Morris, which is:

$$q_t = k_{id} \cdot t^{0.5} + C \quad (2)$$

where, k_{id} is the intra-particle diffusion rate constant (mg/g $min^{0.5}$), q_t (mg/g) is the amount of metal ions adsorbed at time t, C (mg/g) is the intercept which represents the thickness of the boundary layer.

3.2.5.2. Lagergren's pseudo-first-order and pseudo-second-order kinetic models

The Lagergren's pseudo-first-order kinetic model is based on the assumption that the adsorption process depends only on the number of metal ions present in the aqueous

solution and the available binding sites on the adsorbent at any particular period (Ho 2004; Ho and McKay 1999). The integrated form of Lagergren's pseudo-first-order kinetic model can be expressed as follows (Lagergren 1898):

$$log(q_e - q_t) = log(q_e) - \left(\frac{k_1}{2.303}\right) \cdot t \quad (3)$$

where, q_t, q_e are the amount of metal ions adsorbed (mg) per unit dry weight of adsorbent (g) at any particular time t (min) and equilibrium, and k_1 is the pseudo-first-order rate constant (min^{-1}). The corresponding values of the pseudo-first-order rate constant and q_e were calculated from the intercept and slope of the linear plot of $log\ (q_e - q_t)$ versus t. k_1 and q_e are calculated from the slope and intercept from this plot.

The pseudo-second-order kinetic model is based on the assumption that the rate controlling step of an adsorption process is chemical adsorption (Acharya et al. 2009; Hadi et al. 2015; Saini and Melo 2013). The integrated form of Lagergren's pseudo-second-order kinetic model can be expressed as follows (Ho and McKay 1999; Lagergren 1898):

$$\frac{t}{q} = \frac{1}{(k_2 \cdot q_e^2)} + \frac{1}{q_e} t \quad (4)$$

where k_2 (g mg^{-1} min^{-1}) is the pseudo-second-order rate constant. Values of k_2 and q_e were calculated from the intercept and slope of the linear plot of t/q_t versus t.

3.2.6. Thermodynamic studies

Batch experiments were conducted with 10 mg/L metal ion solutions and were mixed with 0.2 g/L of Melanin for Hg (II), Cr (VI), Pb (II) and Cu (II) studies while 0.8 g/L Fe-Melanin and 2 g/L Cu-Melanin were used for As (III) and As (V) removal at different temperatures (288 K, 298 K, 308 K, 318 K and 328 K) to evaluate thermodynamics of the adsorption process.

3.2.6.1. Determination of activation energy

A linear relationship of rate constant versus temperature using Arrhenius equation gives the value of activation energy required for the heavy metals to bind to Melanin. The Arrhenius equation is given as:

$$ln\, k_2 = ln\, A - \frac{E_a}{R \cdot T} \quad (5)$$

Where E_a the activation energy for adsorption, k_2 is the second order rate constant, A is the Arrhenius factor, R is the universal gas constant, and T is the absolute temperature.

3.2.6.2. Evaluation of Thermodynamic parameters

Thermodynamic parameters such as standard free energy change (ΔG^0), enthalpy (ΔH^0) and entropy (ΔS^0) change help to identify whether the adsorption process is favourable or not. A negative Gibbs free energy change indicates that the adsorption is favourable. These thermodynamic parameters were determined to investigate the feasibility of adsorption through the information obtained from the following equations:

$$\Delta G^0 = -RTlnK_c \quad (6)$$

$$lnK_c = \frac{\Delta S^0}{R} - \frac{\Delta H^0}{RT} \quad (7)$$

where K_c is the Langmuir equilibrium constant, R is the universal gas constant (8.314 $J \cdot mol^{-1}K^{-1}$), T is the temperature in Kelvin.

3.2.7. Batch adsorption isotherm studies

Isotherm studies were conducted by using 0.2 g/L of Melanin for Hg (II), Cr (VI), Pb (II) and Cu (II) studies while 0.8 g/L Fe-Melanin and 2 g/L Cu-Melanin were used for As (III) and As (V) removal at different desired concentration ranging from 5 mg/L to 25 mg/L. Two parameter isotherm models such as Langmuir and Freundlich adsorption isotherm models and three parameter isotherm model - Redlich Peterson model were used to evaluate the relationship between adsorbed and residual aqueous concentrations of metal ions at equilibrium.

Isotherm helps to describe the interaction between the adsorbent and adsorbate as per the assumptions of each isotherm. Several factors such as the concentration of metal ions in the solution, their relative adsorbing abilities and the degree of competition among the ions to bind to the active sites of adsorbent determine the shape of isotherms. Langmuir isotherm developed on the assumption of adsorption homogeneity such as

uniform energy of adsorption with no transmigration of metal ions in the plane of the adsorbent surface, non-interaction between the adsorbed metal ions and availability of all identical binding sites for monolayer adsorption. The linear form of Langmuir isotherm can be expressed as follows (Langmuir 1918):

$$\frac{C_e}{q_e} = \left(\frac{1}{q_{max}}\right)\left(\frac{1}{b}\right) + \frac{C_e}{q_{max}} \quad (8)$$

where, C_e (mg/L) is the equilibrium concentration of metal ions, q_e (mg/g) is the amount of metal ions adsorbed per specific amount of adsorbent at equilibrium, q_{max} is the maximum loading capacity, which is the amount of adsorbate required to form monolayer and b represents the affinity of adsorbent to adsorbate.

From the affinity, constant b given in Equation 9, a dimensionless constant called separation factor, R_L which helps to define whether the adsorption process is favourable or not was calculated as follows (Saini and Melo 2013; Wang et al. 2015b):

$$R_L = \frac{1}{1 + b \cdot C_i} \quad (9)$$

where, C_i (mg/L) is the initial metal ion concentration. The value of R_L>1 implies unfavourable adsorption process, R_L = 1 is linear, 0< R_L< 1 represents favourable adsorption process, R_L = 0 implies that the adsorption process is irreversible.

Freundlich adsorption isotherm model is developed on the assumption that the metal uptake occurs on a heterogeneous surface by multilayer adsorption with the lateral interaction between adsorbed species on the surface of the adsorbent. The linear form of Freundlich isotherm can be expressed as follows (Freundlich 1906; Saini and Melo 2013):

$$ln\, q_e = ln\, K_F + \left(\frac{1}{n}\right) ln\, C_e \quad (10)$$

Where q_e (mg/g) is the equilibrium metal uptake capacity, C_e (mg/L) is the residual metal ion concentration, *1/n* and K_F refer to the intensity of adsorption and Freundlich constant, respectively.

The three-parameter model adsorption isotherm, the Redlich-Peterson (RP) model is expressed in its linear form as

$$\frac{C_e}{q_e} = \frac{1}{A \cdot B} + \left(\frac{1}{A}\right) C_e^g \quad (11)$$

Where *A* and *B* are R-P isotherm parameters having unit L/mg and *g* is an exponential term whose values range from 0 to 1 ($0<g<1$) (Wu et al. 2010).

3.2.8. Ternary adsorption studies

Equal concentration of 10 mg/L of Cr (VI)-Hg (II)-Cu (II) and Pb (II)-Hg (II)-Cu (II) ternary mixture solutions maintained at pH 4 ± 0.5 and 5 ± 0.2 respectively and volume 50 mL were taken as the feed for multicomponent metals adsorption analysis. The mixture was orbitally agitated at 150 rpm for 5 hours and 318 K temperature. The residual heavy metal ion concentrations of all metals were analysed using ICP-OES after equilibrium time and amount adsorbed was calculated by the Equation (1).

3.2.9. Melanin impregnated hydrogel

Dried biosynthesised Melanin was made to impregnate into the hydrogel and was used for adsorption studies. 1.2 mL of N, N-Diethyl acrylamide (Merck, India), 0.02 g of Ammonium peroxodisulpahte (APS, ≥98%, Merck, India), 0.016 g of N, N′-methylene bisacrylamide (BIS, ≥98%, Merck, India) was dissolved in 5 mL of distilled water maintained at 30 ºC. The required quantity of dried Melanin was added to the solution and sonicated using a probe ultrasonicator for 15 minutes. To this homogenised solution, 50 µL of N, N, N′, N′- tetramethylethylenediamine (TEMED, ≥99%, Merck, India) was added, and then the hydrogel was formed. The hydrogel was then equilibrated in distilled water for 48 hours with the water changed every 8 hours to remove all the unreacted chemicals. The hydrogel was then vacuum dried at 50 ºC (Long and Hiroshi 2008).

3.2.10. Melanin coated PVDF membrane

Polyvinylidene fluoride (PVDF) membranes of diameter 47 mm and 0.45 µm pore size were procured from Axiva Sichem, India. PVDF membranes were surface activated by wetting with methanol for 15 minutes. The PVDF membranes were then washed with distilled water thrice to remove methanol from the surface. The surface activated discs

were kept immersed in water until use to avoid the drying and thereby losing the activation. Dried Melanin was dissolved in distilled water maintained at pH 12 and to which, the surface activated discs were soaked. The pH of the solution was then changed to pH 2. The system was made to shake at 150 rpm and 30 ºC for 24 hours. Melanin coated PVDF discs were dried at 50 ºC and was used for adsorption studies (Sono et al. 2012).

3.2.11. Melanin impregnated activated carbon

Purified and dried Melanin was suspended in distilled water and alkalized to pH 12, enabling the Melanin to dissolve in water completely. To this solution, an equal quantity of activated carbon (Darco KB, 100-325 particle mesh size, Sigma Aldrich, India) was added, and immediately the pH of the solution was acidified to 2. The system was then made to shake in an orbital shaker at 30 ºC for 3 hours and 150 rpm. After 3 hours, the solution was centrifuged at 3000 rpm for 10 minutes, followed by washing the pellet using distilled water and then dried to use for adsorption experiments. The wash water and supernatant were alkalized to pH 12, and the OD at 400 nm was checked using spectrophotometer (Genesys 10S) to estimate the quantity of Melanin, which was unbound to activated carbon.

3.2.12. Continuous adsorption studies

Melanin impregnated activated carbon was packed in a column to conduct dynamic adsorption studies. Melanin was impregnated on to activated carbon in the ratio of 1:5 (1 part of activated carbon and 5 parts of Melanin). A polypropylene column of inner diameter 4.5 mm and 60 mm long was used for continuous studies in an upward flow set up. Column Frits (1/2 inch, 2µ porosity, Sigma Aldrich, India) to hold the adsorbent was supported on a 75 µ sized steel support. The schematic is shown in Figure 3.1.

The effects of adsorbate inlet concentration, flow rate and adsorbent loading in the column were studied by varying each parameter and keeping the other two parameters constant. Flow rates of 0.5, 1 and 1.5 mL/min were maintained using a peristaltic pump (Fisher Scientific, 13-876-2 Variable-Flow Peristaltic Pump, USA) by an upward flow set up through the bottom of the column, keeping the adsorbent loading and inlet concentration constant. To study the effect of adsorbent loading; 100, 75 and 50 mg

Melanin impregnated activated carbon was packed in the column keeping the other factors consistent. Inlet heavy metal concentration is an important parameter of column studies and the adsorption of 1, 3 and 5 mg/L of heavy metals onto 100 mg Melanin impregnated activated carbon was studied. The concentration of heavy metals in outflow samples were analysed after fixed intervals of time by ICP-OES. The pH of the inlet solutions was adjusted as per the optimum pH obtained for maximum adsorption from the batch pH studies for each heavy metal.

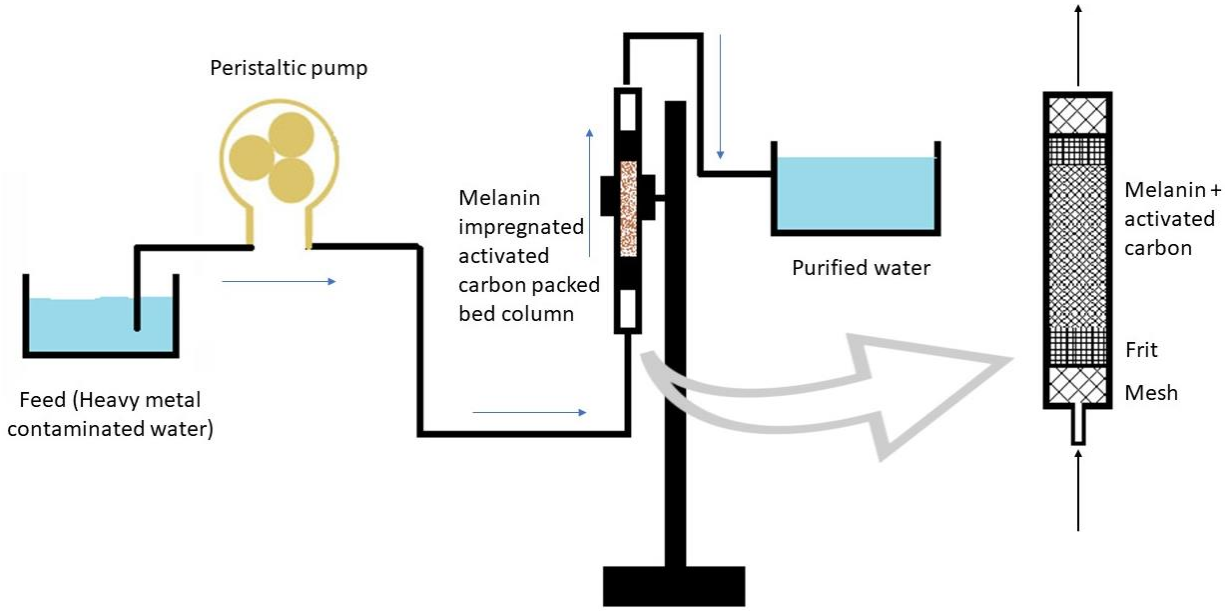

Figure 3.1. Schematic representation of the continuous adsorption system

The breakthrough time and breakthrough curves are the important characteristics that describe the process and kinetic performance of the operation of a packed column. The breakthrough curve illustrates the behaviour of the heavy metal ions adsorption from the aqueous medium to the Melanin impregnated on the activated carbon (Hayati et al. 2018). The breakthrough curve (S shaped curve) for fixed bed height and the flow rate is the ratio of the effluent concentration to the influent concentration as a function of time or volume. The breakthrough point on the breakthrough curve is where the effluent concentration generally reaches about 0.1% of the influent concentration (C_o), and the exhaustion point of the column is usually 95% of its influent value (Dwivedi et al. 2008). The time required to attain the breakthrough concentration is called breakthrough time.

The value of the total mass of metal adsorbed q_{total} for a given feed concentration and the flow rate is equal to the area under the plot of the adsorbed metal concentration C_{ad} ($C_{ad}= C_0–C_t$) (mg/L) vs. t (min) of the breakthrough curve and can be calculated from Equation:

$$q_{total} = \frac{Q}{1000}\int_{t=0}^{t=t.total} C_{ad}\, dt \tag{12}$$

where Q is the volumetric flow rate (mL/min), t_{total} is the total flow time (min), C_{ad} is the concentration of metal removal (mg/L) (Han et al., 2009).

Equilibrium metal uptake or the maximum capacity of the column for removal of metal ions from the inlet solution, $q_{e(exp)}$ (mg/g), in the column is calculated as the following:

$$q_{e\ (exp)} = \frac{q_{total}}{m} \tag{13}$$

where m is the mass of adsorbent in column (g). The total amount of metal ion entering column (W_{total}) is calculated from the following equation

$$W_{total} = \frac{C_0 \cdot Q \cdot t_{total}}{1000} \tag{14}$$

moreover, the removal percentage of metal ions can be obtained from equation

$$Y = \frac{q_{total}}{W_{total}} \times 100 \tag{15}$$

where Y is the ratio of the maximum capacity of the column (q_{total}) to the total amount of metal ion sent to column (W_{total}).

3.2.12.1. Continuous adsorption isotherms

To model the adsorption in column breakthrough experiments, Thomas model is one of the widely used models. Thomas model assumes that there is plug flow in the bed, the adsorption equilibrium follows the Langmuir adsorption model, and the kinetics of adsorption follows a second-order reversible reaction without axial dispersion. Equation 16 describes the Thomas model as:

$$\frac{C_t}{C_0} = \frac{1}{1+exp\left(\frac{K_{TH}q_0 x}{v} - K_{TH}C_0 t\right)} \tag{16}$$

where K_{TH} is the Thomas constant (mL/min·mg), C_t is the effluent heavy metal concentration (mg/L). C_o is influent metal ion concentration, q_o is the amount of metal ions adsorbed per gram of Melanin impregnated activated carbon (mg/g), x is the mass of the adsorbent (g), v is the volumetric flow rate (mL/min), and t is the flow time (min) (Lezehari et al. 2012).

Adam-Boharts model is used to describe the breakthrough in a fixed bed adsorption process for the initial state of operation. The Adam-Boharts model is based on the theory of surface reaction, which states the reaction is between the adsorbate and adsorbent in the column is not immediate. It assumes that equilibrium is not instantaneous, and the adsorption rate is proportional to the adsorption capacity remaining on the adsorbent. The nonlinear equation of Adam-Boharts model is:

$$\frac{C_t}{C_0} = \exp\left(K_{AB}C_0 t - K_{AB}N_0\frac{z}{v}\right) \quad (17)$$

where K_{AB} is the Adam Boharts kinetic constant (L/min·mg), N_o is the adsorptive capacity (mg/g), C_t is the effluent heavy metal concentration (mg/L), C_o is influent metal ion concentration, z is the column bed depth (cm), v is linear velocity (cm/min), and t is the flow time (min) (Ghasemabadi et al. 2018; Mahdi et al. 2018).

3.2.13. FTIR, EDS and XPS analysis of heavy metal adsorption on Melanin

Melanin was made to contact with 25 ml of 10 mg/L of Hg (II), Cr (VI), Pb (II) and Cu (II) solutions at 318 K at specific pH. Similarly, iron and copper functionalised Melanin was made to contact with As (III) and As (V) solutions at 318 K. After 24 hours of incubation at 200 rpm, Melanin was separated from the solutions by centrifugation (5000 rpm for 5 minutes) and washed once with distilled water to remove the unbound metal ions and the Melanin pellet obtained after centrifugation was air dried. The Fourier transform infrared spectroscopy (FTIR) was conducted for the dry Melanin powder by the ATR method, and the spectrum was documented in the range of 4000-400 cm^{-1}. Electron dispersive spectroscopy was performed to confirm the binding of heavy metals to Melanin and functionalised Melanin. X-ray photoelectron spectroscopy analysis was conducted to understand the speciation of metal ions after binding and thereby the nature of binding of heavy metals to Melanin.

3.2.14. Desorption of heavy metals and regeneration of Melanin

The reverse process of adsorption in which the adsorbed heavy metals detaches from Melanin in the presence of a desorbing agent like acid or any other solvent is called desorption. Effect and efficiency of different desorbing agents were studied. The efficiency of desorption was calculated using the equation (Vieira and Beppu 2006)

$$\text{Desorption \%} = \frac{desorbed\ amount\ of\ metal\ ions}{adsorbed\ amount\ of\ metal\ ions} \times 100 \qquad (18)$$

The heavy metal solution of concentration 10 mg/L and volume 50 mL was made to contact with 25 mg Melanin impregnated activated carbon keeping all parameters set for maximum adsorption. The Melanin impregnated activated carbon was centrifuged and added to 10 mL solution of different desorbing agents in an Erlenmeyer flask maintained at 100 rpm, 30°C for 3 hrs. The desorbing agents of the study were 0.5N HCl, 2N HCl, 5 N HCl, 1N citric acid and 1N acetic acid. After efficient desorption of heavy metals from Melanin impregnated activated carbon, the adsorption-desorption process was repeated for 4 cycles to understand its reusability.

4. RESULTS AND DISCUSSION

4.1. Characterisation of Melanin

The biologically synthesised Melanin is subjected to different characterisation techniques such as SEM, TEM, FTIR, TGA, DSC, particles size analysis, zeta potential analysis, XRD and BET analysis to analyse its properties and assess its potential as an adsorbent.

4.1.1. Particle size and electron microscopy study

Figure 4.1 shows the particle size distribution of Melanin. Melanin showed a mean particle size of 32 ± 0.98 nm giving a very low polydispersity index. Fig. 4.2 (a) shows the SEM image, and Fig. 4.2 (b) and (c) shows the TEM images of biosynthesised Melanin at 10 nm and 0.2 microns, respectively. The Melanin appeared as spherical particles in the TEM images at different magnifications while the SEM images manifested it as an agglomeration of small spherical particles confirming Melanin to be nanosized, spherical particles.

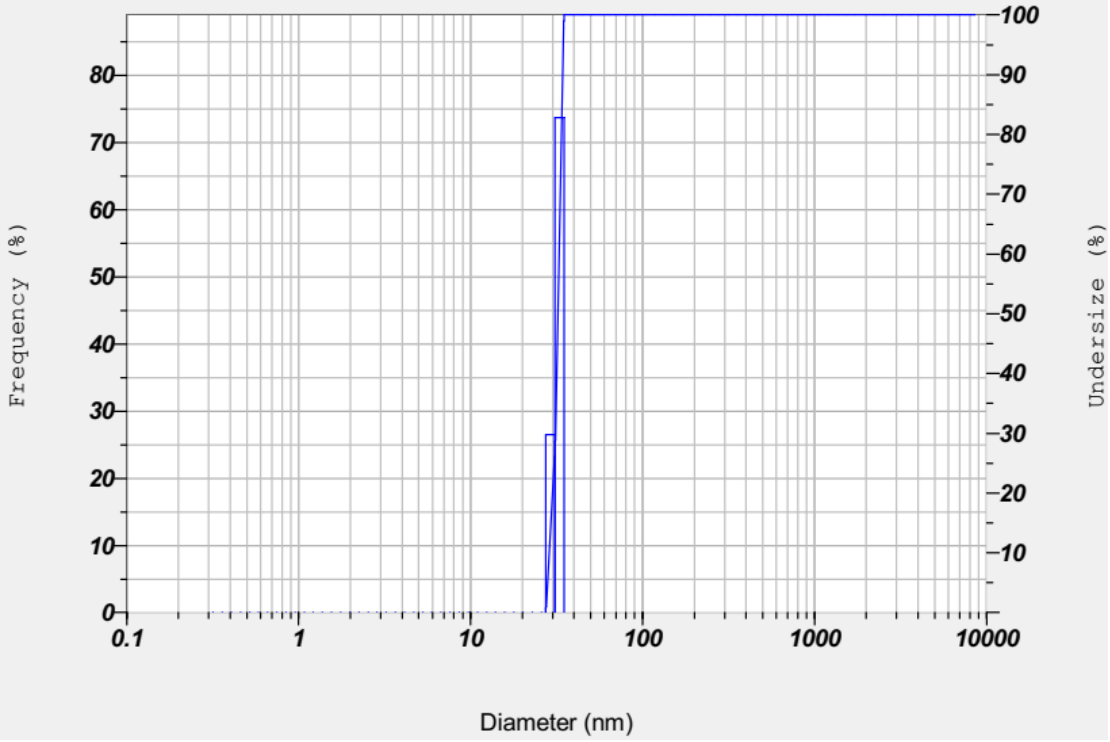

Figure 4.1. The particle size distribution of biosynthesised Melanin

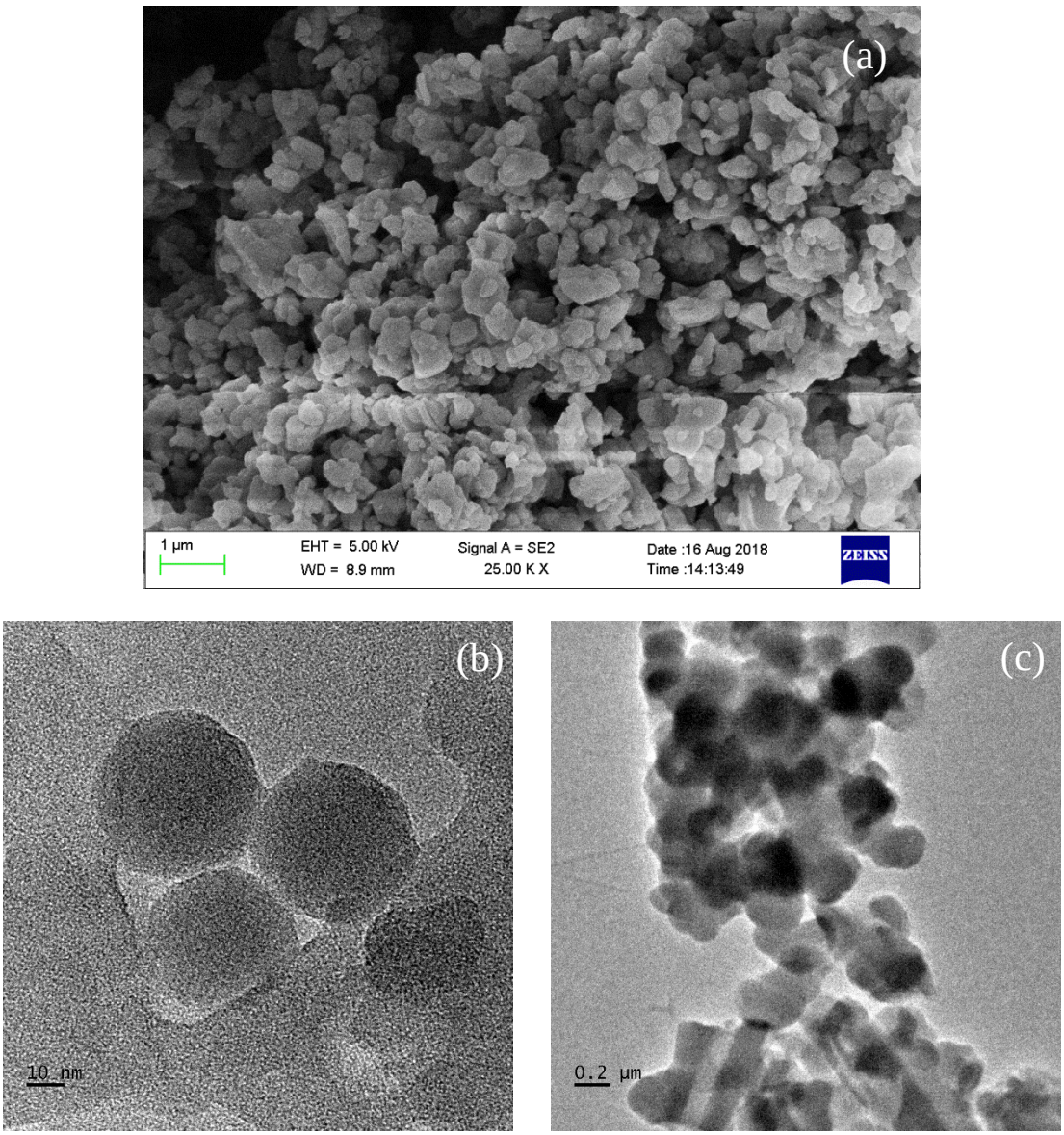

Figure 4.2. (a) SEM image of biosynthesised Melanin at a magnification of 1µm and TEM images of Melanin (b) at 10 nm and (c) at 0.2 microns.

4.1.2. Fourier-Transform Infrared Spectroscopy (FT-IR) Analysis

Fourier-transform infrared spectroscopy was used to detect the vibrational characteristics of the functional groups present in Melanin to which the heavy metals are likely to bind. FTIR spectra of biosynthesised Melanin is shown in Fig. 4.3. Significant peaks of biosynthesised Melanin at around 3100-3500 cm^{-1} are mainly due to the stretching vibration of carboxylic/phenolic –OH group and –NH stretching. A sharp peak at 2977 cm^{-1} and a small peak at around 2882 cm^{-1} can be attributed to

phenolic/carboxylic –C-H stretching vibrations. Peaks at around 1720-1700 cm^{-1} indicate –C=O stretching of the carboxylic group. The peaks around 1240-1200 cm^{-1} indicate –C-N/ –C-O stretching and –C-O-H asymmetric stretching of carboxylic groups.

The peak at around 1641.91 cm^{-1} was due to aromatic –C=C- stretching, $-COO^-$ asymmetric stretching and –C=O of quinone group. Peaks at 1443.17 cm^{-1}, 1568.28 cm^{-1}, 1524 cm^{-1} correspond to the aromatic ring and C-H bonds in Melanin. The peak at 1304 cm^{-1} is attributed to –C-O-H bending vibration (Silverstein and Bassler 1962).

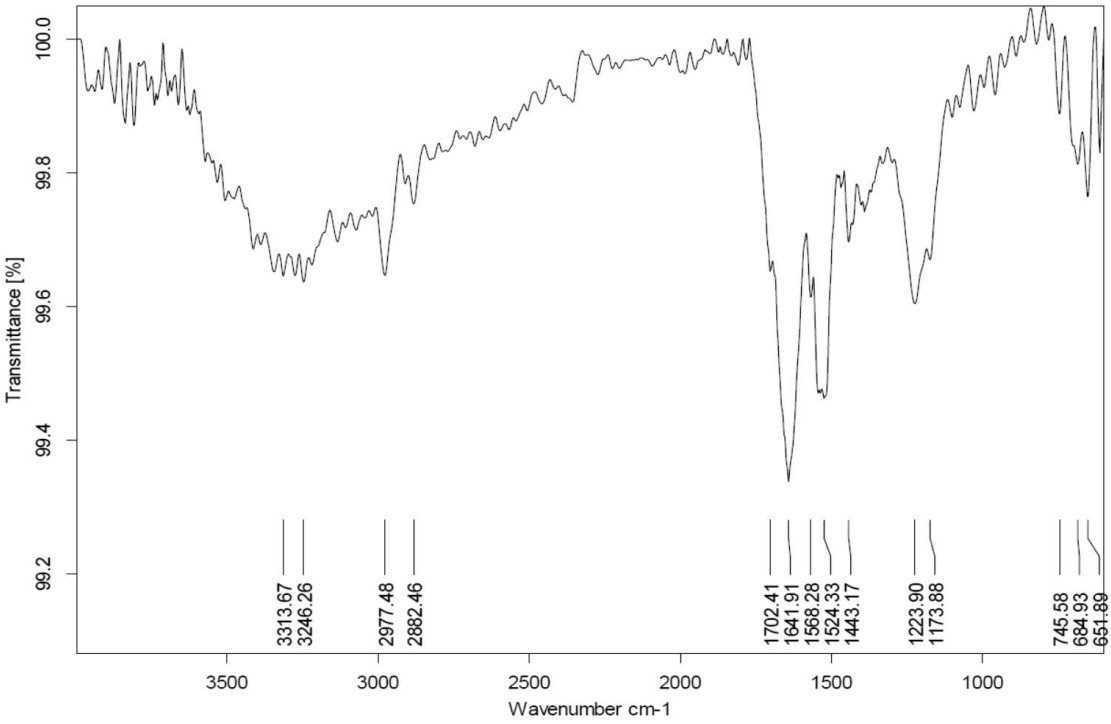

Figure 4.3. FT-IR spectra of Melanin Produced by Pseudomonas stutzeri

4.1.3. Zeta potential study

The surface electric charge developed in Melanin at different pH is determined by conducting zeta (ζ) potential measurement of Melanin maintained at fixed pH conditions (Fig. 4.4). The average surface charge of a molecule is a function of charges possessed by entire functional groups present in a molecule. It indicates the surface negativity of melanin which favours the cationic adsorption (Pathirana et al. 2019). Melanin has four major functional groups out of which three of them namely -COOH, -CO and -OH develops a negative charge while the -NH group will express a positive

charge in an aqueous medium. At pH 4, Melanin will have an overall surface charge of -45.3 mV, which is the highest negative charge Melanin can acquire, and at this pH, maximum cations bind to Melanin. The negative zeta potential showed a decreasing trend in either direction of the pH scale and got a maximum positive surface charge of +6.12 mV at pH 1.

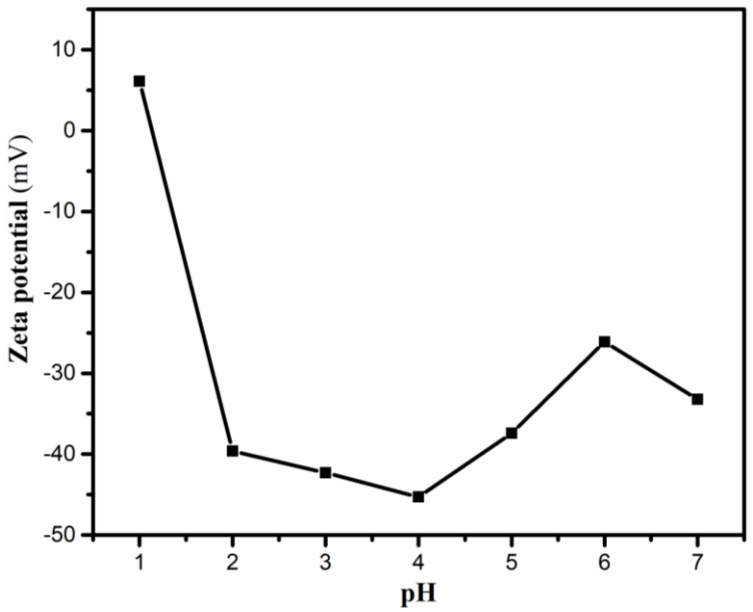

Figure 4.4. Zeta potential of Melanin at different pH without background electrolyte

Binding of heavy metals to Melanin is not only dependent on the charge of Melanin at different pH but also on the speciation of heavy metals at different pH which will be discussed in the section on the effect of pH on adsorption. An inert electrolyte is sometimes added before zeta potential measurement to maintain constant ionic strength as well as to nullify the effect of ligand complexity due to various ions present in groundwater. To understand the impact of counter ions on the zeta potential of melanin background electrolyte was not added in this study (Erdemoğlu and Sarıkaya 2006).

4.1.4. BET surface area analysis.

The Brunauer-Emmett-Teller surface area and pore diameter were analysed at 77.4 K temperature and 1 bar pressure by measuring the nitrogen gas adsorption and desorption (Fig. 4.5). BET is of at most relevance as far as an adsorbent is concerned since the sorptive process are a function of surface area (Castro et al. 2018). The

average surface area is found to be 26.455 m²/g, the average pore volume is 0.061 cc/g, and the pore diameter is 3.657 nm.

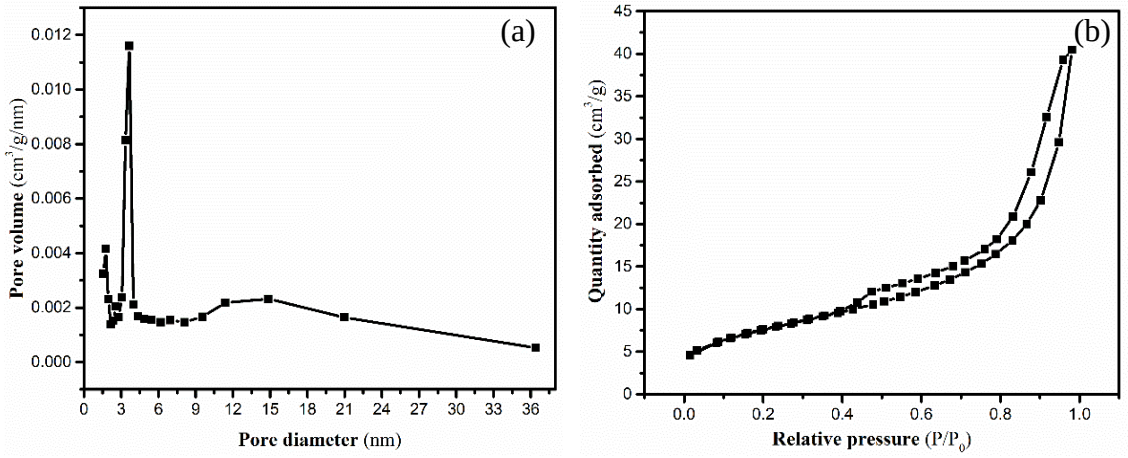

Figure 4.5. (a) BET (b) Pore size distribution

4.1.5. Thermo-gravimetric analysis and differential scanning calorimetry

The thermo-gravimetric analysis and differential scanning calorimetry were conducted to find the thermal stability of biosynthesised Melanin at increasing temperatures till 400 ºC (Fig. 4.6 (a) and (b)). TGA and DSC analysis have shown an endothermic peak and absorbance of latent heat at around 120°C, which indicates that weight loss is due to the moisture removal from Melanin till 120°C. It also showed that Melanin is completely stable till 160°C until which there is no degradation of Melanin due to thermal gradience. Degradation of Melanin started from 260°C and got exhausted by 375°C.

4.1.6. Scanning electron microscopy of functionalized Melanin

The SEM images depict the surface morphology of Melanin before and after functionalization (Fig. 4.7). Melanin seems to be spherically shaped with even surface morphology. The heat treated and $KMnO_4$ treated Melanin have fine granular particles on the surface. These granular particles are oxides of iron and copper what got impregnated to Melanin by functionalization of Melanin to which arsenic groups are adsorbed.

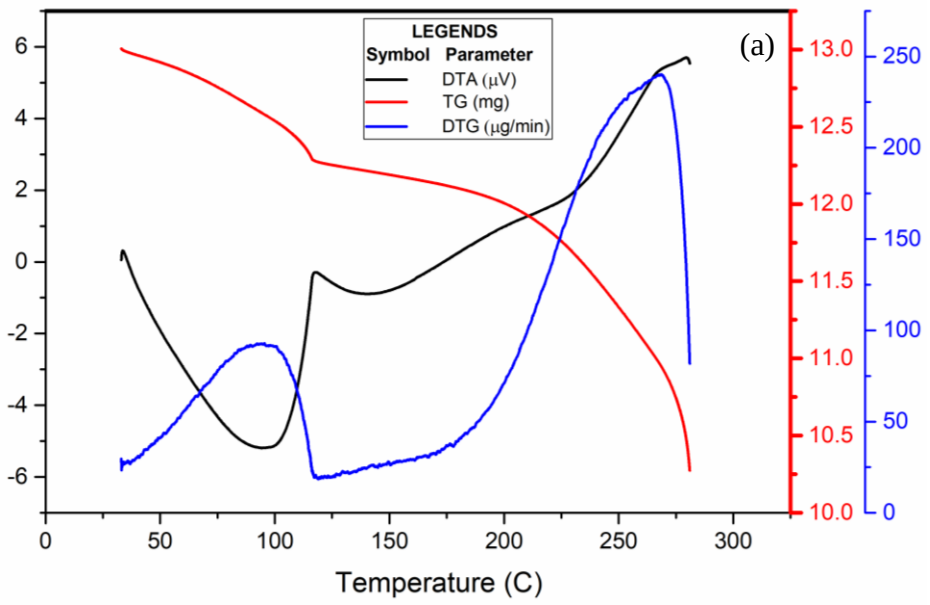

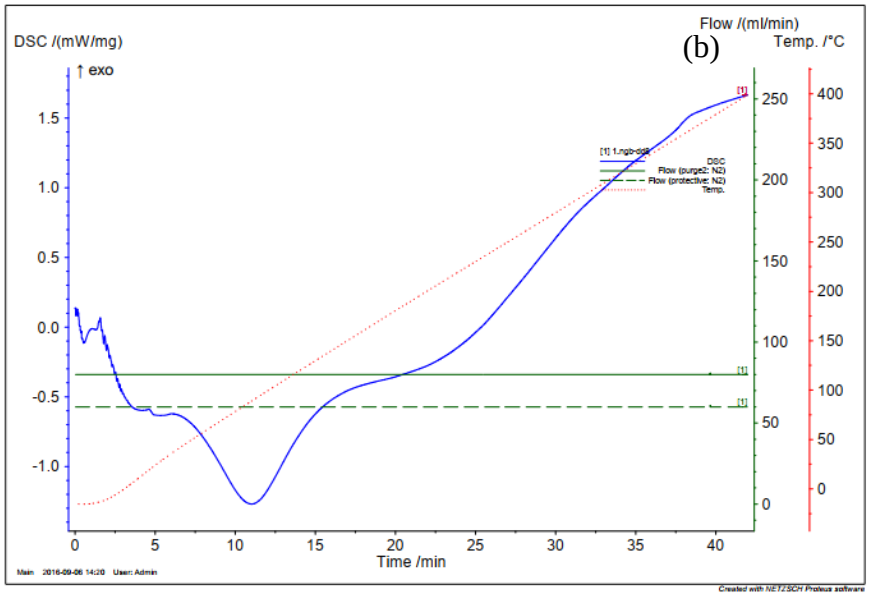

Figure 4.6. (a) TGA and (b) DSC of biosynthesised Melanin

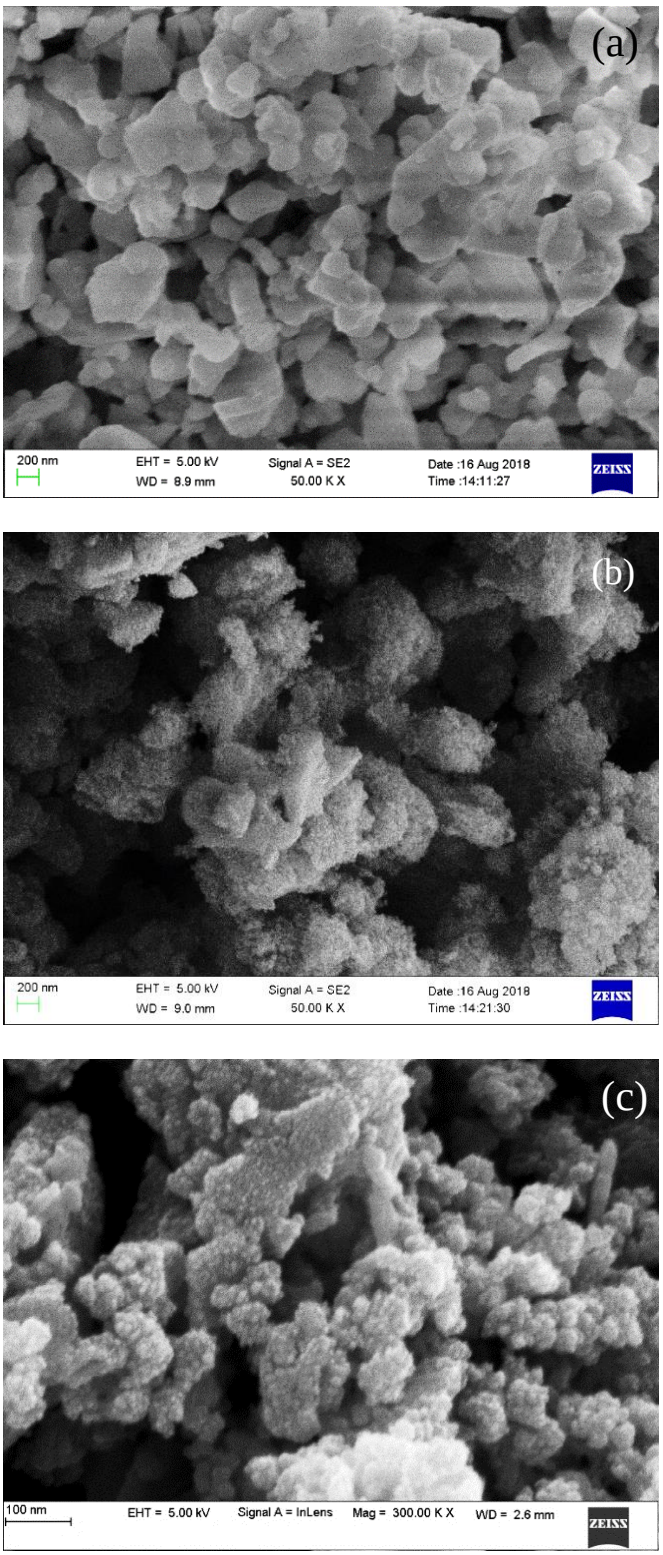

Figure 4.7 (a) SEM image of Melanin at 200nm magnification (b) iron bound Melanin after heat treatment (c) copper bound Melanin after $KMnO_4$ treatment.

4.1.7. Fourier transform infrared spectroscopy of functionalized Melanin

In the case of Fe-Melanin, the functional groups on binding with iron ions showed different vibrational and structural characteristics compared to pure Melanin. As shown in Figure 4.8, the transmittance intensity of Melanin has increased after functionalization with iron. The peak of Melanin at 656.01 cm^{-1} is the characteristic of C-H bend which got shifted down to 632.69 cm^{-1} after iron adsorption and heat treatment. Similar kind of vibrational stretching is seen for Melanin at 687 cm^{-1}, which is a characteristic of N-H wag. The =C-H bond at 774.69 cm^{-1} also had vibrational change as well as intensity increase. The C-C stretch corresponding to 1414.71 cm^{-1}, N-H bend indicated at 1614.47 cm^{-1}, C=O stretch observed at 1707.24 cm^{-1} and -OH group at 323.48 cm^{-1} showed a shift in wavenumbers with a significant increase in transmittance intensity.

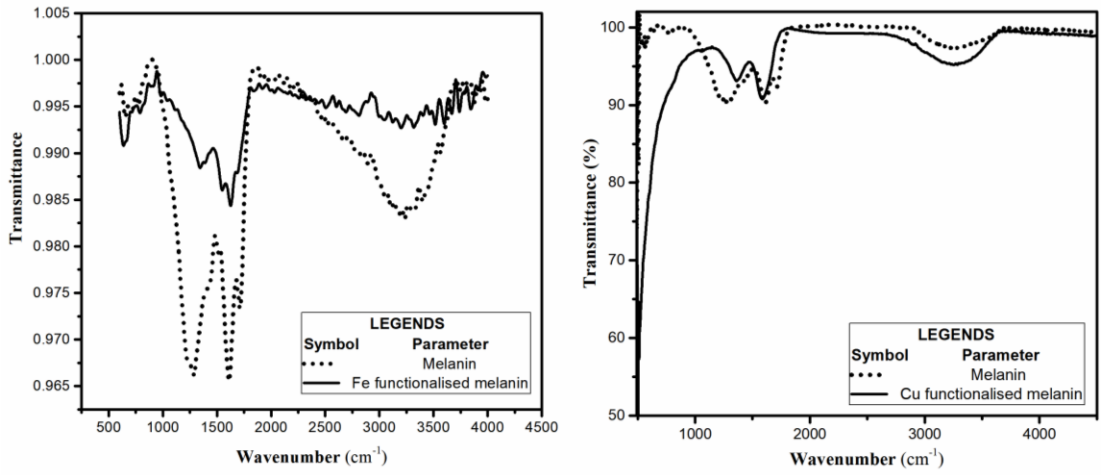

Figure 4.8. FTIR spectra of Melanin with iron functionalized Melanin and copper functionalized Melanin.

The FTIR spectrum analysis of copper functionalised Melanin showed that, unlike iron functionalized Melanin, transmittance peak of Cu-Melanin did not shift to downward wavenumbers. The transmittance intensity increased after copper treatment. The transmittance at 1288.22 cm^{-1} which is the characteristic of C-O stretching of alcohol, carboxylic acid and carbonyl groups, 1607.38 cm^{-1} which denoted N-H bend of amine group present in Melanin, 3265.86 cm^{-1} which is the characteristic of -OH groups of alcohols and carboxylic acids respectively, showed an increase in intensity of transmittance after adsorption, confirming the adsorption of copper to the functional

groups (Pongpiachan 2014; Silverstein and Bassler 1962). The peak corresponding to the wavenumber 500.1 cm^{-1} indicates the existence of copper in the form of cupric oxide (CuO) (McDevitt and Baun 1964) and hence confirms the impregnation of copper to melanin.

4.1.8. XRD analysis

The powder X-ray Diffraction pattern of melanin, iron functionalised melanin and copper functionalised melanin are shown in Fig. 4.9. The change in phase of melanin on iron and copper treatment were studied and found that melanin has an amorphous state.

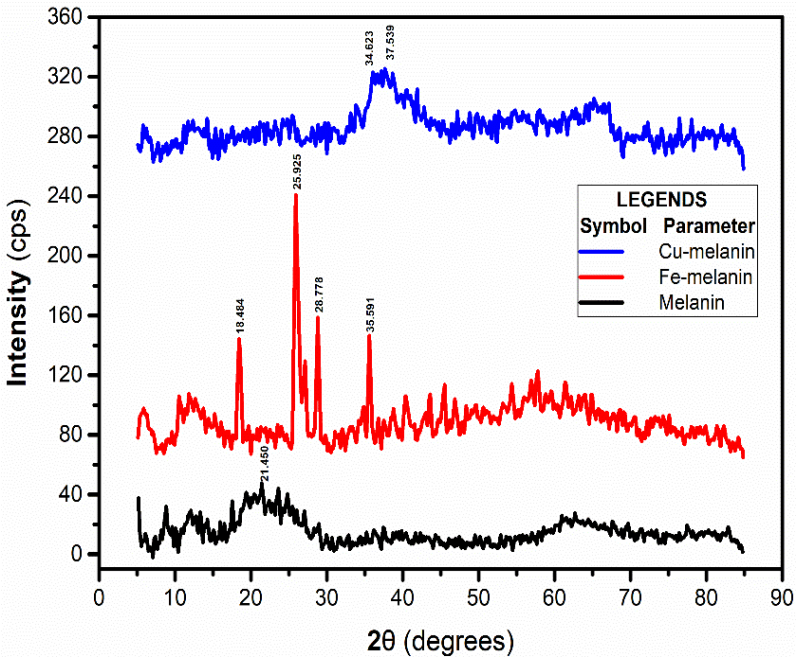

Figure 4.9. Powder XRD pattern of melanin, Fe-melanin and Cu-melanin

The 2θ values in Fe-melanin such as 16.484°, 25.925°, 28.778° and 35.591° indicate that iron is impregnated in melanin as Fe_2O_3 (Demirezen et al. 2019; Khatamian et al. 2017; Maji et al. 2018). The 2θ peaks shown by copper functionalised melanin at 34.623°, 37.539° confirms the formation of CuO nanoparticles and its impregnation onto melanin (Martinson and Reddy 2009).

4.2. Adsorption studies on the removal of heavy metals using Melanin

4.2.1. Effect of pH and the mechanism of adsorption of heavy metals to Melanin

The effect of pH on heavy metal uptake was scrutinised in the range of 1.0 to 7.0 (Fig. 4.10 and 4.11). The study was limited to pH 7 since Melanin starts to dissolve at the alkaline environment above pH 7.5. The surface of Melanin contains functional groups such as -COOH, -CO, -OH and NH, and the mechanism of adsorption is the chelation of metal ions to these functional groups at certain pH. The surface charge of adsorbent, the degree of ionisation and speciation of the metal ions are affected by the pH of the solution (Zhang et al. 2015). The functional groups develop charges based on the solution pH, which makes a physical or chemical interaction with the heavy metals and thereby forms a physical or chemical bond with it (Raouf and Raheim, 2017). Adsorption of heavy metals using Melanin depends mainly on the ionic state, the type of functional groups and the metal ion chemistry in solution. The hydronium (H_3O^+) ions present at acidic pH protonate the functional groups in Melanin. At pH above 4, the concentration of hydronium ions decreases, resulting in negatively charged functional groups of Melanin, to which the Pb (II), Hg (II) and Cu (II) can bind. As the pH increases further, the negative charge will decrease, leading to the decrease of metal ion binding (Hadi et al. 2015). Effect of pH on Pb (II) adsorption study was limited to pH 5 because Pb (II) precipitates to form sparingly stable or highly stable compounds such as $Pb(OH)^+$ above pH 5.5 (Bradl 2004) (Speciation chart of Pb, Hg, Cr, Cu and As are shown in Appendix Fig. 1, 2, 3, 4 and 5).

Mercuric ions exist majorly as $HgOH^+$ above pH 4 and will bind to the negatively charged functional groups of Melanin. The dominant form of Hg (II) in solution is Hg^{2+} at pH lower than 4, and the functional groups in Melanin develop a positive charge at that pH range, and hence adsorption of mercuric ions to Melanin may not be possible. Thus, efficient adsorption of Hg (II) occurs between pH 4 to 6. Considerable binding of Hg (II) to Melanin is seen until neutral pH (Arias et al. 2017; Li et al. 2017; Zhang et al. 2018).

Cr (VI) exist in different ionic forms in the aqueous solution such as CrO_4^{2-}, $HCrO_4^-$ or $Cr_2O_7^{2-}$ and stability of these forms depends mainly on the pH of the solution. Between the pH range of 2 to 6, Cr (VI) exist in the form of $HCrO_4^-$ and $Cr_2O_7^{2-}$ ions

and as pH increases, the predominant form shifts to chromate ion (CrO_4^{2-}) (Baral et al., 2006; Gupta et al., 2010; Yang et al., 2015). From Fig. 4.10, it is clear that the uptake of Cr (VI) was more at pH 3.0. Lowering the pH leads to protonation of Melanin functional groups to a greater extent and thus the negatively charged (chromate/dichromate) ions in the solution bound to the positively charged functional groups on the surface of Melanin. Further, an increase in the pH above 3.0 decreased Cr (VI) adsorption due to the decreasing net positive surface potential of the Melanin. This incited the repulsion of negatively charged Cr (VI) group and COO^- group of Melanin. However, a decreasing trend in adsorption was observed at pH less than 2.0 because below pH 2; Cr (VI) predominantly exists as H_2CrO_4 (Karthikeyan et al. 2005). For a low pH value, the amino group in solution will get protonated to which the negatively charged chromate group can develop an electrostatic interaction (Vold et al. 2003). As the pH increases, the positive charge of the amino group decreases. The lone pair of electrons on the nitrogen of the amino group chelates with the metal ions such as Cu (II), Pb (II) and Hg (II) is forming a chelate complex bond between them (Mende et al. 2016). Above pH 6.0, the decrease in metal uptake may be due to the competition between the hydroxyl ions and Cr (VI) ions (Yang et al. 2015; Zhang et al. 2015). However, other mechanisms like physical adsorption have led to the maximum uptake of Cr (VI) around 88% at lower pHs (Acharya et al. 2009).

Adsorption of any metal ion on adsorbent depends on its atomic radius, electronegativity and ionisation energy. Lead and copper have higher electronegativity and lower ionisation energies to form ions, thus readily binding to the functional groups in Melanin. Higher the electronegativity, stronger will be the interaction to the active sites (Allen and Brown 1995). Even though mercury has high electronegativity and atomic radius compared to chromium and copper, high ionisation energy might be the reason for less mercuric adsorption on to Melanin. The atomic radii, electronegativity and ionisation of different metals of study are catalogued in Appendix Table 1.

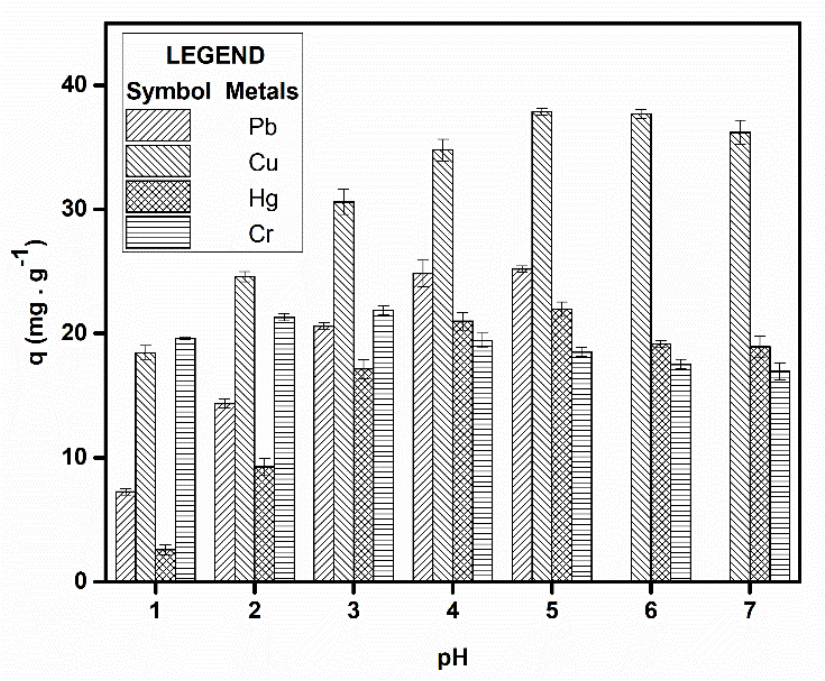

Figure 4.10. Effect of pH on heavy metal uptake (C_i = 10 mg/L, W = 0.2 g/L, rpm= 200, shaking diameter = 25 mm)

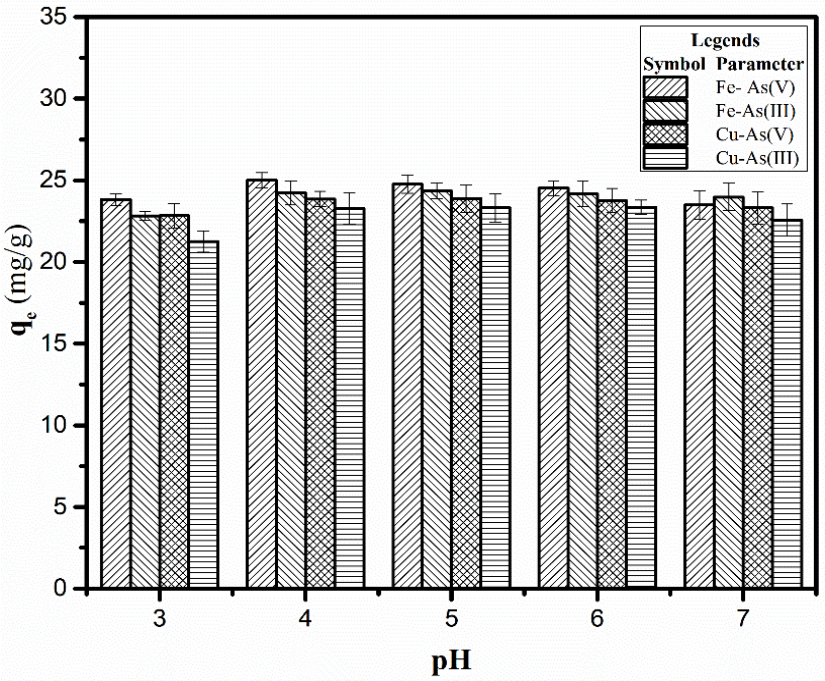

Figure 4.11. Effect of pH on heavy metal uptake (C_i = 10 mg/L, Fe-Melanin = 0.8 g/L, Cu-Melanin= 2 g/L, rpm = 200, shaking diameter = 25 mm)

The pH studies of adsorption of As (V) and As (III) on Fe-Melanin as well as Cu-Melanin showed that maximum adsorption took place in the pH range of 3 to 6 (Fig.

4.11). To be precise, pH 4 showed the maximum amount of adsorption of arsenic species in the case of Fe-Melanin. More than 99% of both As (III) and As (V) was removed from 10 mg/L individual solutions of As (III) and As (V) using 20 mg Fe-Melanin at pH 4 and 50 mg Cu-Melanin at pH range of 4 to 6. Cu-Melanin showed almost the same adsorption capacity at a pH range of 4 to 6. Iron oxide in the aqueous medium will possess a hydroxyl group on its surface (≡FeOH). At lower pH, the iron oxide bound on the surface of Melanin will get protonated ($\equiv FeOH_2^+$) to develop a surface positive charge to which the negatively charged arsenic groups can bind. From pH 5.5 to 9, the iron oxide acquires a neutral charge due to an equal number of positively charged protons and negative charge of hydroxyl groups and that is called a point of zero charge (Liu et al. 2001). As (V) exists predominantly as $H_2AsO_4^-$ in the pH range of 3 to 5 and $HAsO_4^{2-}$ in the range of 5 to 11 (Babaee et al. 2018) and below pH 3, As (V) exists as H_3AsO_4. At pH 4, the attraction between negatively charged arsenic species and positively charged iron oxide present in Melanin will have maximum electrostatic attraction leading to the maximum adsorptive removal of arsenic (Cornell and Schwertmann 1996). In the case of copper treated Melanin, literature has indicated that the point of zero charges for copper oxide is in the basic region. As found by Guedes et al., the point of zero charges for copper oxide is at 7.9 while the maximum positive charge is attained at 4, and after 5.7 it started approaching to the point of zero charge. Arsenic species in the anionic state gets adsorbed to the copper oxide bound to Melanin at pH range of 4 to yield maximum adsorption, and till pH 6, it showed a considerable amount of adsorption (Lenoble et al. 2005).

Arsenic sustains, in its pentavalent ionic state at oxic conditions while the ionic trivalent state of arsenic can be derived only after pH 9 (Xiong et al. 2017). Arsenic exists in the trivalent form in the groundwater which is more toxic and difficult to be removed due to its non-ionisation at neutral pH. The arsenite is hence oxidised to arsenate and adsorbed by iron impregnated in Melanin (Ouma et al. 2018; Ramos Guivar et al. 2018). The iron in the ferric state has catalysed the oxidation of arsenite to form arsenate in the presence of oxygen and acidic condition by Fenton reaction. Majority of the arsenic is then bound to iron in pentavalent state while a little part of As (III) can bind to ferric hydroxide at below neutral pH through weak forces of

interaction (Giles et al. 2011; Ociński et al. 2014) Similarly, copper also have the property of catalysing the oxidation of trivalent form of arsenic to pentavalent form in presence of oxygen and pentavalent forms along with small quantities of trivalent form of arsenic may bind to the Cu-Melanin (Prasad et al. 2011). The impregnated copper and iron start to dissolve in solution from pH 3, and hence the study was not performed at pH lower than 3. (Goswami et al. 2012; Pillewan et al. 2014).

Metal adsorption is dependent on pH because different metals exhibit different ionisation equilibria at different pH. This affects the adsorption of each heavy metal on any given adsorbent. All adsorbents adsorb metals with different efficiency at different pH. Therefore, the adsorbent dose requirement varies to compensate for reduced efficacy. The physisorption is very much sensitive to the pH of the solution and therefore, adsorbents based on physical adsorption are required in large quantities. Melanin selectively adsorbs cations because of ionic charge interaction. Therefore, it can adsorb the metal ions at lower concentrations. Melanin requirement is also less since it adsorbs heavy metals by chemical interactions and it adsorbs metal ions even at neutral pH with good efficiency, however, with a longer equilibrium time (Saini and Melo 2013). Mass transfer limitations could be the reason behind longer time requirements because the experiments were performed at very low initial concentrations par with the groundwater heavy metal concentration.

4.2.2. Effect of contact time on adsorption

Adsorbent - Adsorbate contact time required for the effective binding of metal ions to the functional groups present in Melanin is a crucial factor in the case of adsorption experiments, and the results are shown in Fig. 4.12 and 4.13. Equilibrium state was attained within 90 minutes of contact time for all metals. As the figures depict, the entire adsorption process can be defined by two phases. The first phase corresponds to an initial fast uptake phase, which was mainly due to the high concentration gradient and availability of more binding sites on melanin which subsequently reached equilibrium in the second phase mainly due to the decline of the concentration gradient and active metal binding sites deficit (Saini and Melo 2013)

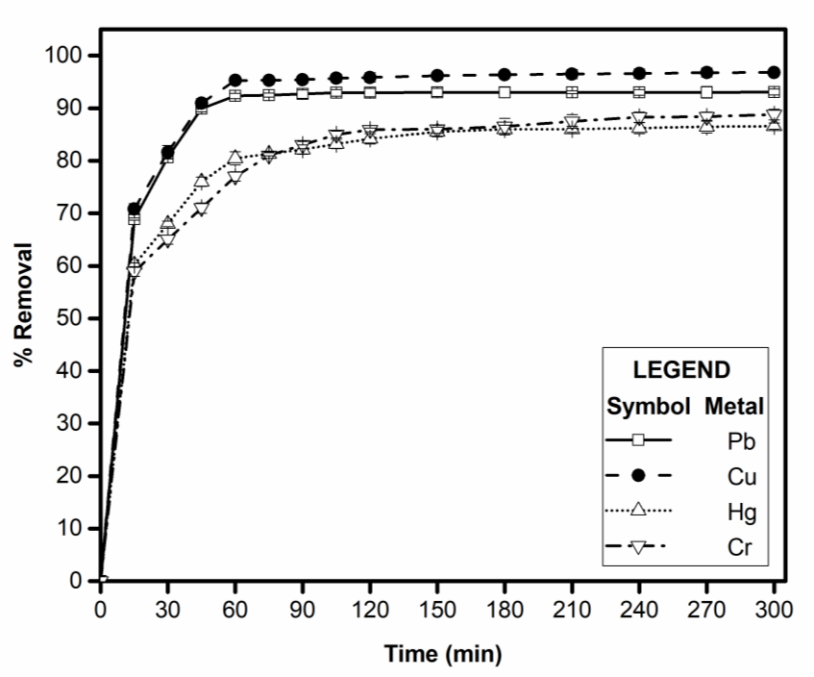

Figure 4.12. Effect of contact time on heavy metal uptake (C_i = 10 mg/L, W = 0.2 g/L, rpm = 200, shaking diameter = 25 mm)

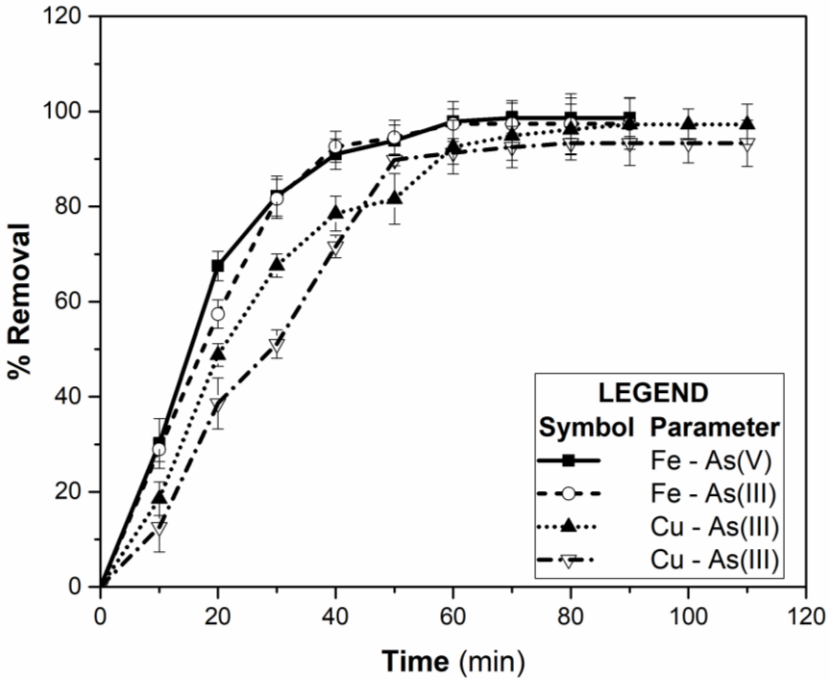

Figure 4.13. Effect of contact time on heavy metal uptake (C_i = 10 mg/L, Fe-Melanin = 0.8 g/L, Cu-Melanin= 2 g/L, rpm = 200, shaking diameter = 25 mm)

In the case of Hg (II), Pb (II), Cr (VI) and Cu (II), maximum binding of heavy metals happened within the first 15 minutes and next 75 minutes showed relatively uniform adsorption. Higher initial metal uptake capacity of Melanin suggests the potential for efficient heavy metal removal. Equilibrium was attained within 50 minutes from the start of the experiment in the case of Fe-Melanin to remove As (III) and As (V) while it took 30 minutes more for Cu-Melanin to attain equilibrium. To understand the kinetic mechanism of adsorption, Lagergren's pseudo-first order, pseudo-second order, and intraparticle diffusion models were modelled.

4.2.3. Kinetic Modelling of adsorption on Melanin

Majority of the controlling mechanism of an adsorption process is investigated using the intra-particle diffusion model, Lagergren's pseudo-first-order and Lagergren's pseudo-second-order kinetic model.

4.2.3.1. Intra-particle diffusion model

The kinetic data were further analysed to understand the diffusion mechanism by an intraparticle diffusion model. According to the Weber and Morris model, the adsorption process is restrained by intra-particle diffusion if the plot of q_t versus $t^{0.5}$ is a straight line and the adsorption process is controlled by two or more steps if there are multiple linear plots (Doke and Khan 2017).

The plot of q_t versus $t^{0.5}$ (Figure 4.14 and 4.15) for Hg (II), Pb (II), Cu (II), Cr (VI), As (III) and As (V) adsorption on biosynthesised, copper and iron functionalized Melanin demonstrated multi-linear plots suggesting that the intra-particle diffusion may not be the only rate-limiting step. As seen in the figures, the adsorption of all heavy metals comprises of two phases. The first phase indicates that mass transfer resistance is limited to the initial stages of adsorption. In the initial stage, the adsorption happens by the boundary layer diffusion of metal ions from the bulk solution onto the external surface of Melanin, whereas the later stages of adsorption are due to the intra-particle diffusion of the metal ions (Fierro et al. 2008).

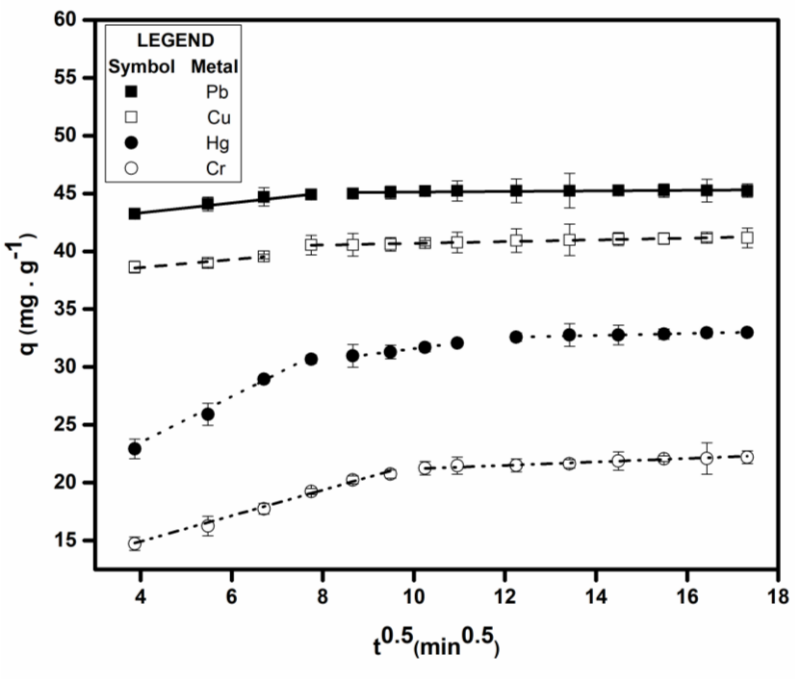

Figure 4.14. Intra-particle diffusion model (Ci = 10 mg/L, W = 0.2 g/L, rpm= 200, shaking diameter = 25 mm)

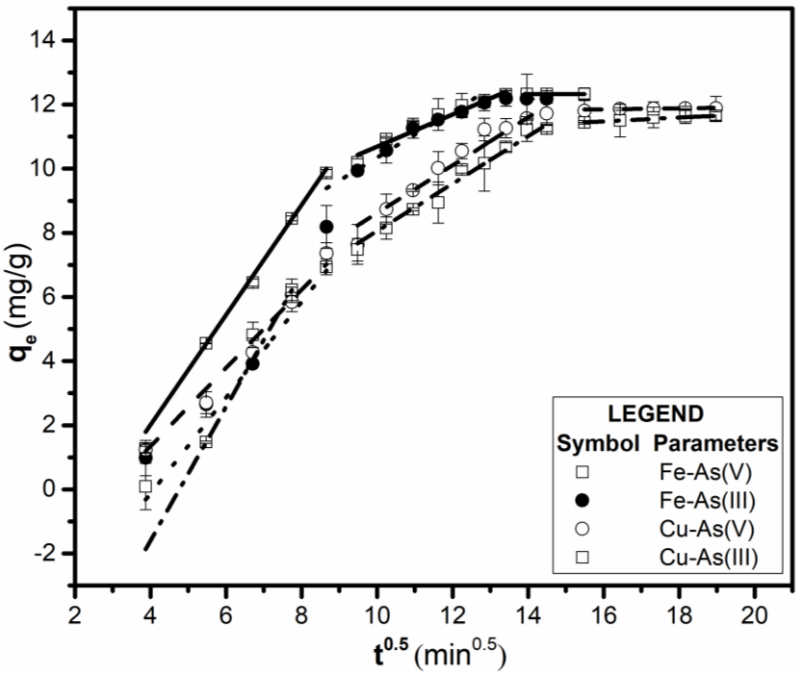

Figure 4.15. Intra-particle diffusion model (C_i = 10 mg/L, Fe-Melanin = 0.8 g/L, Cu-Melanin= 2 g/L, rpm = 200, shaking diameter = 25 mm)

Since the straight line of the second phase of adsorption was not passing through the origin, intra-particle diffusion may not be the only rate-limiting step. Therefore, the adsorption data were further analysed using Lagergren's pseudo-first-order and pseudo-second-order kinetic models to evaluate the rate-limiting step (Aly et al. 2014).

4.2.3.2. Lagergren's pseudo-first-order and pseudo-second-order kinetic models

To examine the mechanism of sorption and the rate-limiting steps, the kinetic data of metal ion removal were modelled with the Lagergren's pseudo-first and second-order kinetic models. The coefficient of determination was adopted from the experimental data fitted by linear regression analysis in the respective models (Matouq et al. 2015). The parameters of Lagergren's pseudo-first-order and second-order kinetic models are listed in Table 8. The validity of each kinetic models was predicted by comparing the results, and it is evident that the experimental data of heavy metal adsorption on the biosynthesised Melanin fitted well with the Lagergren's pseudo-second-order kinetic model (Figure. 4.18 and 4.19). The coefficient of correlation was found to be higher for the pseudo-second-order kinetic model than the pseudo-first-order kinetic model, and the theoretically calculated q_e values of the pseudo-second-order model are comparable to the experimental data. Thus, validating the assumption that the adsorption of Hg (II), Pb (II), Cr (VI) and Cu (II) on Melanin, As (III) and As (V) to functionalised Melanin, is chemical adsorption by exchange or sharing of valence electrons between adsorbent and adsorbate.

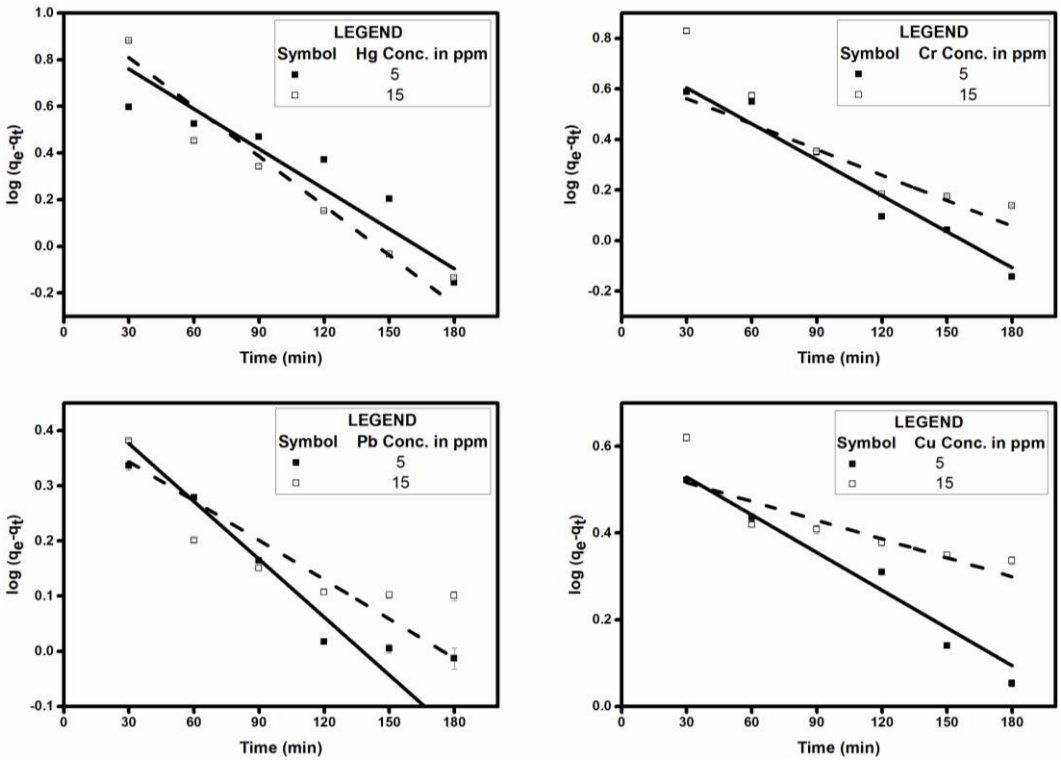

Figure 4.16. Lagergren's Pseudo-first-order kinetic model (w = 0.2 g/L, rpm = 200, shaking diameter = 25 mm)

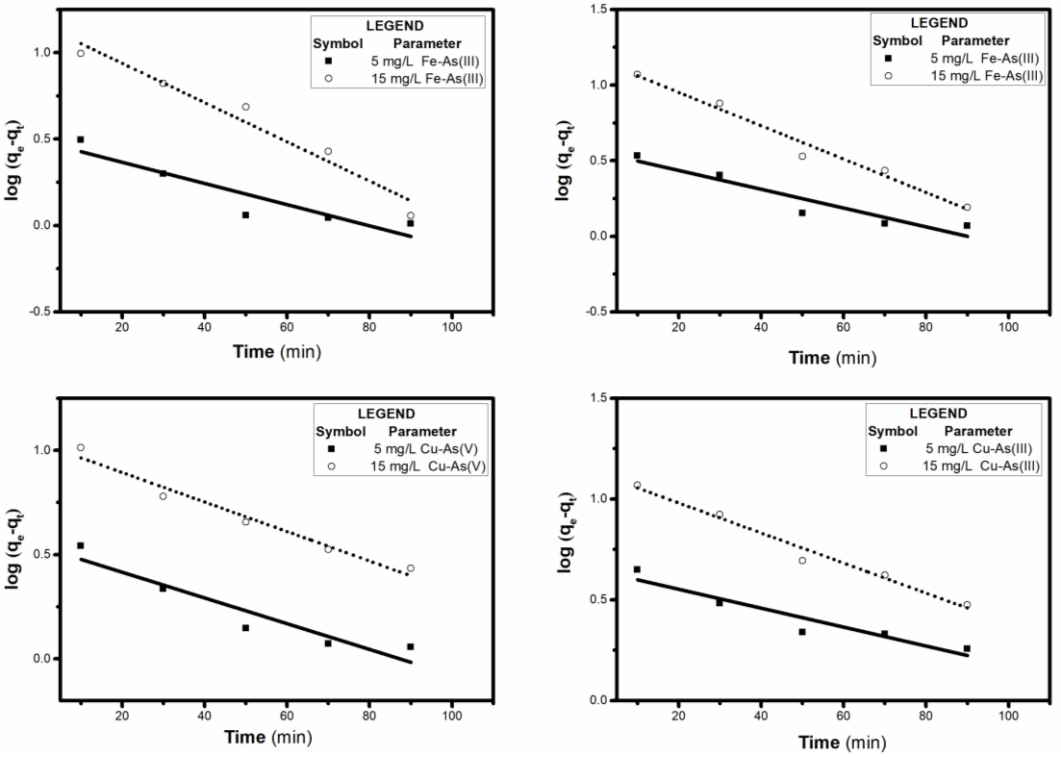

Figure 4.17. Lagergren's Pseudo-first-order kinetic model (Fe-Melanin = 0.8 g/L, Cu-Melanin= 2g/L, rpm = 200, shaking diameter = 25 mm)

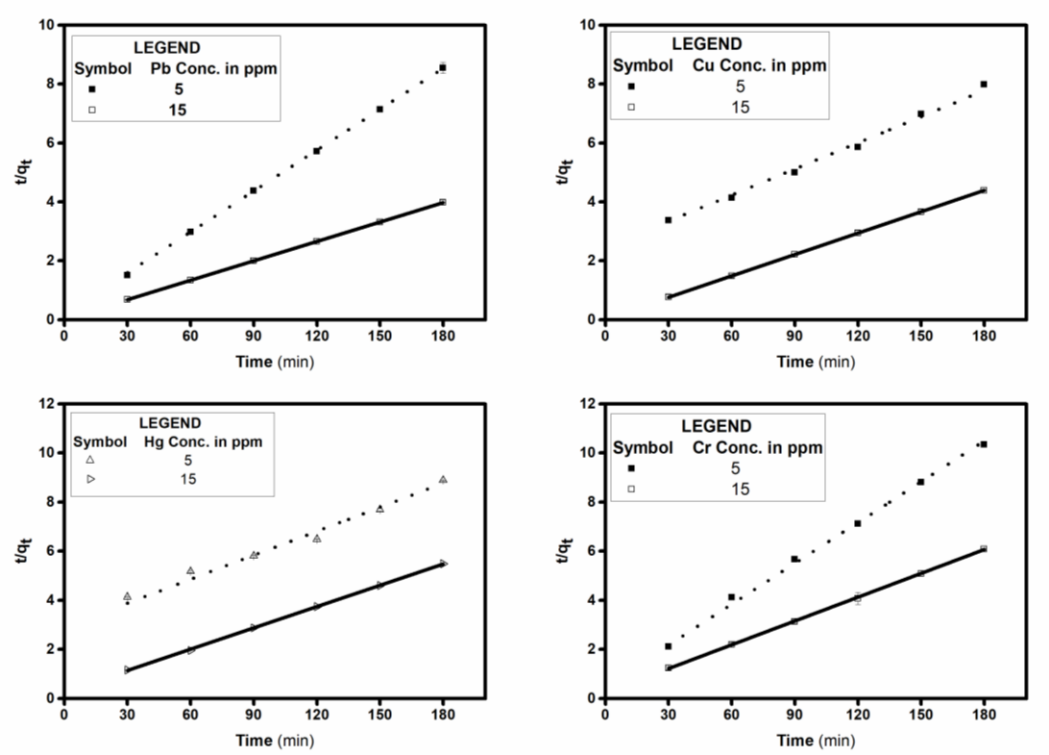

Figure 4.18. Lagergren's Pseudo-second-order kinetic model for heavy metals adsorption (w = 0.2 g/L, rpm = 200, shaking diameter= 25 mm)

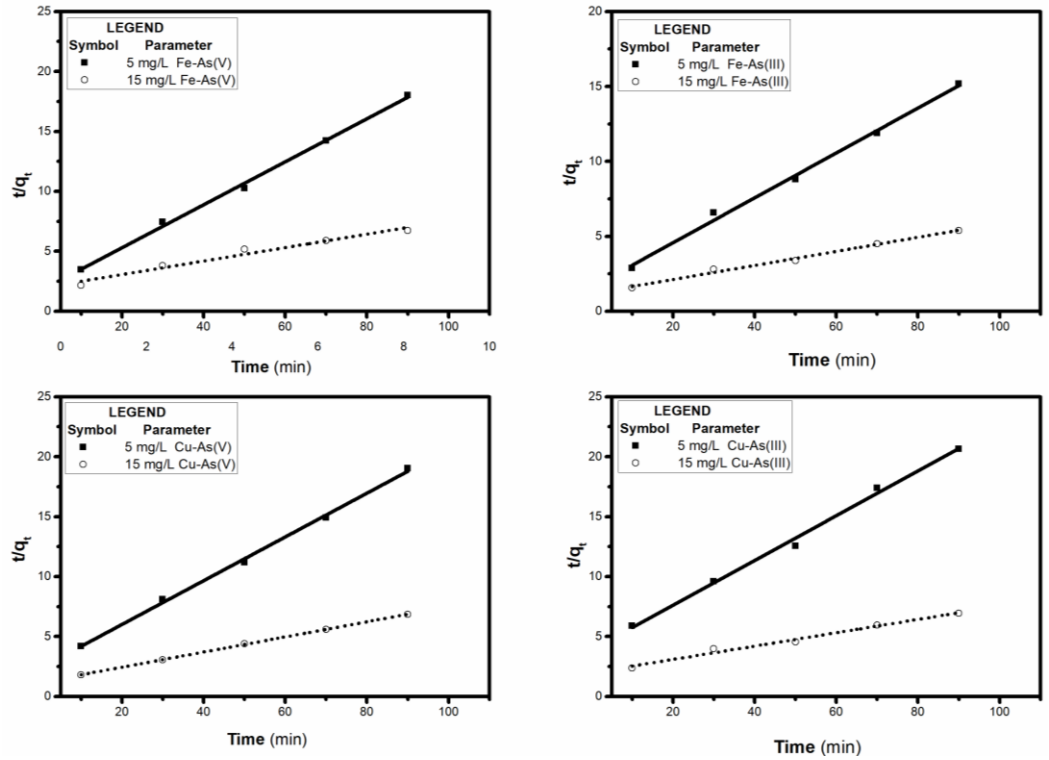

Figure 4.19. Lagergren's Pseudo-second-order kinetic model (Fe-Melanin = 0.8 g/L, Cu-Melanin= 2 g/L, rpm = 200, shaking diameter = 25 mm)

Table 8: Adsorption kinetic parameters of heavy metal adsorption on Melanin

Heavy metal and concentration	**Experimental $q_{e,exp}$ (mg/g)**	**Pseudo-first-order kinetic model**			**Pseudo-second-order kinetic model**		
		k_1 (min^{-1})	**$q_{e,cal}$ (mg/g)**	**R^2**	**k_2 (g/mg· min)**	**$q_{e,cal}$ (mg/g)**	**R^2**
Pb 5 mg/L	21.05	0.018	3.69	0.95	64.7×10^{-05}	21.61	0.99
Pb 15 mg/L	45.24	0.017	5.75	0.81	31.7×10^{-05}	45.54	0.99
Cu 5 mg/L	22.45	0.018	4.48	0.96	35.6×10^{-05}	33.83	0.99
Cu 15 mg/L	40.99	0.032	9.29	0.65	12.8×10^{-05}	41.32	0.99
Hg 5 mg/L	19.50	0.015	4.06	0.89	36.5×10^{-05}	30.70	0.98
Hg 15 mg/L	32.76	0.027	8.18	0.96	4.99×10^{-05}	34.61	0.99
Cr 5 mg/L	17.40	0.016	4.09	0.98	27.0×10^{-05}	18.04	0.98
Cr 15 mg/L	29.62	0.025	6.69	0.96	14.3×10^{-05}	30.94	0.97
As (V) 5mg/L (Fe-Melanin)	6.03	1.45	1.88	0.91	2.5×10^{-03}	6.71	0.98
As (V) 15mg/L (Fe-Melanin)	14.54	3.11	3.87	0.96	2.8×10^{-04}	15.19	0.98
As (III) 5mg/L (Fe-Melanin)	6.03	1.66	2.06	0.95	1.6×10^{-04}	8.70	0.97
As (III) 15mg/L (Fe-Melanin)	16.27	3.09	3.83	0.97	1.7×10^{-04}	17.09	0.97
As (V) 5mg/L (Cu-Melanin)	5.86	1.25	1.72	0.84	2.3×10^{-04}	5.94	0.99
As (V) 15mg/L (Cu-Melanin)	14.22	2.85	3.44	0.98	1.8×10^{-04}	14.21	0.99
As (III) 5mg/L (Cu-Melanin)	5.68	1.56	1.97	0.93	9.8×10^{-04}	6.71	0.97
As (III) 15mg/L (Cu-Melanin)	14.02	2.92	3.55	0.97	1.1×10^{-04}	15.96	0.98

4.2.4. Effect of temperature on adsorption

Temperature is an important factor that affects adsorption. Hence, the effect of temperature on adsorption of heavy metals on Melanin was studied at different temperatures 288, 298, 308, 318 and 328 K, and the result obtained is shown in Fig.4.20 and 4.21. It is noticeable that higher temperatures favoured the adsorption process in case of all studied metal ions, suggesting it to be an endothermic process. The increase in uptake capacity at higher temperatures may be due to the increase in collision frequency between the adsorbent and the metal ions (Acharya et al. 2009; Saini and Melo 2013). With an increase in system temperature, the metals ions will attain more kinetic energy to diffuse from the bulk phase of the solution to the solid phase of the adsorbent. At higher temperatures, some of the surface components attached to Melanin can get dissociated leading to the generation of more active sites to which the heavy metal can bind (Akpomie et al. 2015).

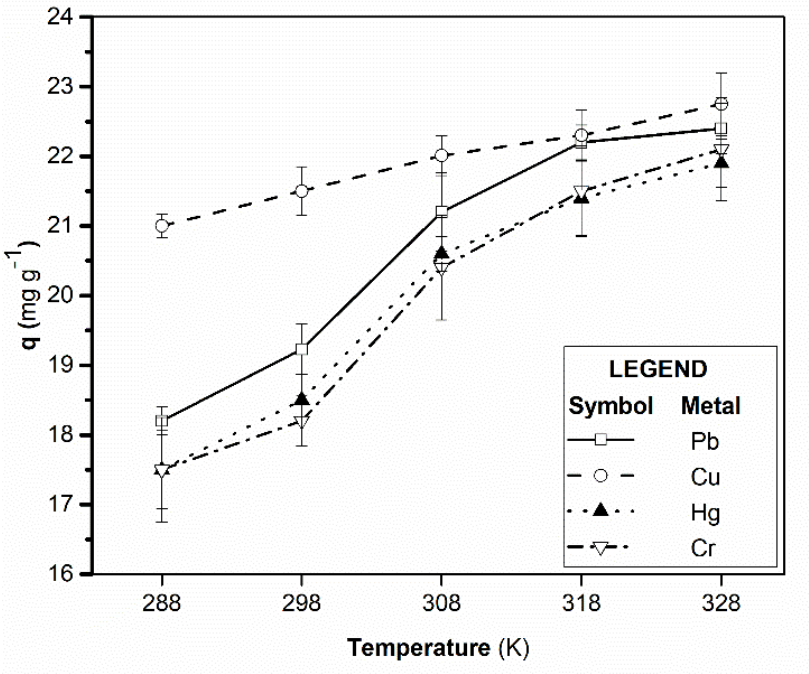

Figure 4.20. Effect of temperature on heavy metals uptake (C_i = 10 mg/L, w = 0.2 g/L, rpm = 200, shaking diameter = 25 mm)

4.2.4.1. Evaluation of Thermodynamic parameters

The thermodynamic parameters such as enthalpy, entropy and Gibb's free energy are calculated by applying experimental data in characteristic equations (Equation 6 and 7)

and are listed in Table 7. Based on these thermodynamic parameters, the nature of adsorption of heavy metals to Melanin is explained.

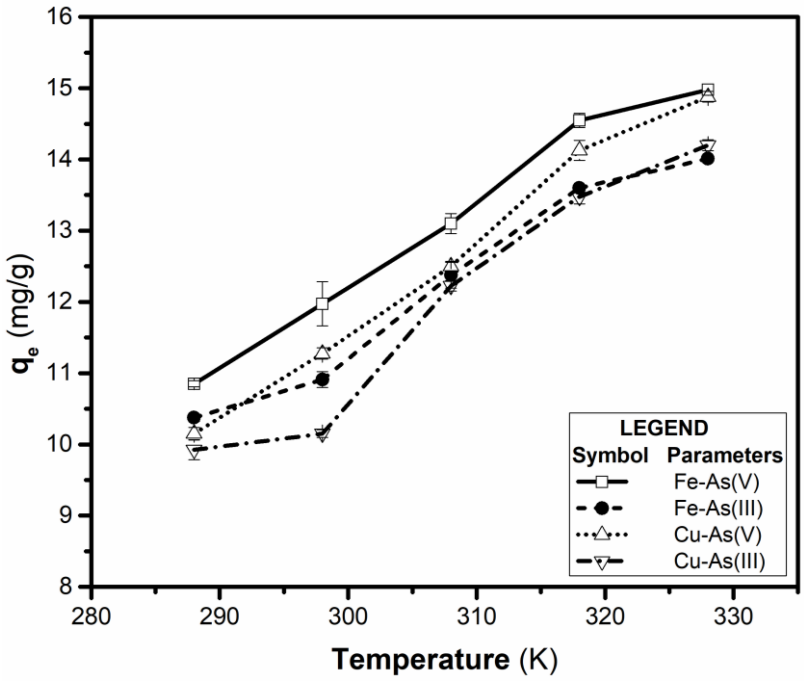

Figure 4.21. Effect of temperature on heavy metals uptake (C_i = 10 mg/L, Fe-Melanin = 0.8 g/L, Cu-Melanin= 2 g/L, rpm = 200, shaking diameter = 25 mm)

There are multiple approaches to consider *K* value for the calculation of Gibbs free energy. One way is to calculate the slope and intercept of the linear plot of *ln* K_c versus *1/T*, and from the Van't Hoff equation, the thermodynamic parameters like enthalpy, entropy and Gibbs free energy are calculated (Acharya et al. 2009). However, the value of *K* obtained from the Langmuir isotherm have the dimension of L/mg which leads to the erroneous calculation of ΔG^0 using Equation 7 since the units of ΔG^0 and *RT* is J/mol (Anastopoulos and Kyzas 2016). According to Milonjić (2007), the Langmuir equilibrium constant need to be made dimensionless before it is used for ΔG^0 calculation by multiplying *K* with 55.5 (molar concentration of 1 Kg water). Further studies reported by Zhou and Zhou (2014) illustrated the need for multiplying the molecular weight of adsorbate to find the new dimensionless *K* for ΔG^0 calculation. As per the new method, ΔG^0 is calculated using K_L (L/mg) by:

$$\Delta G^0 = -RT \ln (K_L \times M_{adsorbate} \times 1000 \times 55.5) \quad (20)$$

The negative value of ΔG° at all studied temperatures indicates the thermodynamic feasibility and spontaneous nature of the adsorption process. Furthermore, a decrease in the value of ΔG^{o} with the increase in temperature confirms that at temperatures near 328 K, adsorption is more spontaneous and favourable (Acharya et al. 2009). The positive values of ΔH^{o} suggest that the present adsorption study was endothermic and also the positive value of ΔS^{o} indicates the increase in randomness at the solid/solution interface during the adsorption process (Schneider et al. 2007).

Table 9. Thermodynamic parameters for heavy metal adsorption

Heavy metals	**ΔH^{o} (kJ/mol)**	**ΔS^{o} (kJ/mol K)**	**ΔG^{o} (kJ/mol)**			
			288 K	**298 K**	**308 K**	**318 K**
Hg (II)	85.45	0.15	-40.66	-35.75	-35.66	-34.61
Pb (II)	91.11	0.18	-40.21	-37.55	-38.61	-39.59
Cr (VI)	74.95	0.12	-36.59	-34.38	-34.37	-32.22
Cu (II)	73.52	0.13	-42.44	-37.88	-38.40	-40.06
As (V) (Fe-Melanin)	64.78	0.11	-35.74	-32.35	-32.20	-32.37
As (III) (Fe-Melanin)	74.61	0.13	-39.98	-34.97	-34.57	-33.72
As (V) (Cu-Melanin)	63.50	0.10	-36.37	-33.32	-32.95	-33.12
As (III) (Cu-Melanin)	73.91	0.13	-40.62	-34.93	-35.46	-34.54

4.2.5. Activation energy studies

The minimum kinetic energy required to carry out a reaction is called activation energy. It is the measure of the energy barrier crossed by the adsorbate to bind to the active sites in the adsorbent. The Lagergren's pseudo-second-order rate constant is found out by conducting a kinetic study at a varying temperature to measure the activation energy. A plot of inverse temperature verses Lagergren's pseudo-second order constant using the Arrhenius equation gives the activation energy required by different metal to bind to Melanin. Type of adsorption can be deciphered from the magnitude of activation energy value (Ali et al. 2016; Saleh 2016).

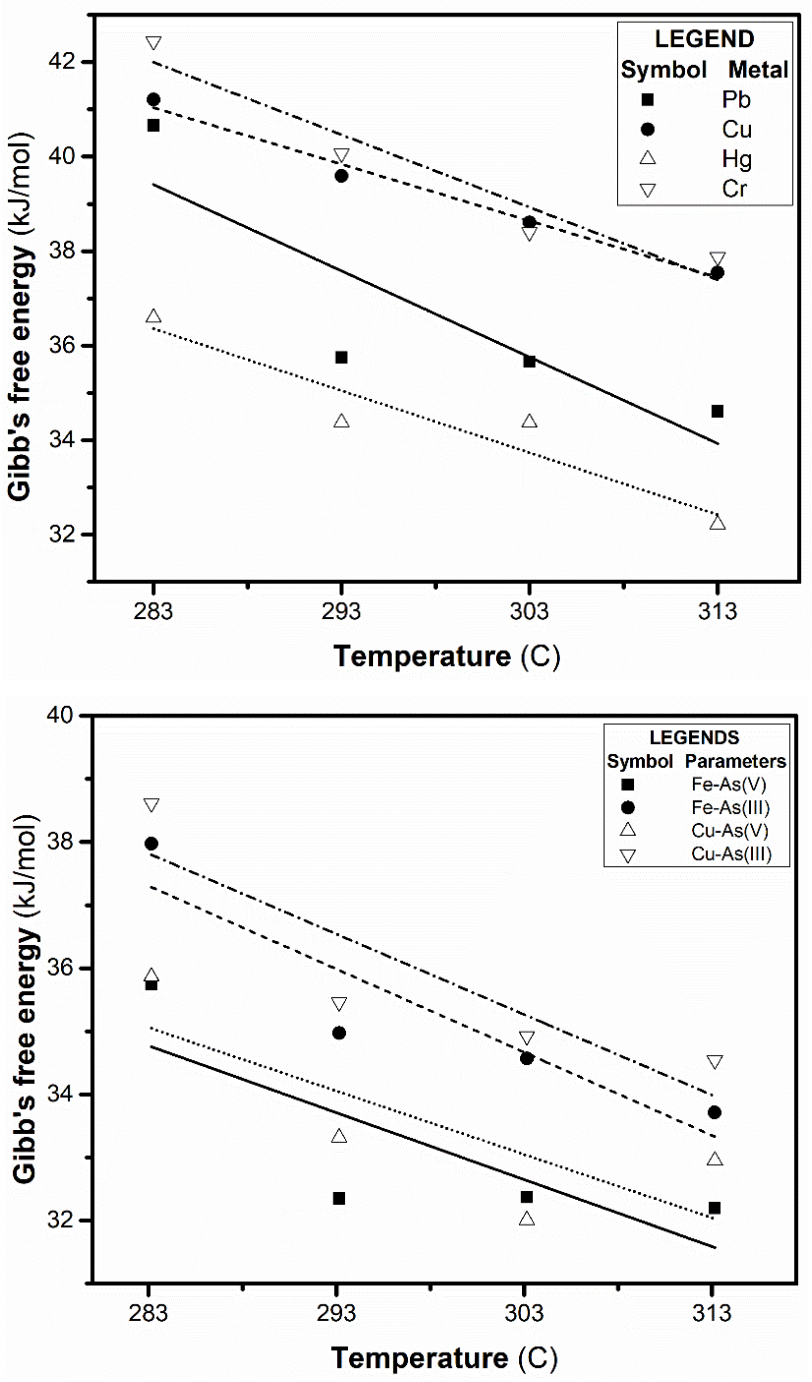

Figure 4.22. Van't Hoff plot for heavy metal adsorption.

The values of activation energy ranging from 40 to 800 kJ/mol infer that the type of adsorption is chemisorption. Chemisorption being a specific process involves strong forces usually by forming strong bonds between the adsorbent and adsorbate (Saleh 2016). The activation energy of heavy metal adsorption on Melanin was calculated, using Equation 5 and values were 16.3, 19.3, 18.3 and 14.8, kJ/mol for Hg (II), Pb (II),

Cr (VI), Cu (II) respectively. As (V) and As (III) bound to Fe Melanin have activation energies of 15.69, 17.13 kJ/mol while that of Cu-Melanin is 19.42 and 21.66 kJ/mol respectively. The calculated values of activation energy using the Arrhenius equation for all heavy metals of the study was below 40 kJ/mol inferring that the adsorption of heavy metals to Melanin is by physical adsorption involving chemical bonding.

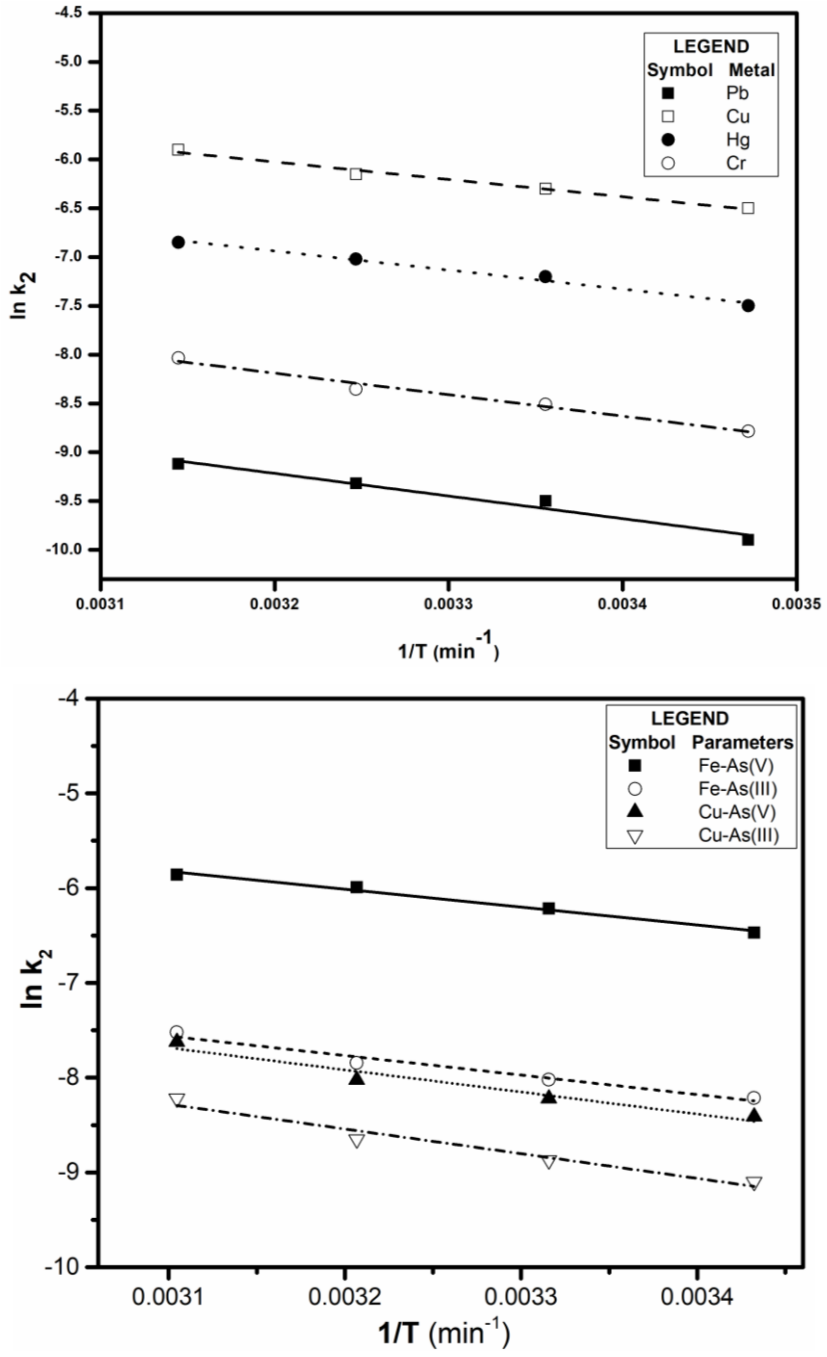

Figure 4.23 Activation energy plot for different metals

4.2.6. Adsorption isotherm studies

4.2.6.1. Effect of initial metal ion concentration on adsorption

The adsorption capacity obtained at different initial metal ion concentration for biosynthesised Melanin and functionalised Melanin is shown in Figures 4.24 and 4.25, respectively. Due to an increase in the collision frequency between adsorbate and adsorbent, an increase in uptake capacity is observed with the rise in initial metal ion concentration (Saini and Melo 2013). The increase in adsorption capacity at higher initial metal ion concentration was due to the higher concentration gradient which is a driving force to overcome the mass transfer resistance between the bulk aqueous phases to the solid adsorbent phase. The percentage efficiency of adsorption will not increase after an absolute concentration of metal ions in the solution because the number of active sites in Melanin is fixed in number and after a particular concentration of metal ions, the active sites get saturated (Akpomie et al. 2015).

From adsorbate variance, experimental data, the distribution coefficient K_D (mL/g), which is one of the important parameters influencing adsorption was calculated. K_D can be described as the ratio of the equilibrium metal ion concentration in solid and in the aqueous phase (Bhainsa and D'Souza 2009; Saini and Melo 2013). K_D value obtained for biosynthesised Melanin was plotted against residual metal ion concentration (Fig. 4.26). Very high values of K_D at a low equilibrium concentration of heavy metals indicate that Melanin can adsorb even at deficient heavy metal concentrations.

4.2.6.2. Equilibrium Modelling

At equilibrium, the relationship between heavy metals adsorbed to Melanin and that present in the aqueous phase is given by an adsorption isotherm. The equilibrium data of heavy metals bound to Melanin and functionalised Melanin are fitted with Langmuir, Freundlich and Redlich-Peterson isotherms models. Langmuir isotherm parameters were calculated from the plot of C_e/q_e versus C_e (Figures 4.27 and 4.28) and are listed in Table 11. The values of R_L obtained for Melanin at different initial metal ion concentrations ranging from 5 to 25 mg/L are in the range of 0 to 1, suggesting a favourable adsorption process.

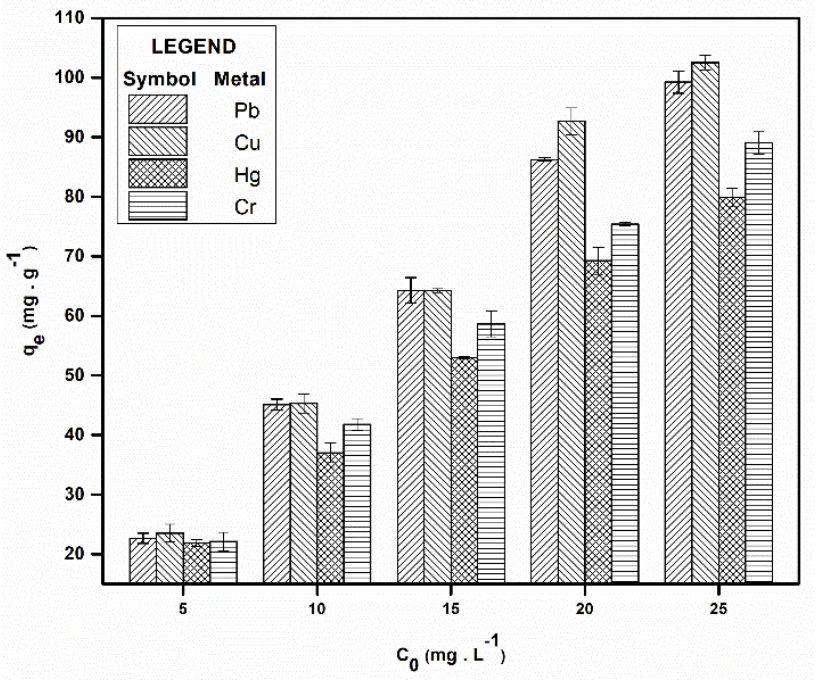

Figure 4.24. Effect of initial heavy metal concentration on uptake capacity (C_0 =5-25 mg/L, w = 0.2 g/L, rpm= 200, shaking diameter = 25 mm)

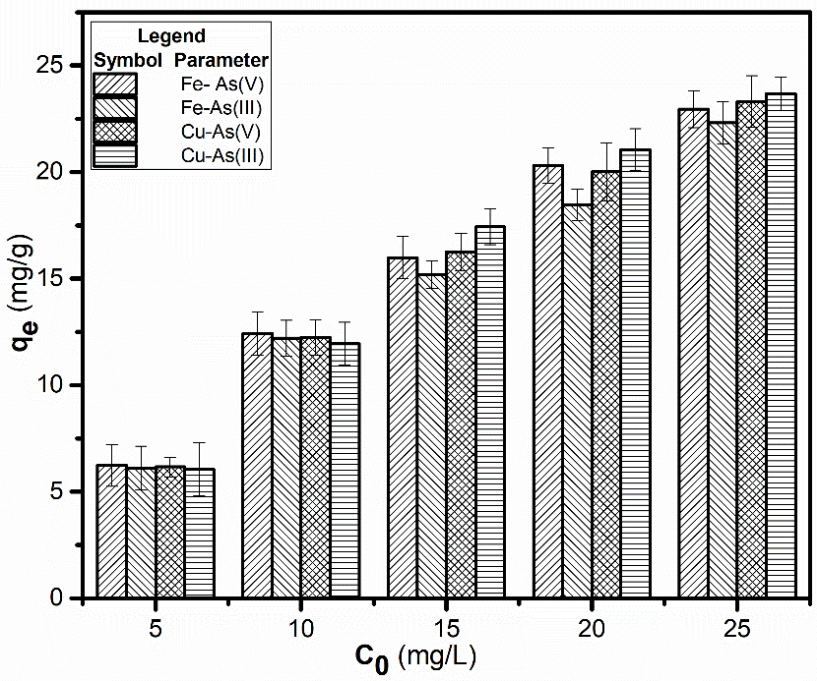

Figure 4.25. Effect of initial heavy metal concentration on uptake capacity (C_0 =5-25 mg/L, Fe-Melanin = 0.8 g/L, Cu-Melanin= 2 g/L, rpm = 200, shaking diameter = 25 mm).

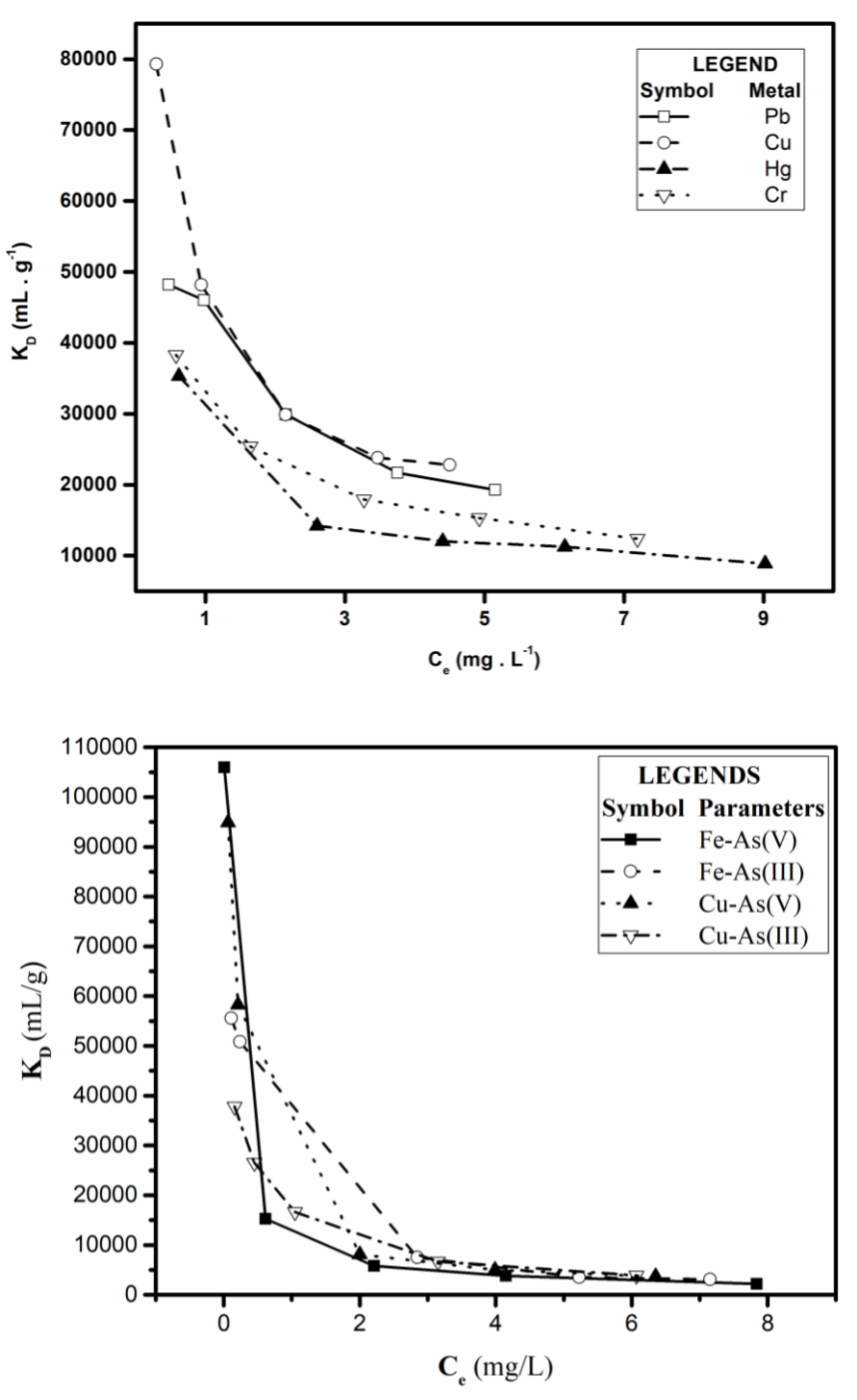

Figure 4.26. The distribution coefficient of heavy metals uptake

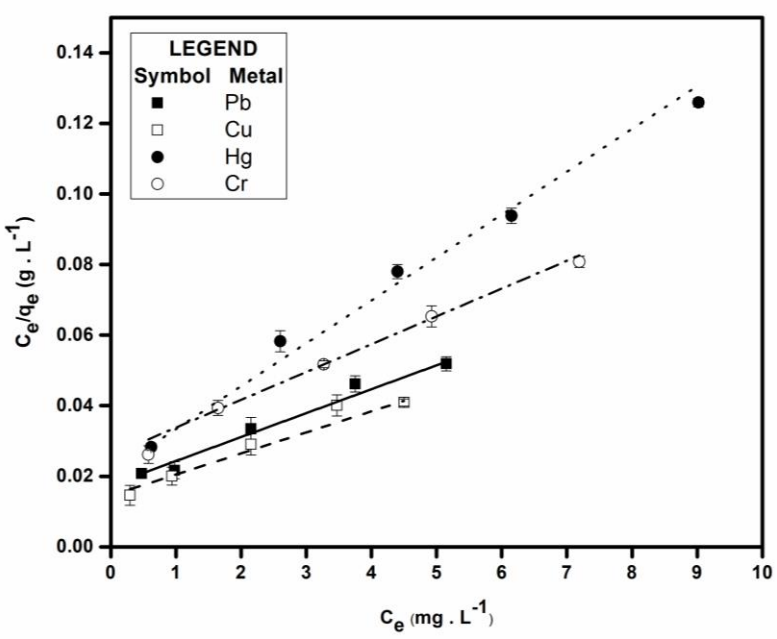

Figure 4.27. Langmuir isotherm for heavy metal uptake (C_o =5-25 mg/L, w = 0.2 g/L, rpm= 200, shaking diameter = 25 mm)

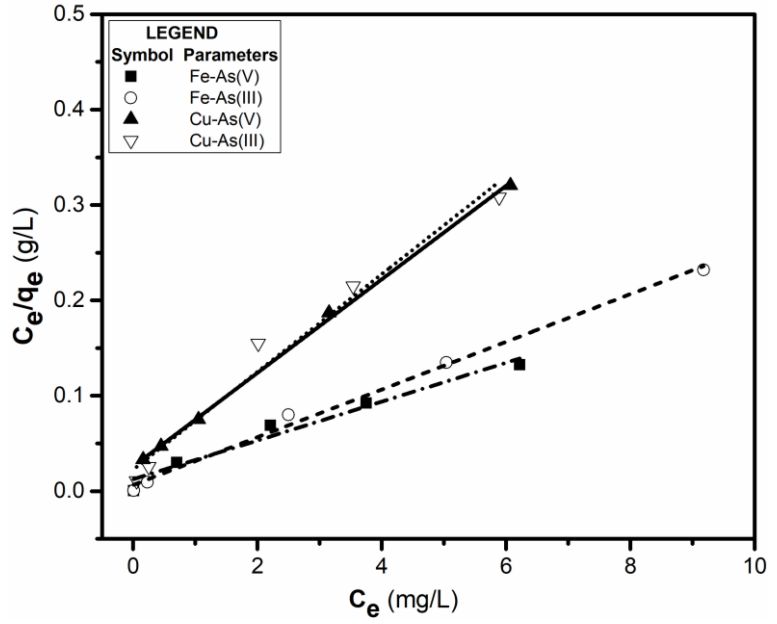

Figure 4.28. Langmuir isotherm for heavy metal uptake (C_i = 5-25 mg/L, Fe-Melanin = 0.8 g/L, Cu-Melanin= 2 g/L, rpm = 200, shaking diameter = 25 mm)

The parameters of Freundlich isotherm for both types of Melanin were calculated from the plot of *ln* q_e versus *ln* C_e (Fig. 4.29 and 4.30) and are listed in Table 11.

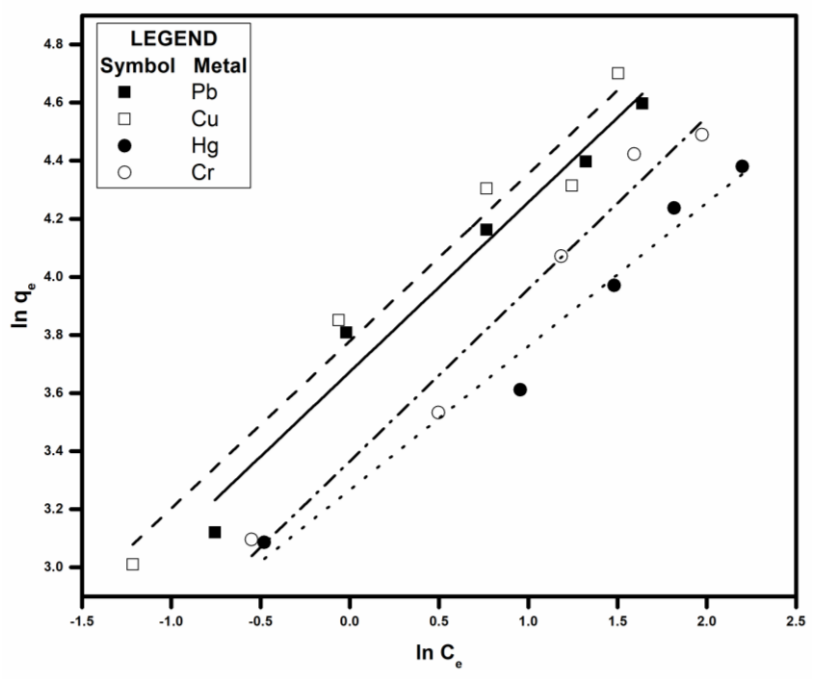

Figure 4.29. Freundlich isotherm for heavy metal uptake (C_0 =5-25 mg/L, w = 0.2 g/L, rpm= 200, shaking diameter = 25 mm)

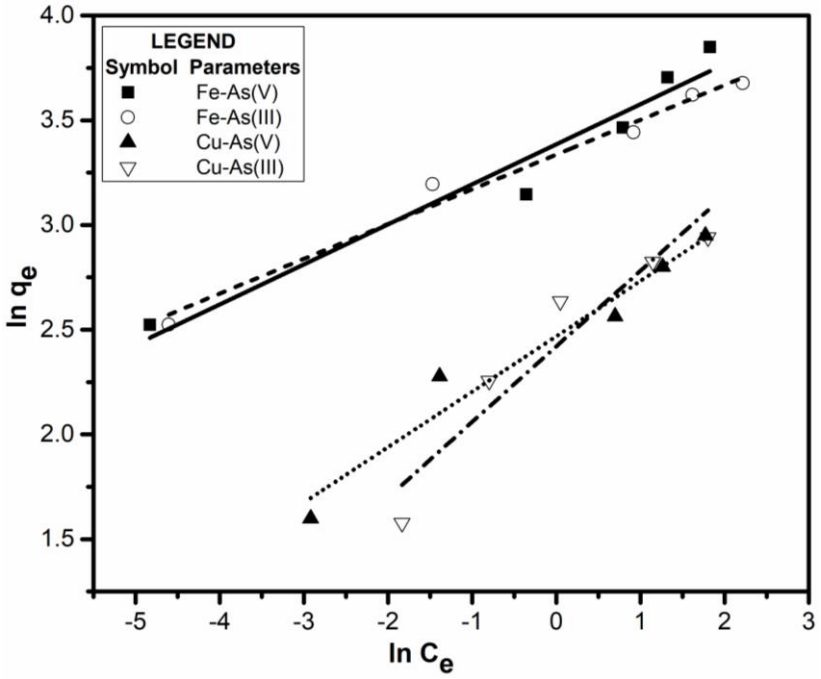

Figure 4.30. Freundlich isotherm for heavy metal uptake (C_i = 5-25 mg/L, Fe-Melanin = 0.8 g/L, Cu-Melanin= 2 g/L, rpm = 200, shaking diameter = 25 mm)

The equilibrium data modelled using Redlich-Peterson isotherms by plotting *ln* C_e/q_e verses *ln* C_e (Fig. 4.31 and 4.32) and the parameters are listed in Table 11.

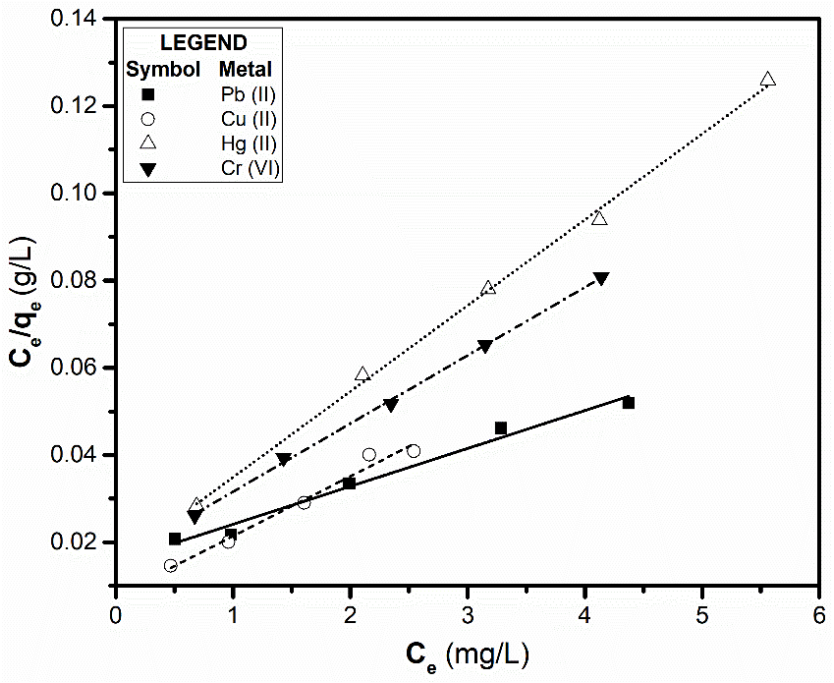

Figure 4.31. Redlich-Peterson isotherm for heavy metal uptake (C_0 =5-25 mg/L, w = 0.2 g/L, rpm= 200, shaking diameter = 25 mm

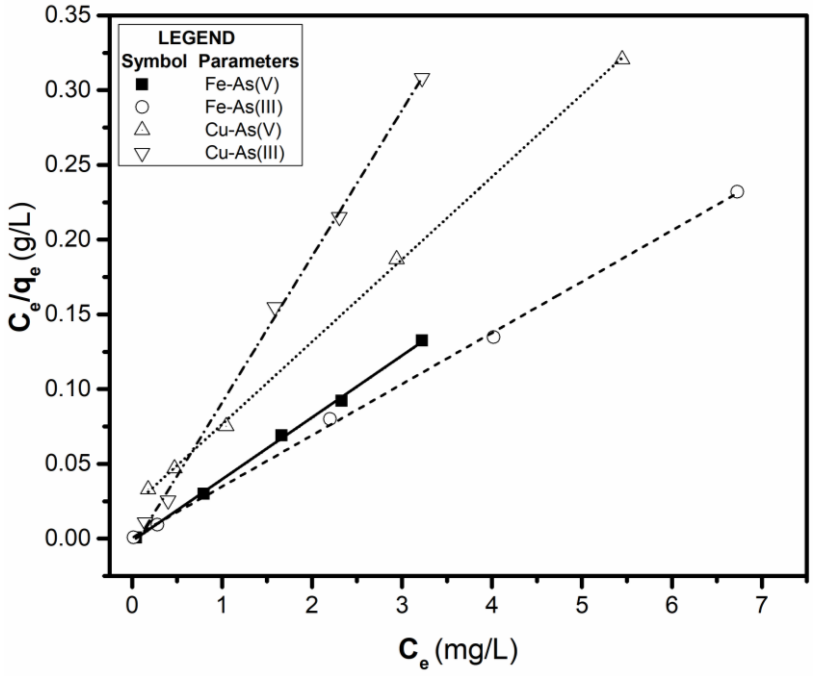

Figure 4.32. Redlich-Peterson isotherm for heavy metal uptake (C_i = 5-25 mg/L, Fe-Melanin = 0.8 g/L, Cu-Melanin= 2 g/L, rpm = 200, shaking diameter = 25 mm)

The applicability of Langmuir and Freundlich isotherm models for heavy metal adsorption on to Melanin was assessed using Equations 8 and 11 respectively by linear

regression analysis. The experimental data fitted well with the Langmuir adsorption isotherm model having a higher correlation coefficient compared to the Freundlich isotherm model with the lower correlation coefficient. The maximum loading capacity obtained for biosynthesised Melanin from Langmuir isotherm plot is 82.37, 147.49, 126.90 and 167.78 for Hg (II), Pb (II), Cr (VI) and Cu (II) respectively. In the case of As (V) and As (III) adsorption to iron and copper impregnated Melanin, the maximum adsorption capacity obtained from Langmuir isotherm model are 50.12 and 39.98 mg/g for As (V) and As (III) adsorption to Fe-Melanin, 20.387 and 19.519 mg/g for As (V) and As (III) adsorption to Cu-Melanin respectively. The value of 1/n for biosynthesised Melanin obtained was between 0 and 1 which infers that the heavy metal adsorption on Melanin is favourable in studied conditions and low 'b' value indicates high affinity of heavy metal ions towards Melanin.

Melanin having high adsorption capacity and high affinity for Hg (II), Cr (VI), Pb (II), Cu (II), As (V) and As (III) metal ions even at lower concentration can be considered as a promising adsorbent for heavy metal removal. The increase in adsorption capacity with an increase in temperature infers that the control mechanism of adsorption is chemisorption. Langmuir isotherm concludes that the adsorption of heavy metal ions to Melanin is limited to the monolayer. The adsorption energy required for binding adsorbate to functional groups in Melanin is the same for all sites. The adjoining adsorbed metal ions do not interfere with each other and also the occupancy condition of an active site is not affected by another site (Can et al. 2016). The adsorption capacity and the operating parameters are compared with the current study.

The three-parameter isotherm, Redlich-Peterson model, have combined features of both Langmuir and Freundlich adsorption isotherms, making it a hybrid adsorption mechanism. As the exponential term *g* tends to zero, the model approximates to Henry's law or follows Freundlich model, and while it tends to 1, the model approximates to Langmuir isotherm model (Soltani et al. 2019). The model proposes linear dependence between the concentration and exponential parameter in the model equation. The equations involving experimental data as well as theoretical predictions, are solved by minimisation procedure using 'Microsoft Excel 365 SOLVER' (Appendix Figures 6 and 7).

Table 10. Isotherm parameters of heavy metal adsorption on Melanin

Heavy metals	Langmuir isotherm model			Freundlich isotherm model			Redlich-Peterson model			
	q_m (mg/g)	b (L/mg)	R^2	K_F (mg/g)	$1/n$	R^2	A	B	g	R^2
Hg (II)	82.37	0.57	0.99	26.21	0.49	0.97	50.81	1.29	0.78	0.99
Pb (II)	147.49	0.38	0.99	39.36	0.58	0.96	114.94	0.06	0.9	0.98
Cr (VI)	126.90	0.30	0.99	28.93	0.59	0.97	64.02	0.98	0.7	0.99
Cu (II)	167.78	0.41	0.97	43.59	0.48	0.96	72.99	1.80	0.66	0.97
As (V) (Fe-Melanin)	50.12	1.61	0.95	29.53	0.19	0.93	24.17	24.06	0.74	0.99
As (III) (Fe-Melanin)	39.98	3.79	0.99	28.11	0.17	0.97	29.24	56.35	0.86	0.99
As (V) (Cu-Melanin)	20.38	2.14	0.99	11.80	0.26	0.94	18.13	2.58	0.94	0.99
As (III) (Cu-Melanin)	19.52	2.26	0.96	11.25	0.36	0.89	10.22	14.18	0.76	0.99

The results show that R-P isotherm fitted well to all the metals similar to Langmuir isotherm (Figures 4.31 and 4.32). However, the arsenic adsorption to different functionalised Melanin showed more fitting towards R-P isotherm than Langmuir isotherm. The values of *g* are closer to 1 inferring that the R-P model approximates to Langmuir isotherm model and hence the Langmuir isotherm assumptions are valid for the adsorption of heavy metals to melanin.

4.2.7. Ternary adsorption studies

Multi-component removal is the most desirable quality for an adsorbent since it can remove many heavy metal contaminants at a stretch and render the water fit for drinking. Adsorption of multicomponent from a system is quite different from single heavy metal adsorption (Sehaqui et al. 2014). The binding and selectivity of heavy metals to Melanin is elucidated and shown in Fig. 4.33 and 4.34.

It is evident from the results that the mono-metal system has better adsorption to Melanin when compared to the multi-metal system. The decrease in adsorption capacity for the ternary system was due to the competition of heavy metals to bind to the active sites in Melanin (Dong et al. 2016). In the case of Pb-Hg-Cu ternary system, there is a 3.4% decrease in adsorption efficiency as compared to individual heavy metal adsorption to Melanin. Similarly, Cu (II) and Hg (II) showed a decrease of 5.8 % and 32 % in efficiency, respectively. In the case of Cr-Hg-Cu ternary system, Cr (VI) showed a 4.1% decrease in adsorption efficiency while Cu (II) and Hg (II) showed 2.7% and 49.21% respectively. From these studies, it is evident that Cu (II) followed by Pb (II) and Cr (VI) have more affinity of binding towards Melanin. Hg (II) did not show improved adsorption during competitive binding for both the ternary systems. From this study, it is evident that Melanin can be used to remove multi-metal from solutions with improved efficiency. Melanin nanoparticles produced by the bacterium have proved to be an efficient adsorbent to remove heavy metals in the presence of other cations. However, the removal of these nanoparticles from the aqueous solution after adsorption is a tedious process.

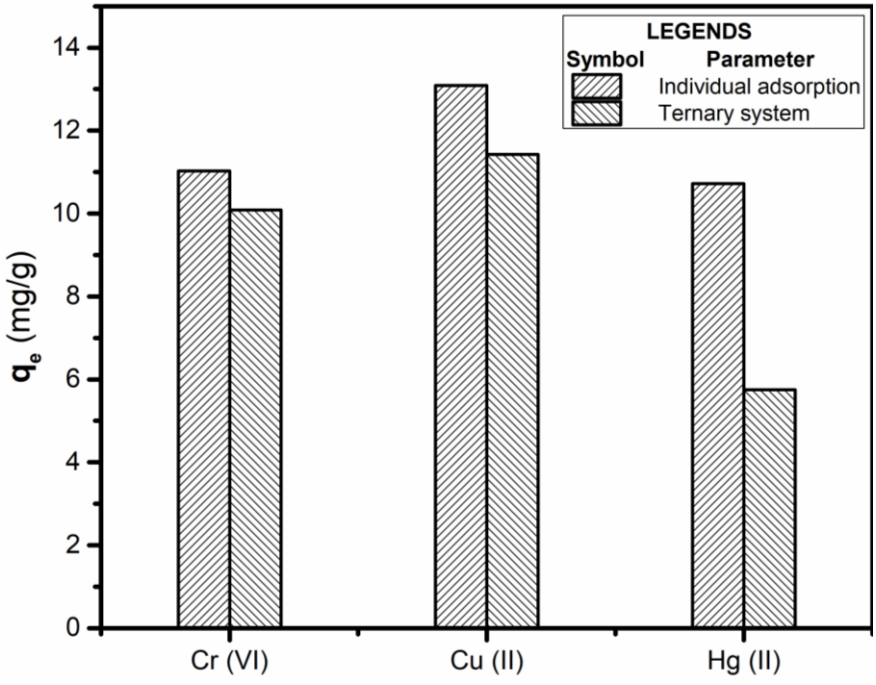

Figure 4.33. Competitive adsorption of Cr (VI), Cu (II) and Hg (II) (C_0 =10 mg/L, W = 0.2 g/L, rpm= 200, shaking diameter = 25 mm)

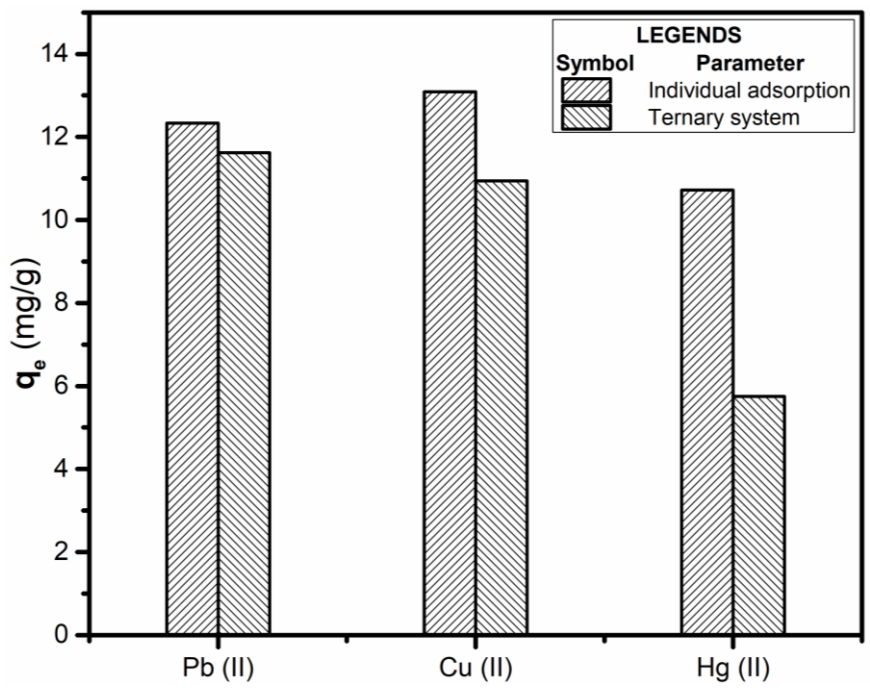

Figure 4.34. Competitive adsorption of Pb (II), Cu (II) and Hg (II) (C_0 =10 mg/L, W = 0.2 g/L, rpm= 200, shaking diameter = 25 mm)

Further, continuous studies with Melanin packed column might incur adsorbent leaking issues with the effluent. To avert the concern pertinent to the size, Melanin was made

to tightly bind onto different matrices such as N, N-Diethyl acrylamide hydrogel, PVDF membrane and activated carbon. Batch adsorption studies were conducted to understand the effect of matrix on the adsorption efficiency of Melanin.

4.3. Adsorption studies of heavy metals on Melanin impregnated hydrogel

4.3.1. Surface morphology studies

Morphological studies of the hydrogel using SEM shows that the hydrogel is highly porous with interconnecting mesh-like structure at 100 µm (Fig. 4.35). On analysis at higher magnifications, the surface of hydrogel seemed to be uniform and continuous. The SEM analysis of Melanin impregnated hydrogel showed the Melanin particles attached to the surface and entrapped within the hydrogel network.

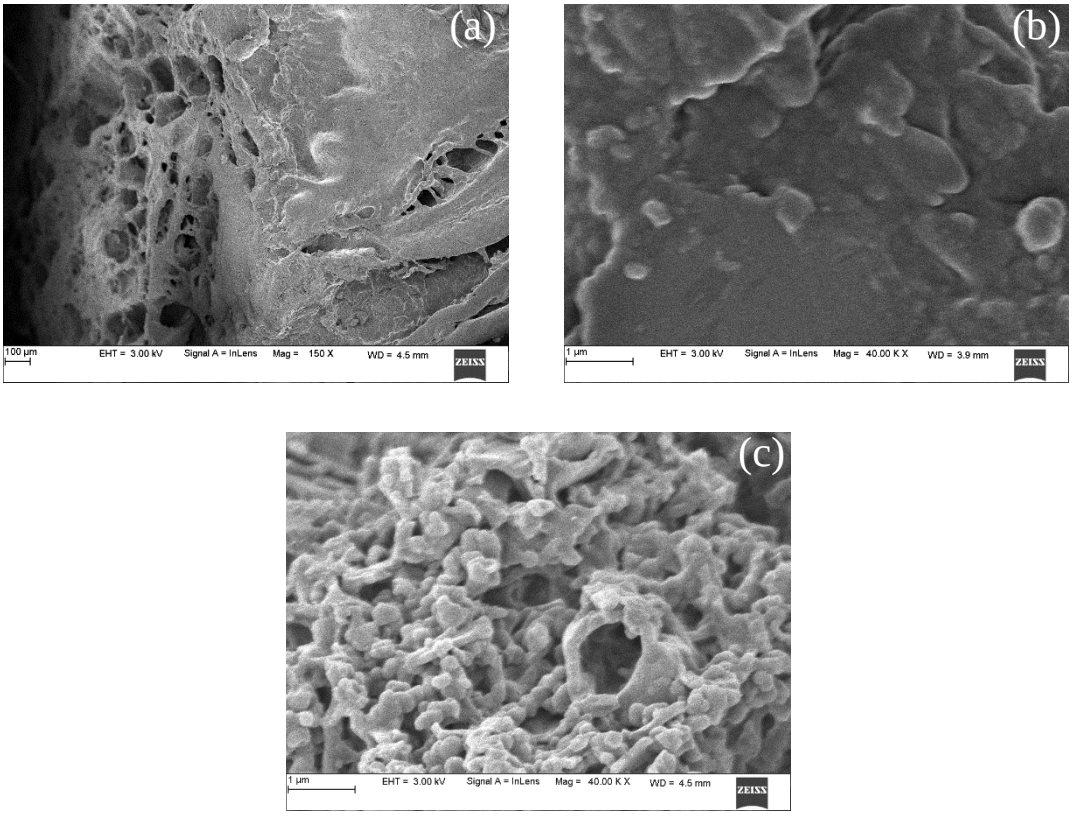

Figure 4.35. SEM images of (a) hydrogel at 100 µm (b) Melanin free hydrogel at 1µm (c) Melanin impregnated hydrogel at 1 µm.

4.3.2. Batch adsorption studies.

4.3.2.1. Effect of pH

Aqueous medium with Cr (VI) concentration of 5 mg/L and volume 50 mL maintained from pH 1 to 7 was equilibrated with 10 mg of Melanin impregnated in the hydrogel. The adsorption of Cr (VI) at different pH by Melanin impregnated hydrogel is depicted in Fig. 4.36. The hydrogel is thermosensitive as well as pH sensitive; that is, it deswells at higher temperatures and lower pH. So the pores of hydrogel will tend to shrink and hence, the easy passage of liquid through the hydrogel is curtailed (Yildiz et al. 2010). Cr (VI) exhibited higher adsorption at neutral pH where the hydrogel was fully swelled. In Fig. 4.36, C_o represents the initial concentration of the heavy metal solution, *w* is the amount of Melanin impregnated in the hydrogel.

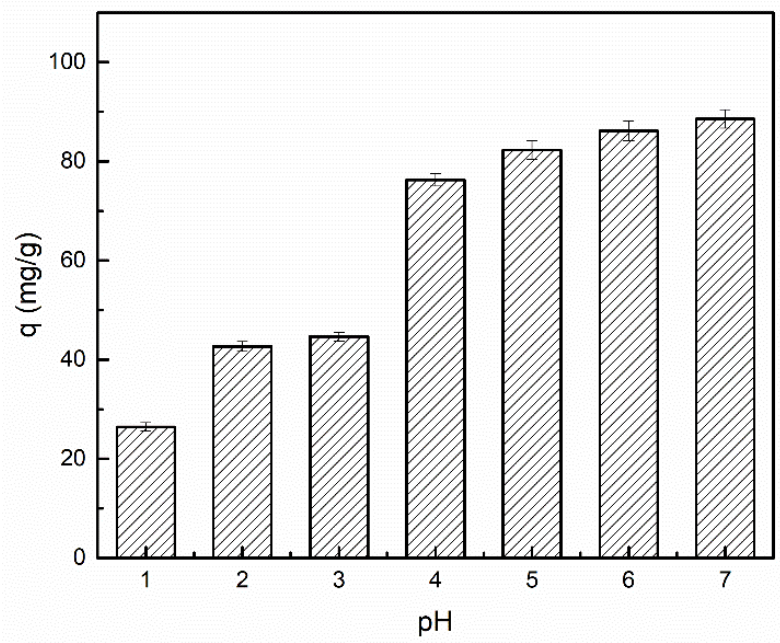

Figure 4.36. Effect of pH on Cr (VI) removal using Melanin impregnated hydrogel. (C_0 =5 mg/L, w = 0.2 g/L, rpm= 150, shaking diameter = 25 mm)

4.3.2.2. Effect of time

Cr (VI) solution of concentration 5 mg/L was individually equilibrated with Melanin impregnated hydrogel and free hydrogel. The equilibrium was attained after 36 hours (Fig. 4.37). When compared to other systems, the hydrogel took a very long time to

attain equilibrium because of the compact structure which hinders the easy movement of water through the pores of the hydrogel.

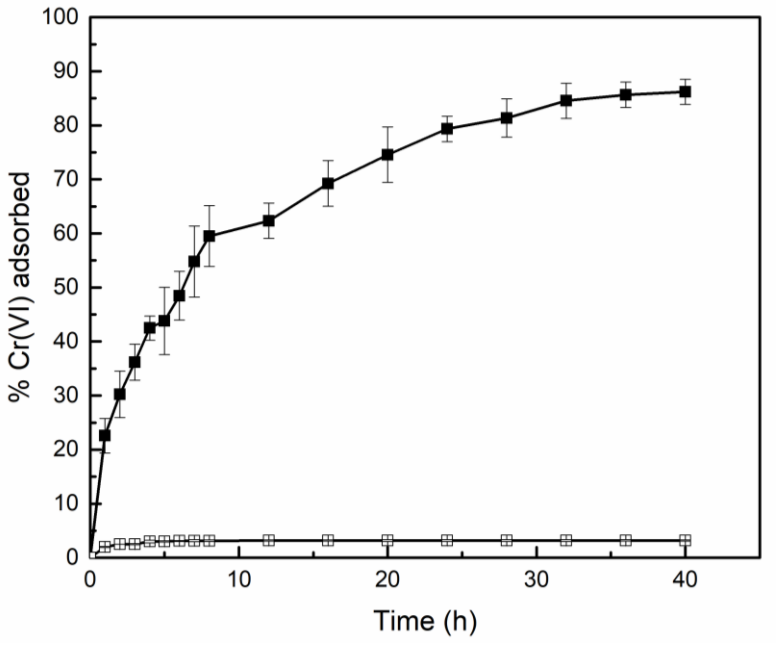

Figure 4.37. Effect of time on adsorption of Cr (VI) on to Melanin impregnated hydrogel (■) and free hydrogel (□). (C_0 =5 mg/L, W = 0.2 g/L, rpm= 150, shaking diameter = 25 mm)

4.3.2.3. Effect of temperature

The study showed that higher temperature favoured higher amounts of adsorption of heavy metals (Fig. 4.38). As the temperature increases, the collision frequency of heavy metals to the active sites in Melanin also increases, thereby leading to improved adsorption of heavy metals. Binding of heavy metals at higher temperatures infers that it is an endothermic adsorption process. The thermosensitive hydrogel shrunk at higher temperatures leading to the contraction of pores to decrease its size and the free flow of water through the hydrogel is hindered. So maximum adsorption of Cr (VI) to Melanin impregnated hydrogel was at 318 K and above which adsorption efficiency started decreasing.

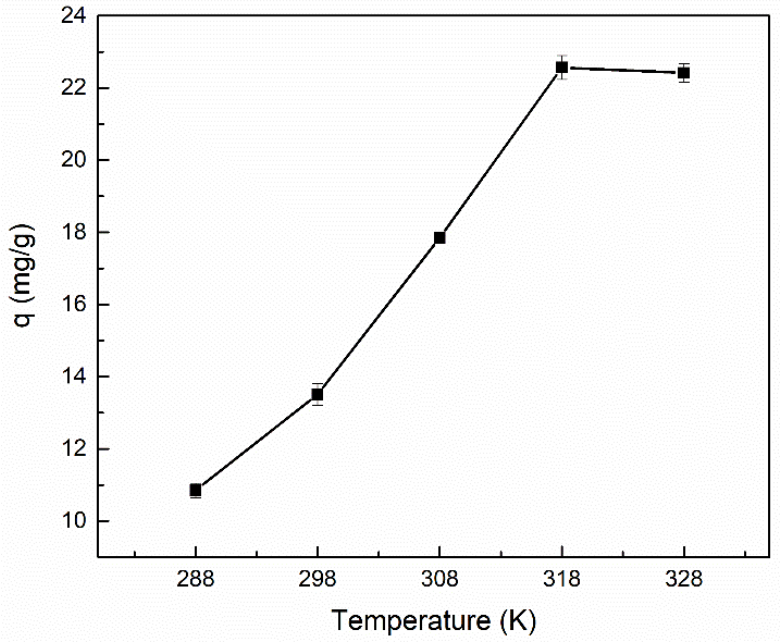

Figure 4.38. Amount of Cr (VI) adsorbed at different temperatures. (C_0 =5 mg/L, W = 0.2 g/L, rpm= 200, shaking diameter = 25 mm)

4.3.3. FTIR studies

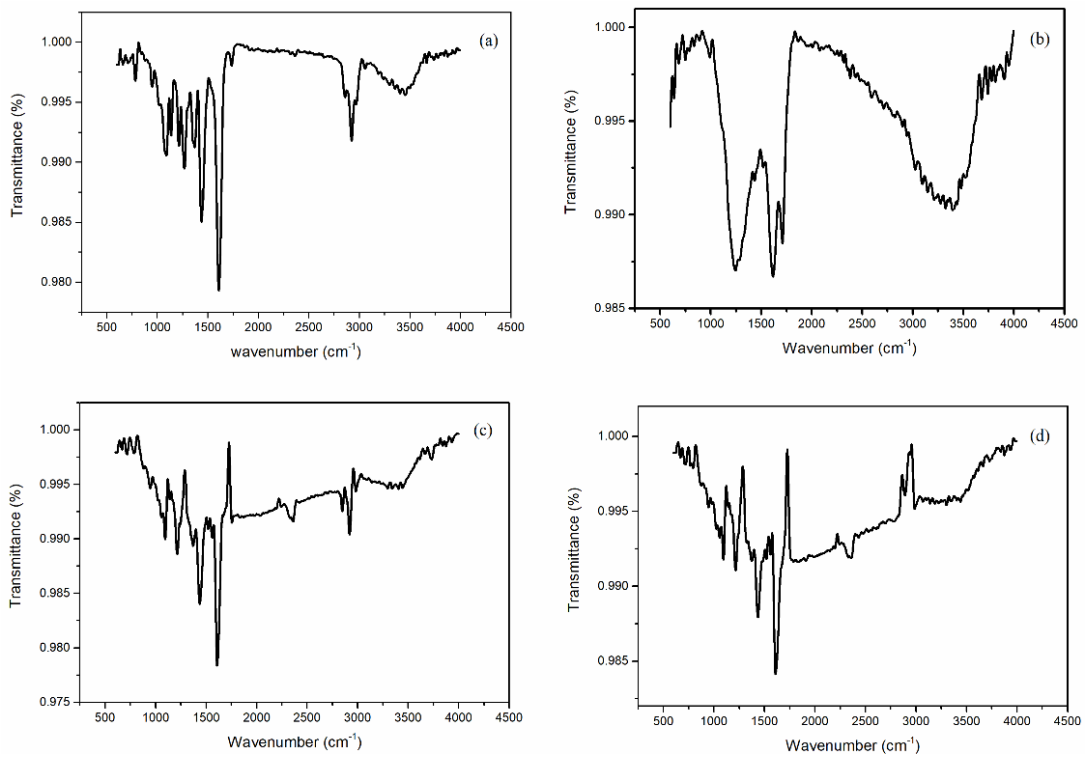

Figure 4.39. FTIR spectrum of (a) hydrogel (b) Melanin (c) Melanin impregnated hydrogel (d) Cr (VI) bound Melanin impregnated hydrogel.

The FTIR spectrum of N, N-diethyl acrylamide hydrogel, has shown the presence of different functional groups. Wavenumber at 1021.55, 1137.27, 1214.91 and 1736.37 cm^{-1} showed the presence of -C=O whereas the wavenumbers corresponding to 1090.22, 1269.10 cm^{-1} indicated the presence of –C-N bonds. 1609.47 cm^{-1} corresponds to N-H group present in the hydrogel while 3403.95 cm^{-1} indicated the –OH bonds. FTIR spectrum of Melanin impregnated hydrogel has shown that the addition of Melanin to the hydrogel has not changed any of the functional groups. Apart from a slight shift and decrease in % transmittance, the Melanin has not chemically reacted with the hydrogel. Wavenumbers 1057.82, 1094.54, 1140.14, 1213.79, 1609.04, 2919.79, 2981.98, 3403.49 cm^{-1} in Fig. 4.39 have shown a shift from its position when compared to pure hydrogel while the wavenumbers 1371.10, 1437.43, 1609.04 cm^{-1} showed only decrease in % transmittance while wavenumber shift was not observed.

Adsorption of Cr (VI) to Melanin impregnated in the hydrogel has shown a shift in wavenumbers, and more importantly, the % transmittance has increased when compared to the Melanin bound hydrogel. Wavenumbers in the spectrum of Melanin impregnated hydrogel has been shifted to 1056.39, 1094.93, 1142.65, 1215.36, 1436.53, 1519.63, 1609.68, 2987.19, 3441.14 cm^{-1}. For all these wavenumbers, transmittance % have increased. The increase in the intensity of peaks indicates the binding of Cr (VI) to Melanin, where the shifting of peaks indicates strong bonding with the functional groups. The FTIR thereby confirms that the Melanin has not reacted and formed bonds with hydrogel and Cr (VI) adsorbed to Melanin.

The studies using Melanin immobilised hydrogel to remove Cr (VI) showed significant adsorptive removal. However, contact time required to reach equilibrium seemed to be very high, which is around 36 hours to attain 88% removal of 5 mg/L of Cr (VI) ions from 50 mL aqueous medium. Moreover, the thermal and pH response of the hydrogel is a limiting factor for its application in groundwater purification. Besides these cons, a certain quantity of Melanin tends to leach out during the curation period of around 24 to 48 hours. Hence the study is limited only to Cr (VI) removal and new matrices are explored to coat Melanin for improved heavy metal removal.

4.4. Adsorption studies of heavy metals on Melanin coated PVDF

4.4.1. Surface characterisation of Melanin coated PVDF

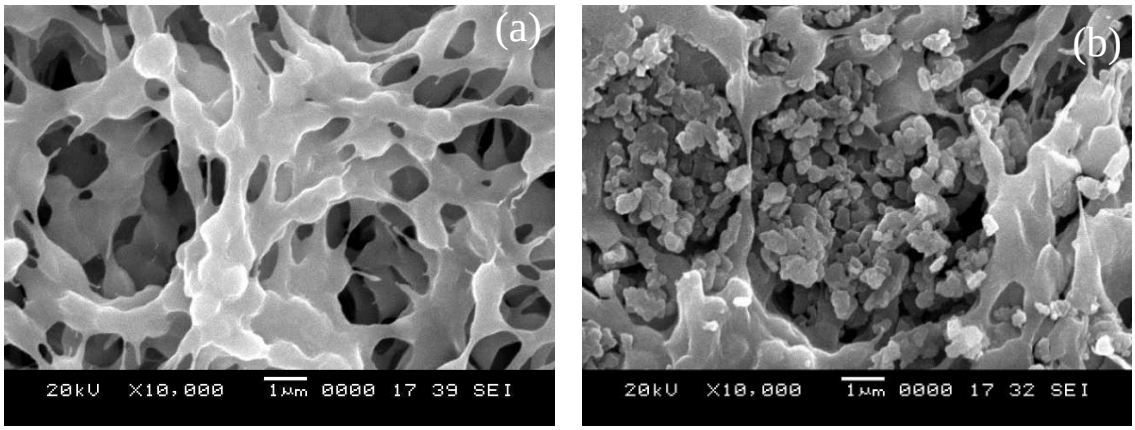

Figure 4.40. SEM images of (a) PVDF membrane (b) Melanin coated PVDF membrane.

The morphology study of PVDF membrane showed in Fig. 4.40 (a) reveals the presence of a large number of pores irregularly distributed and having high interconnectivity. Fig. 4.40 (b) shows that the Melanin coated PVDF membrane has almost uniformly distributed pores with more or less equal in size. Melanin binds to surface activated PVDF membranes through hydrophobic and dipole interactions (Hugli 2012). Melanin has reduced the porosity of PVDF and formed an inseparable layer over the PVDF membrane.

4.4.2. Adsorption studies

Surface activated PVDF membranes were coated with 20 mg Melanin by a dip coating method and was used for adsorption studies. Each membrane was coated with about 5 mg of Melanin and was used for the removal of heavy metal ions from water by adsorption. Adsorption studies using PVDF without PVDF membrane showed hardly any binding of heavy metals on to it.

4.4.2.1. Effect of pH

The adsorption of heavy metals on to Melanin coated PVDF membrane is influenced by the change in pH. Maximum adsorption shown by Cr (VI) was at pH 3, Cu (II), Pb (II) and Hg (II) at 5 (Fig. 4.41).

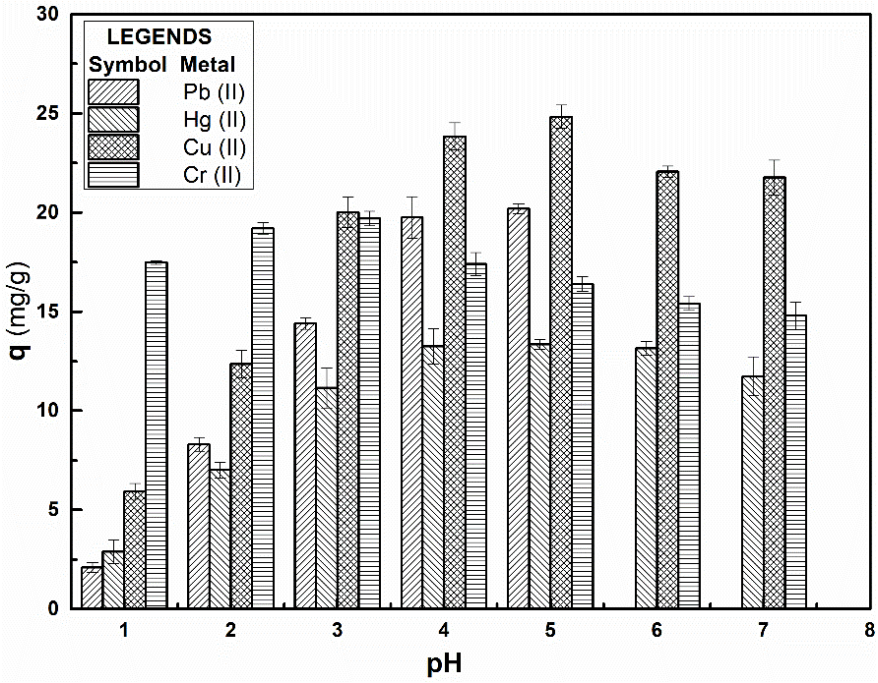

Figure 4.41. Amount of heavy metals adsorbed on to Melanin coated PVDF membranes at different pH (C_0 =5 mg/L, w = 0.4 g/L, rpm= 150, shaking diameter = 25 mm)

4.4.2.2. Effect of contact time

Melanin coated PVDF discs when equilibrated with 5 mg/L of heavy metal solution attained an equilibrium within 3.3 hours (Fig. 4.42). The efficiency of adsorption was decreased due to the unavailability of half of the total active sites which was engaged in binding to PVDF membrane.

4.4.2.3. Effect of temperature

The adsorption of heavy metals to Melanin coated PVDF showed an increasing trend with temperature. The amount adsorbed was maximum at 328 K (Fig. 4.43)

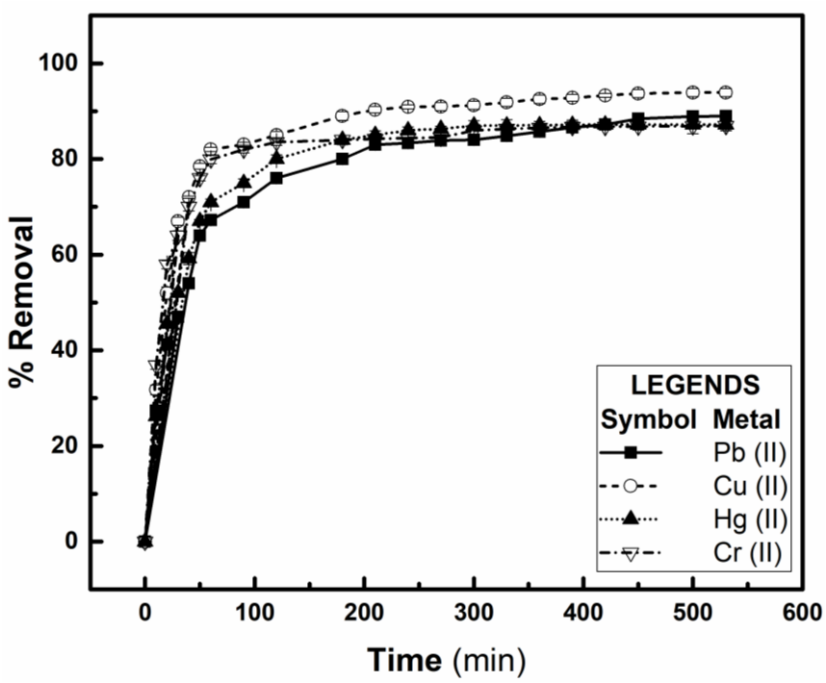

Figure 4.42. Percentage removal of heavy metals with respect to time. (C_0 =5 mg/L, w = 0.4 g/L, rpm= 150, shaking diameter = 25 mm)

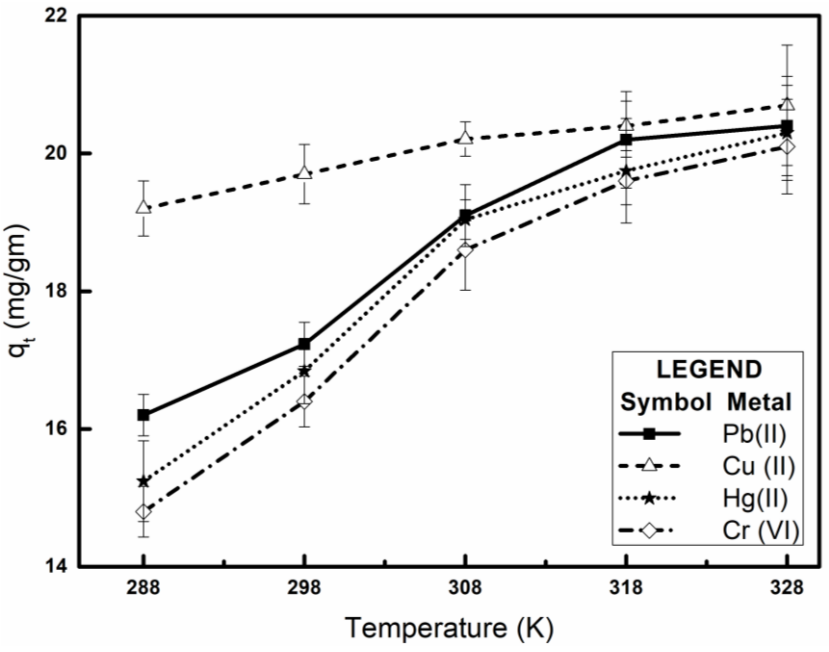

Figure 4.43. Amount of heavy metals adsorbed onto Melanin at different temperatures (C_0 =5 mg/L, w = 0.4 g/L, rpm= 200, shaking diameter = 25 mm)

4.4.3. FTIR studies

The FTIR spectrum of Melanin, PVDF and Melanin coated PVDF membrane was analysed in the range of 400 to 4500 cm^{-1} (Fig. 4.44). The spectrum analysis of surface activated PVDF showed the presence of certain functional groups and bonds. The transmittance peak at 612.896, 761.83, 840.47 cm^{-1} confirmed the presence of alkyl halides, which are the fluorine attached to the carbon in PVDF. The peaks at 795.74, 1181.13 and 2916.72 cm^{-1} indicated the presence of C-H bonds. It also showed the presence of –C-O at 1275.76 cm^{-1} and –OH at 3459.60 cm^{-1}. The FTIR spectrum of Melanin coated PVDF membrane was compared with that of surface activated PVDF membrane and found that many peaks have shifted from higher to lower wavenumbers, the intensity of certain other peaks have decreased which confirms the binding of Melanin to PVDF membrane. The peaks such as 761.83, 840.47, 1181.13,1275.76 cm^{-1} which were present in the PVDF spectrum have been shifted to new wavenumbers of 761.51, 836.36, 1060.25, 1178.01, 1400.24 cm^{-1}. The shift infers the binding of Melanin to these functional groups and forming a stable layer over the PVDF. The peaks at wavenumber 876.95 cm^{-1} showed the presence of an –NH wag, while the 977.92 cm^{-1} indicated the presence of =C-H in the aromatic group of Melanin. The groups at 2796.58 and 3042.94 cm^{-1} indicated the presence of aldehyde groups in Melanin.

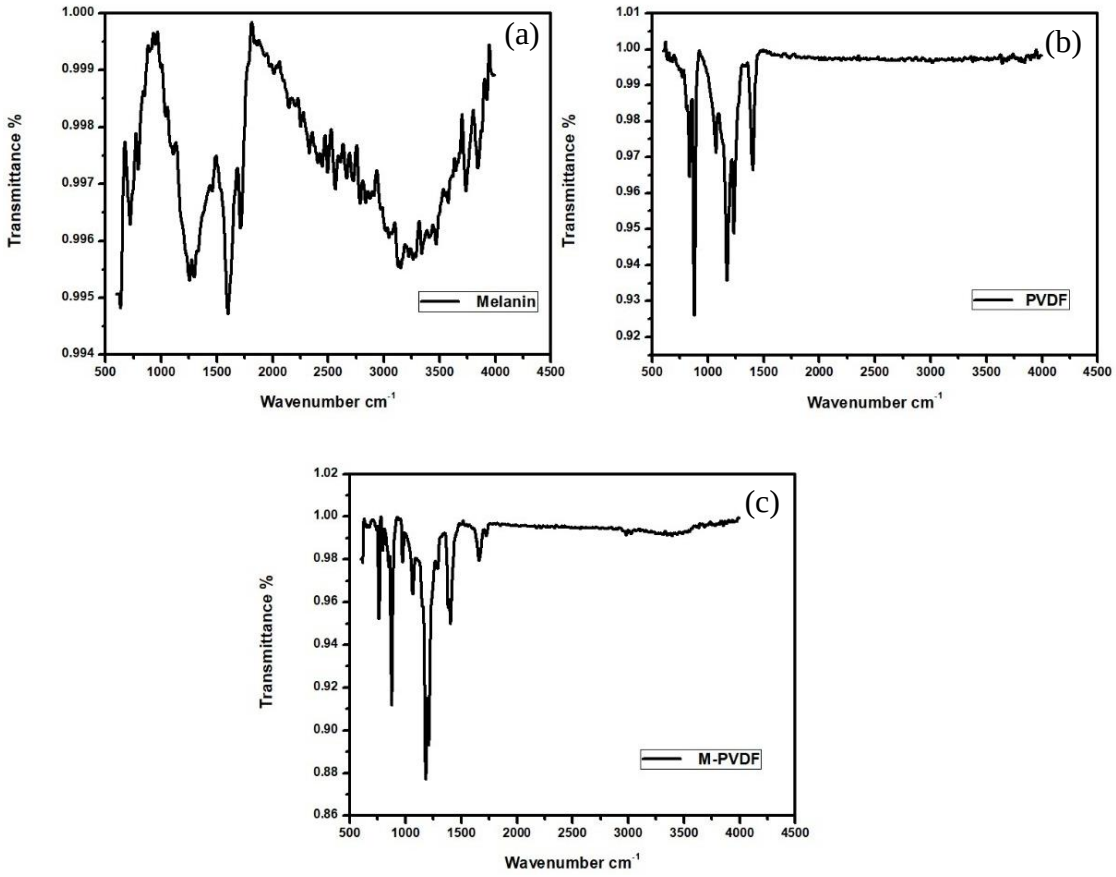

Figure 4.44. FTIR spectrum of (a) Melanin (b) PVDF (c) Melanin coated PVDF.

Considering the economic feasibility, the cost associated with the use of PVDF membranes is high. About half of the active sites of Melanin used for coating was engaged in bonding to PVDF membrane and hence were not available for heavy metal removal. The quantity of Melanin coated onto PVDF membrane was double that of what was used in Melanin impregnated hydrogel for obtaining the same amount of heavy metal removal. This accounts to wastage of Melanin.

4.5. Adsorption studies of heavy metals on Melanin impregnated activated carbon

Activated carbon is known for its adsorption capacities and is conventionally used for the purification of water in the household and commercial scales. Activated carbon has a positive charge in the lower pH range (Dai 1994). Melanin possesses a high negative charge in the pH range from pH 3 to near neutral, and hence it will bind to AC in that pH range by electrostatic and London dispersion forces (Silva et al. 1996).

4.5.1. Characterisation of Melanin bound activated carbon

4.5.1.1. Surface morphological studies with SEM

Fig. 4.45 (a) and (b) shows the SEM images of activated carbon at different magnifications and Fig. 4.45 (c), (d) and (e) shows Melanin impregnated onto activated carbon. Fig. 4.45 (e) shows the uniform coating of Melanin on activated carbon.

4.5.2. Coating studies of Melanin on to activated carbon

Coating studies revealed that efficient binding to Melanin onto activated carbon occurred at temperatures between 30ºC to 35ºC. Hence further coating experiments were conducted at room temperature. The spectrophotometric analysis showed that 98 to 99% Melanin got strongly impregnated on to activated carbon. There was a release of 104 µg of melanin during the first and second wash while further washing did not show melanin liberation from activated carbon.

4.5.3. Adsorption studies

Melanin impregnated activated carbon was used for the removal studies of Hg (II), Pb (II), Cr (VI) and Cu (II) from water. The effect of parameters like time, pH and temperature on removal of heavy metals were studied by batch mode of operation. Melanin impregnated activated carbon showed comparable adsorption efficiencies during optimisation studies of different parameters. Heavy metal studies using activated carbon as control and melanin impregnated activated carbon illustrated that the later had 13 to 15 times more efficiency than former for Hg (II), Cr (VI), Pb (II) and Cu (II) removal.

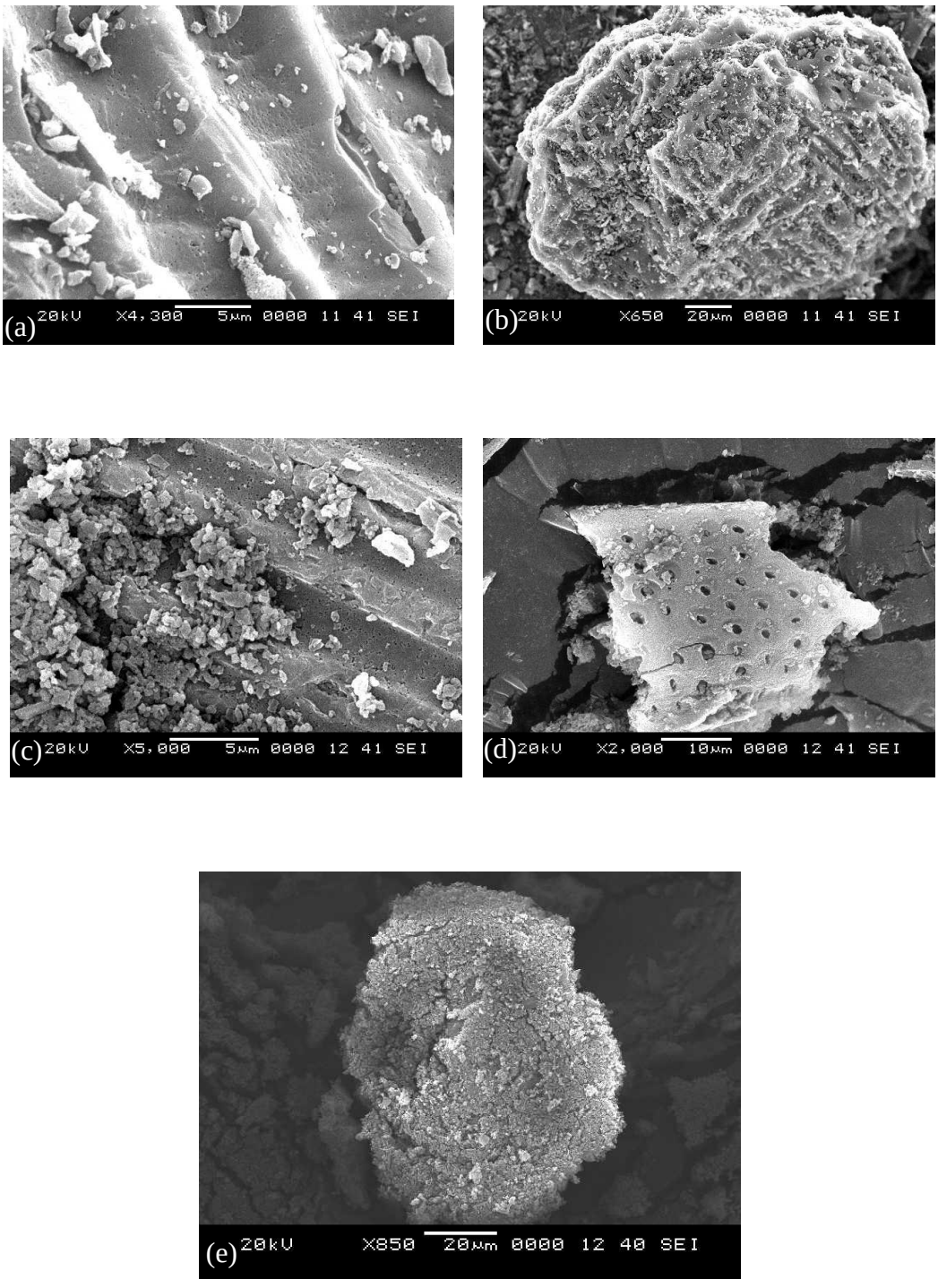

Figure 4.45. SEM images of (a) activated carbon at 5 µm (b) activated carbon at 20 µm; Melanin impregnated activated carbon at (c) 5 µm, (d) 10 µm (e) 20 µm

4.5.3.1. Effect of pH

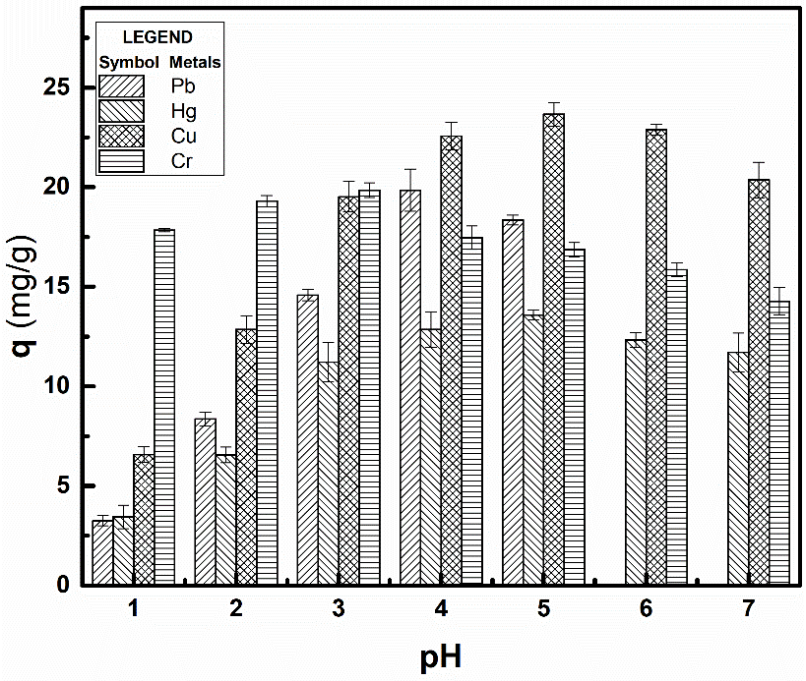

Figure 4.46. Amount of Cr (VI), Pb (II), Hg (II) and Cu (II) adsorbed onto Melanin at different pH (C_0 =5 mg/L, w = 0.2 g/L, rpm= 150, shaking diameter = 25 mm)

The effect of pH on heavy metal uptake was scrutinised in the range of 1.0 to 7.0 (Fig. 4.46). Maximum adsorption of Hg (II), Pb (II) and Cu (II) are observed at pH 5 and Cr (VI) at pH 3. The mechanism and efficiency of heavy metal binding to Melanin impregnated activated carbon is similar to the heavy metal adsorption studies on to free Melanin.

4.5.3.2. Effect of contact time

Adsorbent - Adsorbate contact time required for the adsorption process is a crucial factor in the case of adsorption experiments, and the results are shown in Fig. 4.47. Equilibrium state was attained within 90 minutes of contact time for all metals.

As the figure depicts, the entire adsorption process can be defined by two phases. The first phase corresponds to an initial fast uptake phase, which was mainly due to the high concentration gradient and availability of more binding sites on adsorbent which subsequently reached equilibrium mainly due to the decline of the concentration gradient and active metal binding sites deficit (Saini and Melo 2013). Maximum

binding of heavy metals happened within the first 45 minutes, and the next 120 minutes showed fairly uniform adsorption.

Heavy metal solutions equilibrated with 10 mg activated carbon was also analysed at different time intervals and found that activated carbon could remove only 6 to 8% of Pb (II), Cr (VI) and Cu (II) from 50 mL of heavy metal solution while Hg (II) was not removed by activated carbon. Melanin impregnated activated carbon proved to be 13 to 15 times more efficient in heavy metal removal than activated carbon.

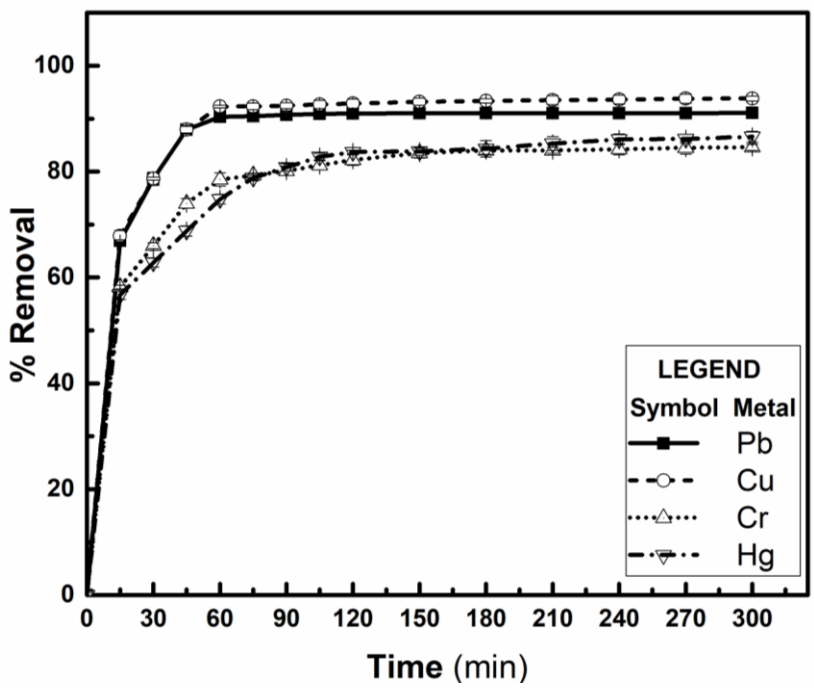

Figure 4.47. Percentage removal of heavy metals with respect to time (C_0 =5 mg/L, w = 0.2 g/L, rpm= 150, shaking diameter = 25 mm)

4.5.3.3. Effect of Temperature

Temperature is an important factor that affects adsorption. Hence, the effect of temperature on adsorption of heavy metals on Melanin impregnated activated carbon was studied at different temperatures 288, 298, 308, 318 and 328 K and the result obtained is shown in Fig. 4.48. It is noticeable that higher temperatures favoured the adsorption process in case of all studied metal ions, suggesting an endothermic process. The increase in uptake capacity at a higher temperature may be due to the increase in collision frequency between the adsorbent and the metal ions (Acharya et al. 2009; Saini and Melo 2013). With an increase in system temperature, the metals ions will

attain more kinetic energy to diffuse from the bulk phase of the solution to the solid phase of the adsorbent. At higher temperatures, some of the surface components attached with the biopolymer Melanin can get dissociated leading to the generation of more active sites to which the heavy metal can bind (Akpomie et al. 2015).

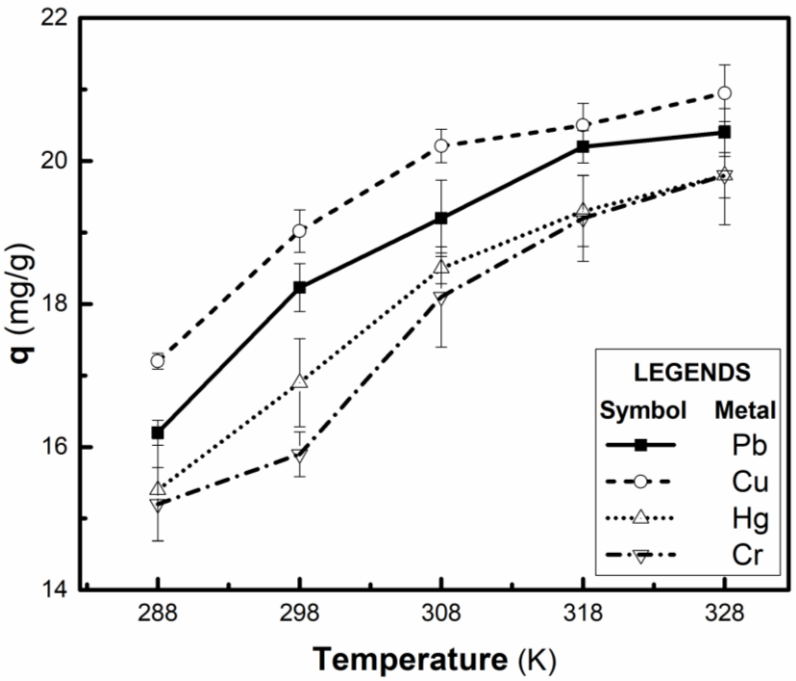

Figure 4.48. Amount of heavy metals adsorbed onto Melanin bound activated carbon at different temperatures (C_0 =5 mg/L, w = 0.2 g/L, rpm= 150, shaking diameter = 25 mm)

4.5.4. FTIR analysis of Melanin bound activated carbon

The FTIR spectrum of activated carbon did not include much of the peaks corresponding to bond stretching and vibrations (Fig. 4.49). Significant peaks were a few like 1228.5 and 3485.4 cm^{-1} which are bond stretching of –C-OH and –OH groups and are merely water content associated with the activated carbon. On the contrary, the Melanin spectrum exhibited a broad range of bond stretching and vibrations. Functional groups such as carbonyl, carboxyl, hydroxyl and amine groups were evident from the spectral studies. Melanin impregnated activated carbon exhibited the presence of functional groups by bond stretching peaks. These functional groups are the result of Melanin bound on to the activated carbon. Significant peaks are at wavenumbers 831.56 cm^{-1} which indicates –NH bond wag, 1022.20 and 1105.3 cm^{-1} indicating –CN stretching. 1647.90 cm^{-1} points the –NH bond stretching. 1711.45 cm^{-1} indicates the

presence of carbonyl groups and 2765.50 cm^{-1} showed the presence of either carbonyl or carboxyl group. –OH bonds were predominantly higher than that activated carbon had which is also from Melanin bound on to it. Carbon-carbon stretching, and vibrations were indicted for being higher than was there in activated carbon. Hence, FTIR analysis confirmed the binding of Melanin on to activated carbon.

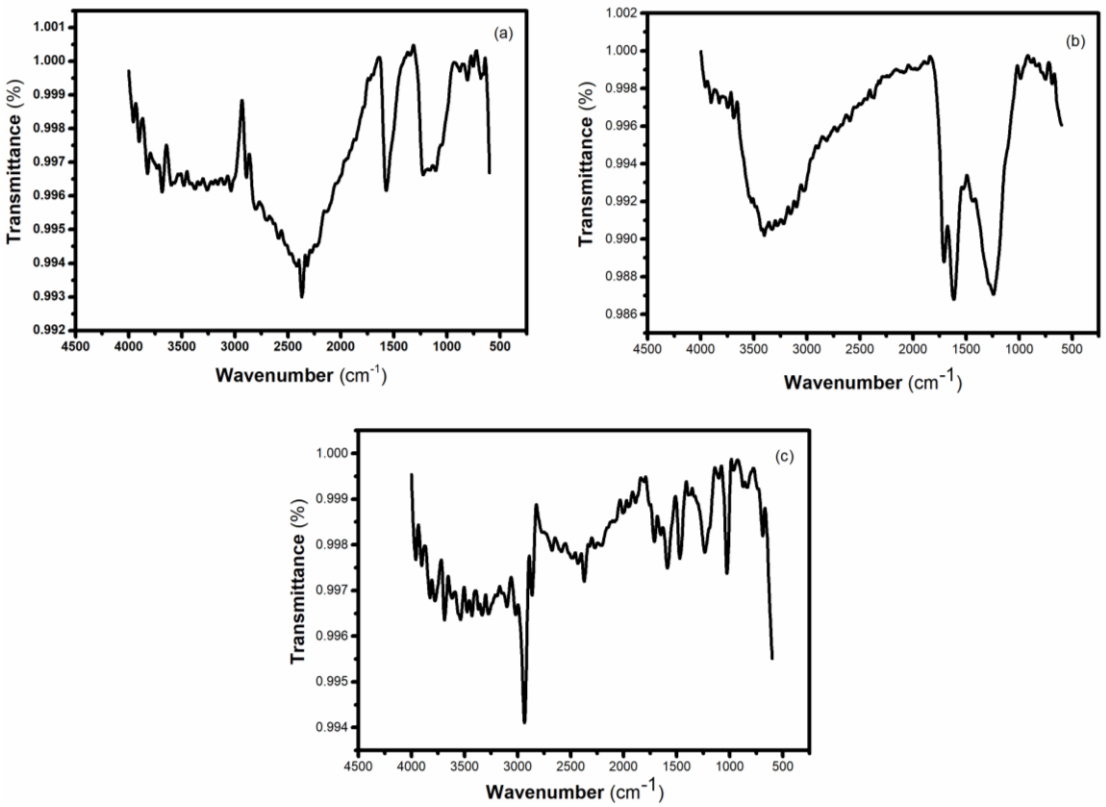

Figure 4.49. FTIR spectrum of (a) activated carbon (b) Melanin (c) Melanin bound activated carbon

4.5.5. Energy Dispersive Spectroscopy (EDS)

Elemental information was analysed from EDS spectra obtained from X-ray emissions caused by the high-intensity electron beam. The presence of heavy metal's peaks in EDS spectrum confirms the adsorption of it onto Melanin. Melanin bound activated carbon was washed with distilled water after adsorption experiments and centrifuged at 3000 rpm for 10 minutes and then dried in a vacuum oven maintained at 50ºC for 12 hours before the EDS analysis was conducted.

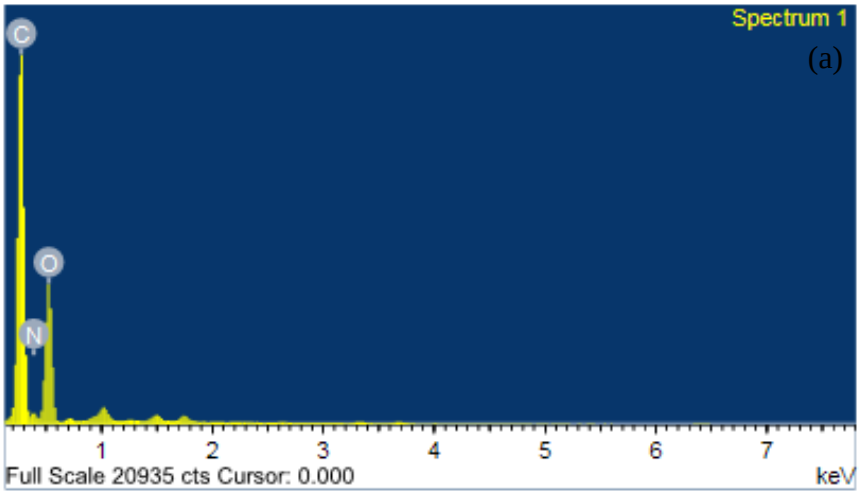
Spectrum 1
(a)
C
O
N
1
2
3
4
5
6
7
Full Scale 20935 cts Cursor: 0.000
keV

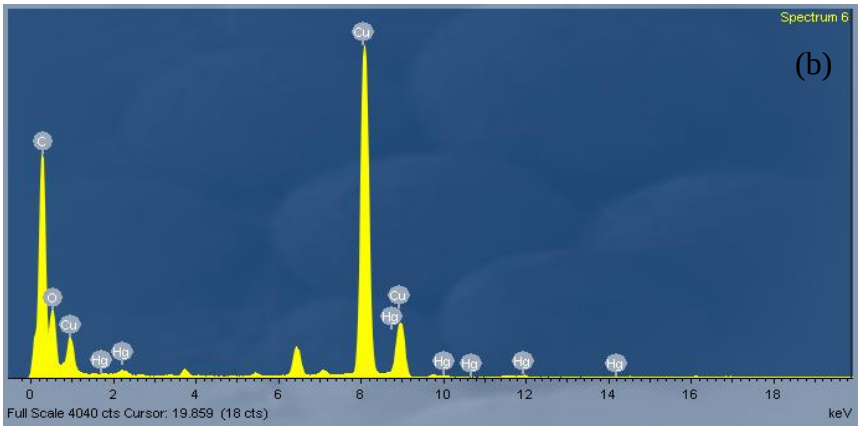
Spectrum 6
(b)
Cu
C
O
Cu
Hg
Hg
Cu
Hg
Hg
Hg
Hg
0
2
4
6
8
10
12
14
16
18
Full Scale 4040 cts Cursor: 19.859 (18 cts)
keV

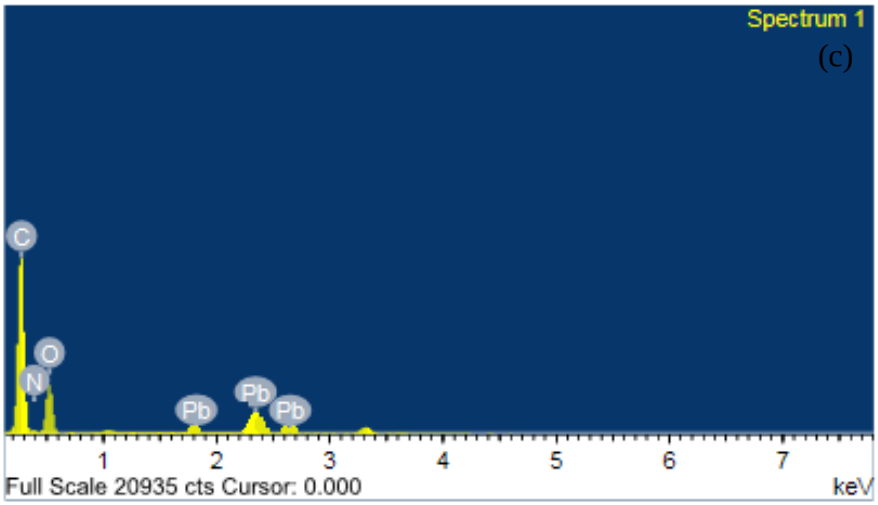
Spectrum 1
(c)
C
O
N
Pb
Pb
Pb
1
2
3
4
5
6
7
Full Scale 20935 cts Cursor: 0.000
keV

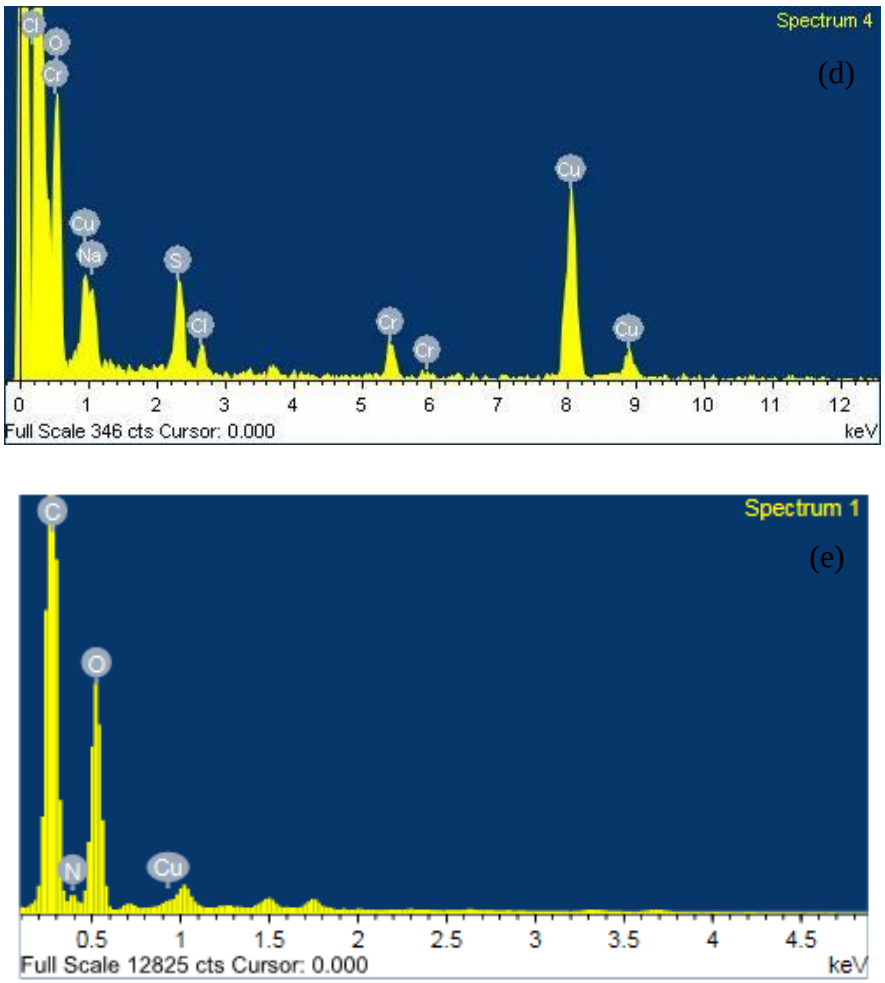

Figure 4.50. EDS analysis of (a) Melanin impregnated activated carbon and Melanin impregnated AC loaded with (b) Hg (II) (c) Cr (VI) (d) Pb (II) (e) Cu (II)

The EDS analysis has confirmed the presence of heavy metals in the Melanin impregnated activated carbon. Figure 4.50 (a) shows the EDS of Melanin impregnated activated carbon while (b), (c), (d) and (e) showed the presence of Hg (II), Cr (VI), Pb (II) and Cu (II) confirming it adsorption to the Melanin bound activated carbon.

Melanin bound activated carbon possess higher efficiency and is economically feasible. Activated carbon has a higher surface area to which Melanin can be uniformly impregnated. Its porous structure allows the intra-particular diffusion of metals from the liquid medium to Melanin impregnated on its surface and enhances heavy metal binding and its removal. Hence the future work direction is intended to be with Melanin impregnated activated carbon

4.6. Fixed bed column studies

To explore the large-scale applicability of Melanin impregnated activated carbon for the removal of heavy metals from drinking water and to understand the real-time effects, column studies need to be conducted using the optimised parameters from the batch studies. Schematic representation of the experimental set up is shown in Figure 3.1. Experiments on the removal of Hg (II), As (III), As (V), Pb (II), Cr (VI) and Cu (II) were conducted by varying one among the three parameters namely flow rate, heavy metal concentration, and adsorbent loading while keeping the other two parameters constant.

4.6.1. Effect of flow rate

The effect of flow rate on heavy metal adsorption was studied by varying the flow rates (0.5, 1 and 1.5 mL/min). The column was packed with 100 mg Melanin impregnated activated carbon, and the inlet heavy metal concentration was 1 mg/L. From Fig. 4.51, it can be inferred that, as the flow rate increases, the steepness of the breakthrough curve increases. This can be due to the short contact time available for the heavy metals to bind to the active sites in Melanin. The active sites which are on the surface of Melanin will be used during high flow rate cases, and the intraparticle diffusion will be onerous leading to steeper breakthrough and a lower amount of adsorption of heavy metals to Melanin (Hayati et al. 2018).

4.6.2. Effect of inlet concentration of heavy metals

The effect of influent adsorbate concentration was studied by varying the heavy metal concentration (0.5, 1, 1.5 mg/L) (Fig. 4.52). 100 mg Melanin impregnated activated carbon was packed in the column, and the heavy metal solution was pumped at a flow rate of 0.5 mL/min for the study. As the heavy metal concentration increased, the breakthrough curve became steeper, and the breakthrough time was also reduced. At higher concentration of heavy metal feed solution, the concentration gradient between the feed solution and active sites in adsorbent will be high, which helps the heavy metals bind swiftly to the surface-active sites and then to diffuse into the pores and bind to the active sites. This leads to the swift exhaustion of the active sites, and hence,

breakthrough occurs faster and breakthrough time is also reduced (Mthombeni et al. 2018).

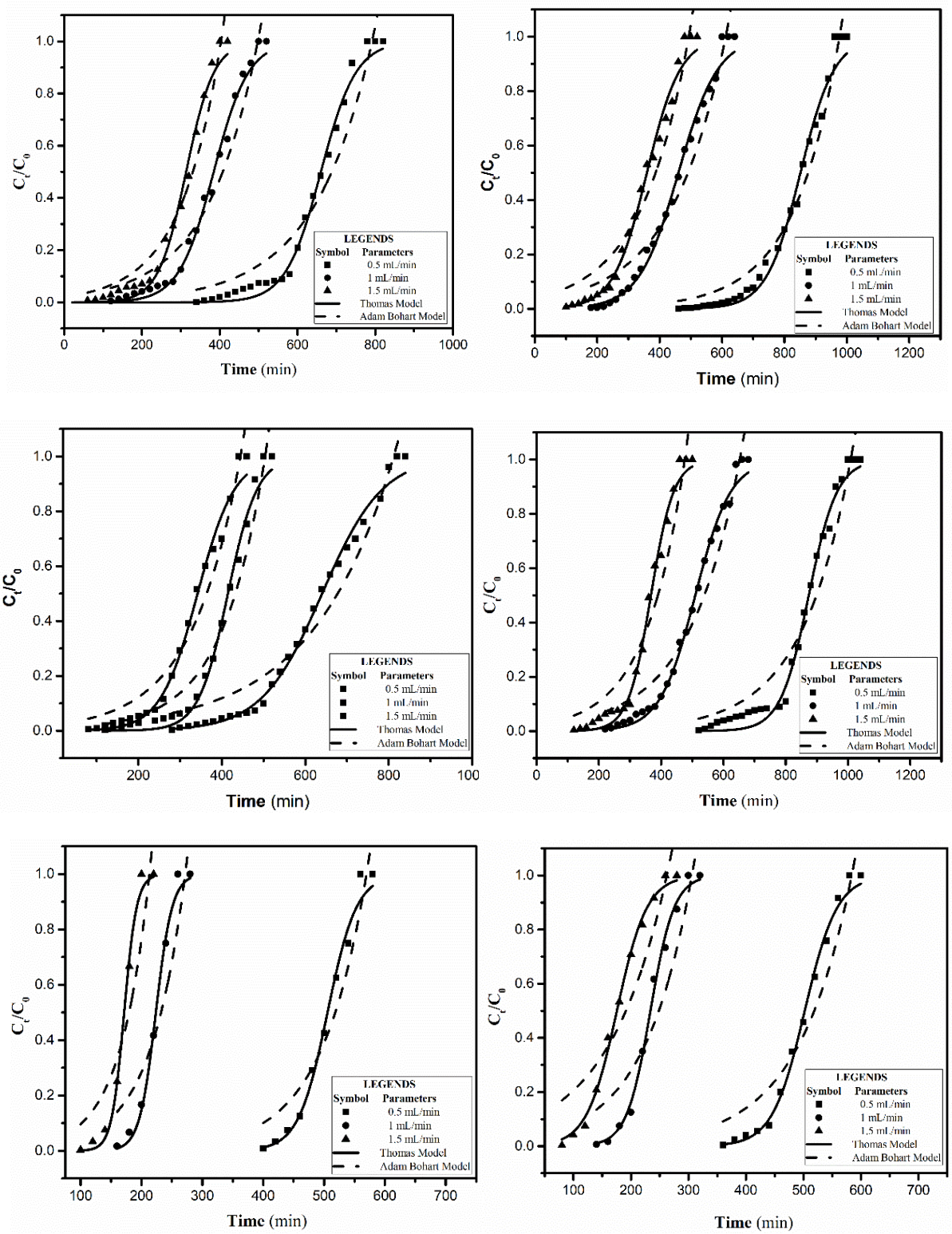

Figure 4.51. Effect of flowrate on breakthrough curve (a) Hg (II) (b) Pb (II) (c) Cr (VI) (d) Cu (II) (e) As (V) (f) As (III) [C_0=1 mg/L, v = 0.5, 1, 1.5 mL/min, w=100 mg, z= 90 mm]

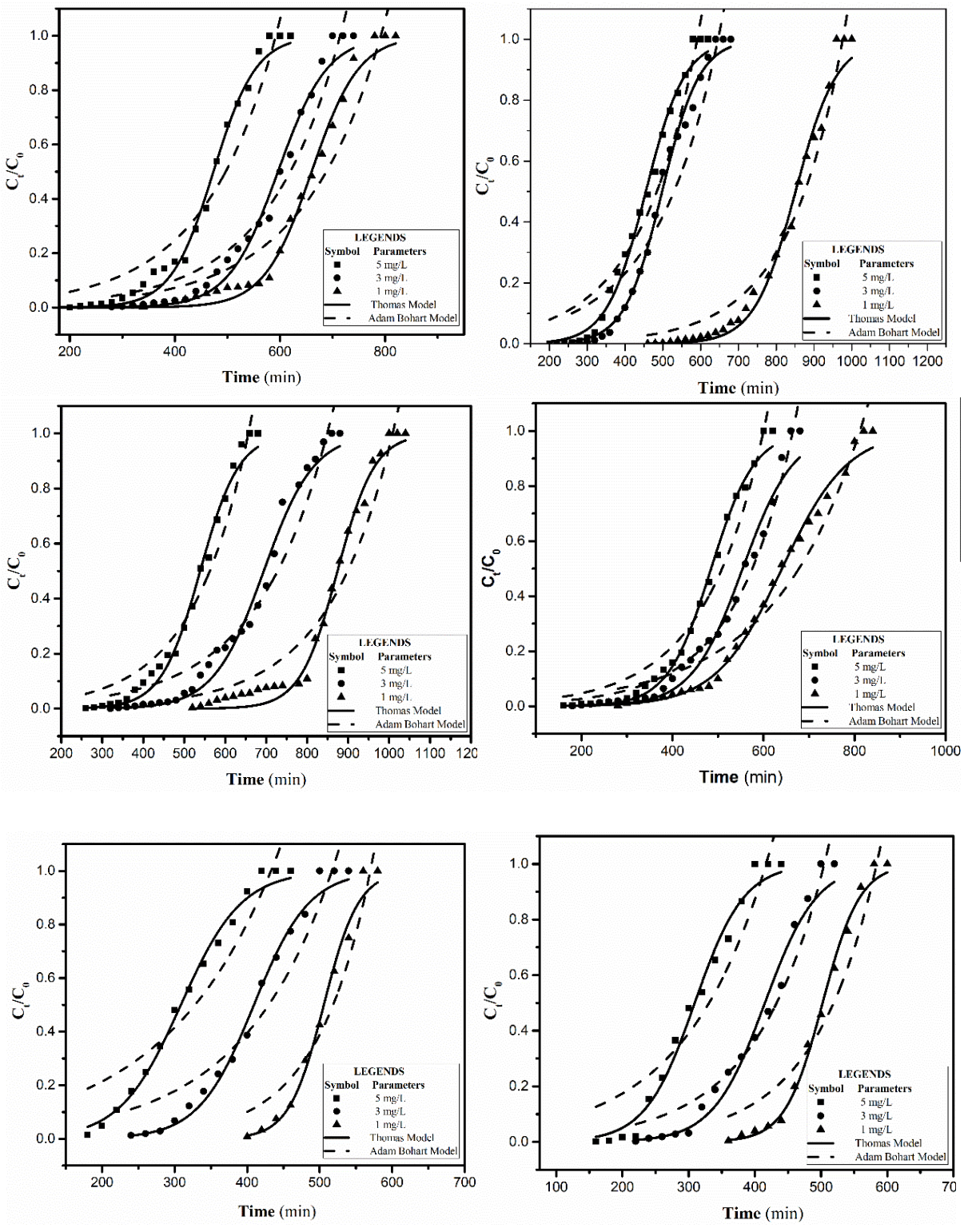

Figure 4.52. Effect of inlet concentration on breakthrough curve (a) Hg (II) (b) Pb (II) (c) Cr (VI) (d) Cu (II) (e) As (V) (f) As (III) [C_o= 1, 3, 5 mg/L, v=0.5 mL/min, w=100 mg, z= 90mm]

4.6.3. Effect of adsorbent loading

Figure 4.53 represents the breakthrough curve for Hg (II), As (III), As (V), Pb (II), Cr (VI) and Cu (II) adsorption at the flow rate of 0.5 mL/min and influent heavy metal concentration of 1 mg/L. Breakthrough point and time were enhanced as the adsorbent loading in the column increased. As adsorbent quantity increases, more active sites are available for the metal ions to bind and also the metal ion solution can be in contact with the adsorbent for a longer time, which improves the adsorption efficiency. Highest adsorption efficiency was achieved when adsorbent loading was highest; in this case, 100 mg of Melanin impregnated activated carbon showed the maximum heavy metal removal (Shahbazi et al. 2013). The parameters like amount adsorbed to the Melanin impregnated activated carbon, total metal ions entering the column, yield in % at different operating conditions are listed in Table 11.

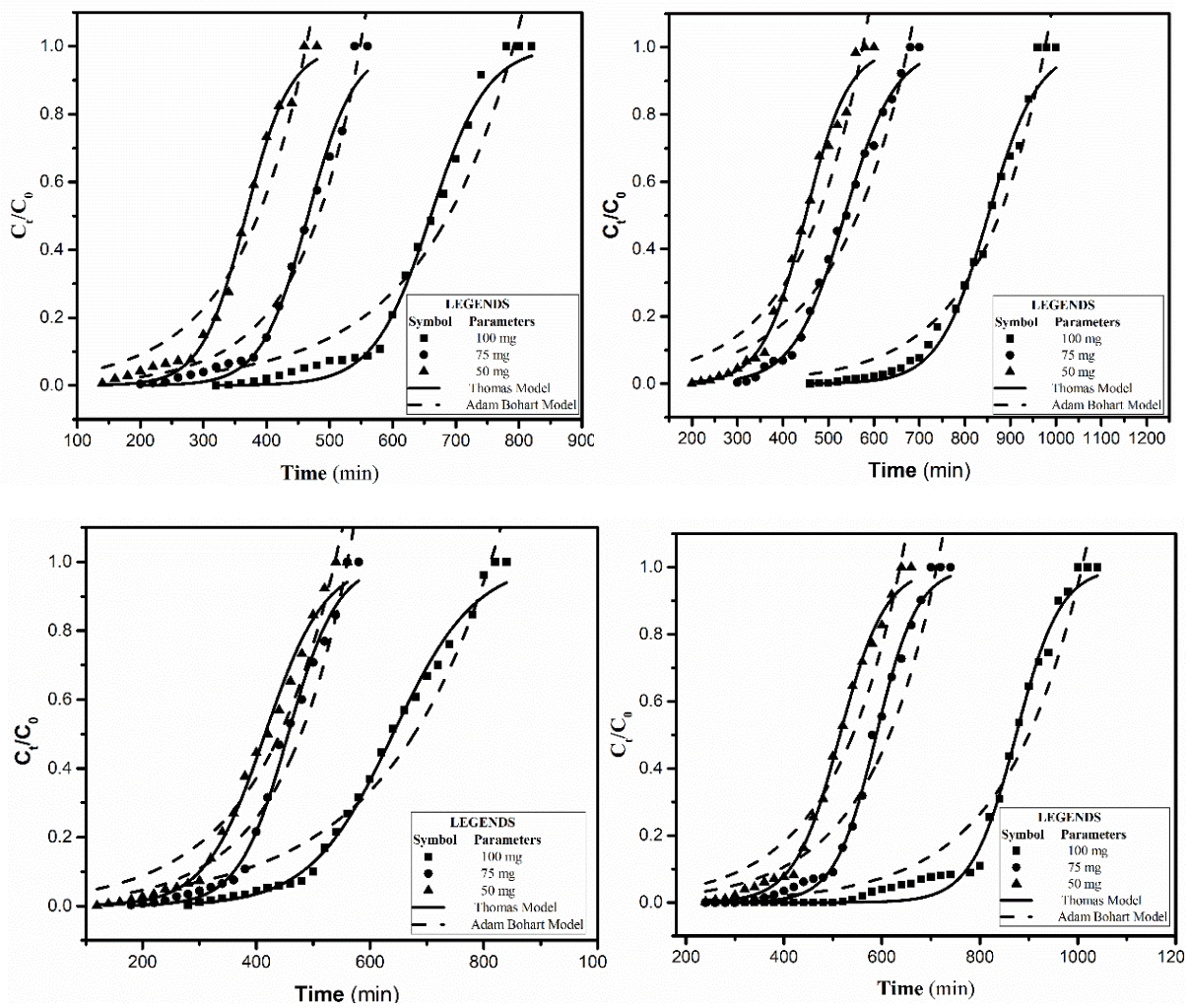

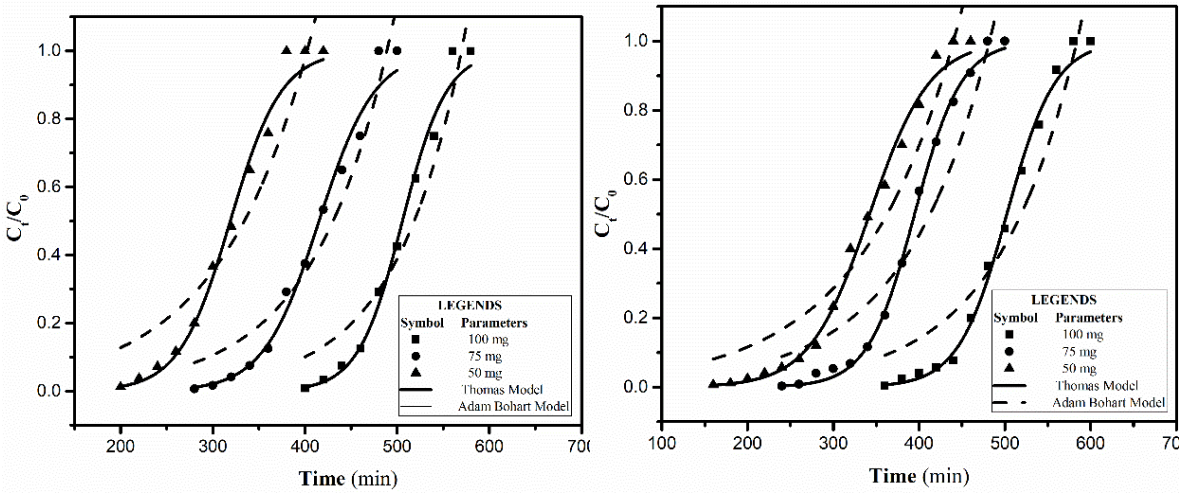

Figure 4.53. Effect of adsorbent loading on breakthrough curve (a) Hg (II) (b) Pb (II) (c) Cr (VI) (d) Cu (II) (e) As (V) (f) As (III) [C_0=1 mg/L, v=0.5 mL/min, z= 45, 67.5, 90 mm]

The breakthrough point was attained within 320 min for Hg (II), 380 min for As (V), 340 min for As (III), 440 min for Pb (II), 260 min for Cr (VI), 500 min for Cu (II). Breakthrough volume obtained at optimised conditions are 160 mL for Hg (II), 190 mL for As (V), 170 mL for As (III), 220 mL for Pb (II), 120 mL for Cr (VI), 220 mL for Cu (II). Continuous adsorption studies using 25 mg activated carbon as the fixed bed was conducted using optimised parameters from the study and the breakthrough curves are shown in Appendix Fig. 8. The breakthrough was attained very fast, and the insignificant quantity of heavy metals seemed to have removed. Batch adsorption studies on removal of mercury using activated carbon showed no significant removal, and hence continuous studies were not performed for the same.

4.6.4. Dynamic adsorption analysis

Thomas model and Adam-Bohart's model were used to study the dynamic adsorption behaviour in the fixed bed column. Experimental data were modelled in Equation 16 and 17 to validate the models. Based on the fitting by linear regression analysis, Thomas model seemed to be valid for the adsorption of heavy metals onto Melanin impregnated activated carbon loaded column. The assumptions of the Thomas model are hence valid in the column adsorption studies for the removal of heavy metals using melanin impregnated activated carbon. The assumptions of the Thomas model are:

1. There is plug flow in the bed.

2. The adsorption equilibrium follows the Langmuir adsorption model.
3. The kinetics of adsorption follows a second-order reversible reaction without axial dispersion.

4.7. Characterisation of Melanin after adsorption of heavy metals

Melanin was analysed after adsorption of heavy metals using FTIR spectroscopy to understand the binding of heavy metals to the functional groups present in melanin. XPS analysis was conducted to understand the state of heavy metals after adsorption to melanin

4.7.1. FT-IR analysis of pure and heavy metal loaded Melanin

Fourier-transform infrared spectroscopy was used to identify the vibrational characteristics of functional groups present on the surface of Melanin (Fig. 4.54). In the FTIR spectrum of Melanin the characteristic absorption band of C-N was identified at wave number 1246.89 cm^{-1}, N-H of the amino group at 1609.52 cm^{-1}, C=O stretching at 1708.09 cm^{-1}, -OH group at 3224.62 and 3330.25 cm^{-1}. The spectrum of heavy metal bound Melanin had shown an increase in % transmittance, indicating that the heavy metals are bound to these functional groups. Increased intensity of the C-N stretching peak at wavenumber 1245.60 cm^{-1} indicated binding of Pb (II) to C-N group of Melanin. Cu (II), Hg (II) and Cr (VI) binding to C-N group were indicated by an increase in % transmittance of the peak at 1245.90 cm^{-1}, 1238.36 cm^{-1} and 1228.68 cm^{-1} respectively.

The transmittance intensity of N-H group at 1609.52 cm^{-1} have increased after Pb (II), Hg (II), Cu (II) and Cr (VI) binding, but have shifted to 1601.23 cm, 1617.39, 1611.17 and 1614.84 cm^{-1} respectively. The shifting of a peak to higher wavenumbers indicates chemical bonding of heavy metals to the functional groups. The functional group, C=O corresponding to wave number 1708.09 cm-1, have also shown an increase in % transmittance and a shift to a lower frequency of 1703.59, 1702.82, 1701.94 and 1704.88 cm^{-1} after Pb (II), Cu (II), Hg (II) and Cr (VI) binding respectively. Shifting of peaks to lower wavenumbers can likely be caused by the high electron density induced by the heavy metals bound adjacent functional groups.

Table 11. Parameters of continuous column adsorption with experimental adsorption column capacity.

Heavy metal	**Inlet concentration, *C* (mg/L)**	**Inlet flow rate, *v* (mL/min)**	**Adsorbent loading, *w* (mg)**	**q_e (mg/g)**	**M_{total} (mg)**	**Yield (%)**
Pb (II)	5	0.5	100	11.03	1.48	74.61
	3	0.5	100	7.65	1.06	72.41
	1	0.5	100	5.23	0.62	83.83
	1	1	100	5.65	0.86	65.92
	1	1.5	100	6.53	1.17	55.78
	1	0.5	75	4.45	0.44	75.46
	1	0.5	50	5.55	0.38	73.67
Cu (II)	5	0.5	100	13.03	1.68	77.45
	3	0.5	100	10.56	1.37	76.73
	1	0.5	100	4.52	0.56	80.90
	1	1	100	5.32	0.66	80.61
	1	1.5	100	5.64	0.83	68.33

	1	0.5	75	4.07	0.39	77.13
	1	0.5	50	5.39	0.35	76.5
Hg (II)	5	0.5	100	11.59	1.61	71.92
	3	0.5	100	9.08	1.18	76.65
	1	0.5	100	3.79	0.49	78.99
	1	1	100	4.29	0.62	68.80
	1	1.5	100	5.13	0.76	67.86
	1	0.5	75	3.51	0.36	76.30
	1	0.5	50	4.09	0.29	71.13
Cr (VI)	5	0.5	100	11.69	1.63	71.62
	3	0.5	100	8.09	1.08	74.58
	1	0.5	100	3.97	0.51	78.39
	1	1	100	4.77	0.65	73.44
	1	1.5	100	6.17	0.86	72
	1	0.5	75	3.74	0.36	77.14

	1	0.5	50	5.06	0.35	72.17
As (V)	5	0.5	100	7.48	1.19	62.61
	3	0.5	100	5.97	0.81	74.13
	1	0.5	100	2.9	0.35	83.33
	1	1.0	100	2.42	0.35	72.02
	1	1.5	100	2.68	0.36	74.72
	1	0.5	75	3.14	0.3	78.54
	1	0.5	50	3.55	0.25	70.48
As (III)	5	0.5	100	7.10	1.14	65.63
	3	0.5	100	6.23	0.83	74.90
	1	0.5	100	2.86	0.36	79.69
	1	1.0	100	2.53	0.38	66.10
	1	1.5	100	2.80	0.47	59.97
	1	0.5	75	2.97	0.3	74.17
	1	0.5	50	3.84	0.26	72.65

Table 12. Adam-Bohart's and Thomas model parameters for heavy metal removal in the fixed bed under different operating conditions.

Heavy metals	***C* (mg/L)**	***v* (mL/min)**	***m* (g)**	**K_{AB} (L/min·mg)**	**N_o (mg/g)**	**R^2**	**K_{TH} (mL/min·mg)**	***q* (mg/g)**	**R^2**	**$q_{e,\ exp}$**
Pb (II)	5	0.5	100	1.27	2.63	0.93	3.78	11.61	0.99	11.03
	3	0.5	100	1.86	1.81	0.9	6.29	7.97	0.99	7.64
	1	0.5	100	5.31	1.11	0.96	14.1	5.53	0.99	5.23
	1	1	100	4.42	1.39	0.95	12.12	5.98	0.99	5.66
	1	1.5	100	5.04	1.68	0.94	14.28	6.97	0.98	6.52
	1	0.5	75	4.82	1.02	0.93	13.77	4.64	0.99	4.45
	1	0.5	50	5.44	1.31	0.93	16.25	5.85	0.99	5.55
Cu (II)	5	0.5	100	1.45	2.92	0.95	4.12	13.74	0.99	13.04
	3	0.5	100	1.79	2.37	0.95	5.09	11.1	0.99	10.56
	1	0.5	100	5.75	0.97	0.93	19.99	4.81	0.99	4.54
	1	1	100	5.56	1.25	0.94	15.98	5.61	0.99	5.32
	1	1.5	100	7.33	1.37	0.92	24.97	6.03	0.99	5.64

	1	0.5	75	6.54	0.91	0.93	21.57	4.32	0.99	4.07
	1	0.5	50	6.56	1.22	0.94	19.49	5.66	0.99	5.39
Hg (II)	5	0.5	100	1.39	2.69	0.92	4.74	12.31	0.99	11.59
	3	0.5	100	2.28	1.99	0.95	6.63	9.54	0.99	9.08
	1	0.5	100	5.59	0.83	0.93	18.43	3.96	0.99	3.79
	1	1	100	6.39	1.04	0.95	18.59	4.61	0.99	4.29
	1	1.5	100	7.99	1.27	0.95	23.22	5.61	0.99	5.13
	1	0.5	75	8.78	0.76	0.97	22.5	3.72	0.98	3.51
	1	0.5	50	7.6	0.97	0.94	23.76	4.40	0.99	4.09
Cr (VI)	5	0.5	100	1.49	2.67	0.96	4.09	12.36	0.99	11.69
	3	0.5	100	2.51	1.79	0.97	5.76	8.59	0.98	8.09
	1	0.5	100	3.98	0.92	0.95	10.58	4.16	0.99	3.97
	1	1	100	7.48	1.14	0.96	21.86	5.39	0.99	4.77
	1	1.5	100	6.62	1.51	0.96	17.26	6.64	0.99	6.18
	1	0.5	75	6.56	0.84	0.94	17.65	3.95	0.99	3.74

	1	0.5	50	5.51	1.22	0.95	14.68	5.39	0.99	5.07
As (V)	5	0.5	100	5.51	0.45	0.89	4.58	8.02	0.99	7.49
	3	0.5	100	2.56	1.4	0.91	8.45	6.34	0.99	5.97
	1	0.5	100	10.41	0.64	0.93	24.76	3.03	0.98	2.9
	1	1	100	14.62	0.56	0.87	21.68	2.68	0.99	2.42
	1	1.5	100	17.27	0.67	0.87	22.3	3.07	0.99	2.69
	1	0.5	75	9.91	0.68	0.94	20.36	3.33	0.98	3.14
	1	0.5	50	8.48	0.84	0.89	16.32	3.82	0.99	3.55
As (III)	5	0.5	100	1.54	1.89	0.89	5.15	8.03	0.99	7.11
	3	0.5	100	3.01	1.41	0.95	7.95	6.64	0.98	6.23
	1	0.5	100	8.88	0.61	0.92	17.48	3.01	0.99	2.87
	1	1	100	10.05	0.641	0.87	14.31	2.8	0.99	2.54
	1	1.5	100	8.12	0.82	0.87	18.78	3.144	0.99	2.81
	1	0.5	75	8.36	0.67	0.9	16.57	3.15	0.99	2.97
	1	0.5	50	7.47	0.92	0.92	12.77	4.10	0.93	3.83

Increase in intensity of transmittance was observed for –OH bonds corresponding to wavenumbers 3224.62 and 3330.25 cm^{-1} after heavy metal adsorption and the peak at 3330.25 cm^{-1} shifted to 3242.12, 3362.77, 3245.10 and 3213.76 cm^{-1} in case of Pb (II), Cu (II), Hg (II) and Cr (VI) binding respectively. Shifting of –OH and –NH functional group peaks to lower from higher wavenumbers is attributed to the binding of heavy metals (Sajjan et al. 2013).

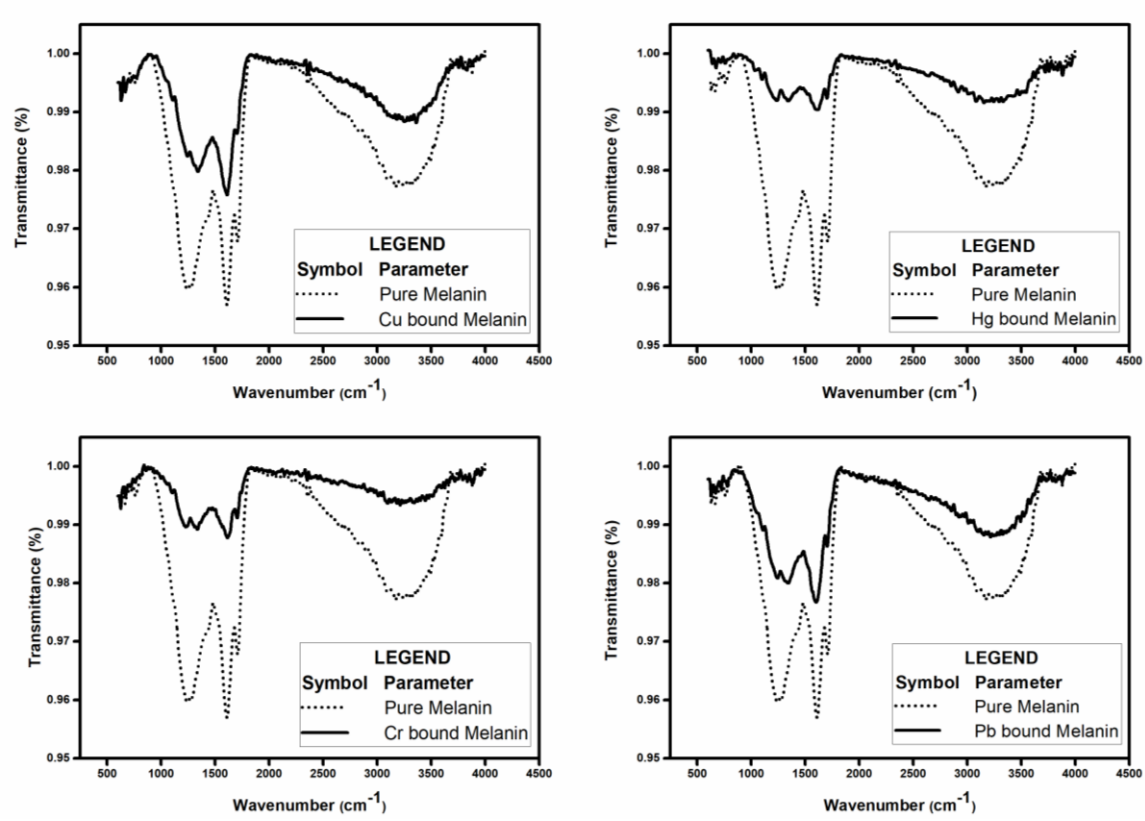

Figure 4.54. FTIR spectra of Melanin and heavy metal adsorbed Melanin

The spectra of Cr (VI) and Hg (II) bound Melanin showed an increase in % transmittance when compared to the spectra of Pb (II), and Cu (II) bound Melanin. Hexavalent chromium predominantly bound as negatively charged $HCrO_4^-$ and $Cr_2O_4^{2-}$ groups to positively charged Melanin. Hg (II) bound to negatively charged Melanin as $HgOH^+$ group. Meanwhile, Cu (II) and Pb (II) bound to negatively charged Melanin as Cu^{2+} and Pb^{2+} ions respectively. Presence of oxygen and hydrogen atoms in the adsorbed complexes of Cr (VI) and Hg (II) may be the reason for increased % transmittance observed (Liao et al. 2002).

FTIR studies revealed that the functionalization using iron followed by the heat treatment did not impart any chemical or physical deformation to Melanin and also showed that iron strongly adsorbed to Melanin (Fig. 4.55). Vibrational, as well as the intensity of transmittance, revealed that As (III) and As (V) have adsorbed to the iron that has been bound strongly to the different functional groups of Melanin.

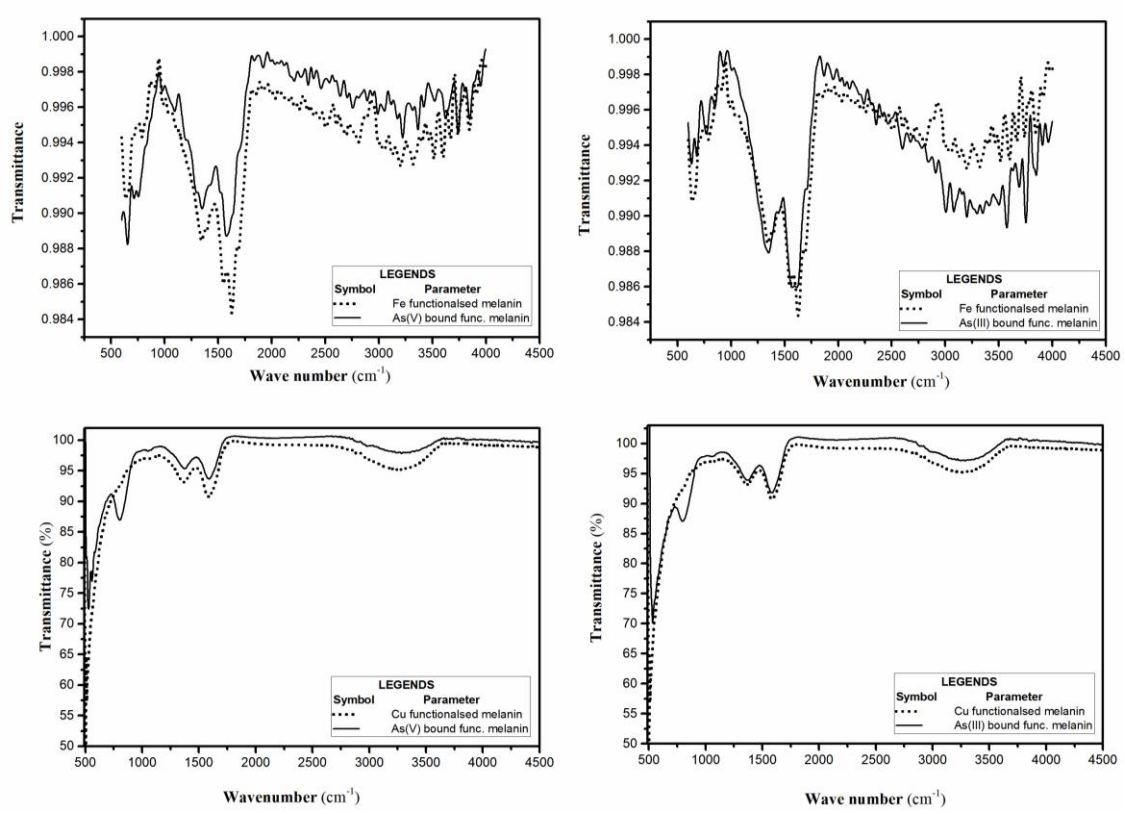

Figure 4.55. FTIR spectra of Melanin and heavy metal adsorbed Melanin

FTIR analysis of Melanin after Cu (II) adsorption and $KMnO_4$ treatment showed that prominently four transmittance peaks are significant. The vibrational stretching at 779.101 cm^{-1} corresponding to C-H out of plane group of aromatic groups in Melanin got shifted to 795.493 cm^{-1} and 808.028 cm^{-1} after As (V) and As (III) adsorption respectively. Unlike Fe-Melanin, the transmittance peak of Cu-Melanin did not shift to downward wavenumbers. The transmittance intensity increased after copper treatment and further increased on adsorption of As (III) and As (V). The transmittance at 1288.22 cm^{-1} which is the characteristic of C-O stretching of alcohol, carboxylic acid and carbonyl groups, 1607.38 cm^{-1} which denoted N-H bend of amine group present in Melanin, 3265.86 cm^{-1} which is the characteristic of -OH groups of alcohols

and carboxylic acids respectively, showed an increase in intensity of transmittance after adsorption, confirming the adsorption of Cu (II) to the functional groups and a forward shift in wavenumber indicated strong chemical bonding of copper and arsenic groups. The change in intensity of peaks confirmed the binding of arsenic groups to copper bound functional groups of Melanin. FTIR study also confirmed that copper adsorption followed by $KMnO_4$ treatment did not alter the basic structure and nature of Melanin (Pongpiachan 2014; Silverstein and Bassler 1962)

4.7.2. X-ray Photoelectron Spectroscopy (XPS)

XPS spectra high-resolution scans were studied for Hg, Cr, Pb and Cu on biosynthesised before and after adsorption. The spectra studies confirmed the adsorption of Hg 4f, Pb 4f, Cr 2p and Cu 2p on Melanin after it was equilibrated with individual solutions of heavy metals (Figure 4.55).

In the case of mercury, binding energy corresponding to $4f_{7/2}$ peak reference materials is only in the range of 99.9 to 101.4 eV (Hutson et al. 2007). The reference point of mercury (Hg^0) is 99.9 eV. The peaks in XPS data show a shift from 99.9 eV to 101.34 eV. The Hg 4f lines centred around 101.34 eV indicates that the Hg is in oxidised form. It must be inferred that there is not any Hg^0 since the $4f_{7/2}$ peak at 99.9 eV has shifted and it can be Hg^{2+} or $HgOH^+$ adsorbed on to Melanin (Wang et al., 2015). The spectrum analysis of lead bound Melanin has led to the identification of Pb $4f_{7/2}$ at 138.57 eV, which is the characteristic binding energy for Pb^{2+} ions. The $4f_{5/2}$ peak at 139.75 eV represents the binding energy of zero charged lead, which represents the adsorbed lead to the functional groups in Melanin (Bertrand and Fleischauer 1980). The spectrum analysis of Cr (VI) bound Melanin has identified a peak Cr $2p_{3/2}$ at 577.56 eV, which was decomposed to three peaks located at 576.35, 577.52 and 579.21 eV. First one corresponds to Cr_2O_3, the second one corresponds to $Cr(OH)_3$, and the last one corresponds to $Cr_2O_7^{2-}$ (Ithurbide et al. 2007).

The XPS results shed light on the mechanism of chromium adsorption. Some of the Cr (VI) ions on binding with positively charged functional groups will get reduced to Cr (III) ions (Duranoğlu et al. 2012). Both Cr (VI) and Cr (III) is adsorbed to the functional groups in Melanin. On analysis of the XPS spectra of Cu (II) bound Melanin, two peaks Cu $2p_{3/2}$ and Cu $2p_{1/2}$ with binding energies 934.08 and 954.03 eV were observed,

which are characteristic peaks of Cu^{2+}. Cu 2p satellite peak at 942.02 eV is also an indication of Cu^{2+}. The peaks corresponding to the binding energies at 931.83 and 952.4 eV can be inferred to Cu^0/Cu^+. The binding energies of Cu^0 and Cu^+ are very close. From XPS data, it can be confirmed that the Cu^{2+} on adsorption to functional groups in Melanin will reduce to Cu^0/Cu^+ (Li et al. 2018).

XPS analysis was performed to study the surface characteristics of copper, iron and As (III) and As (V) bound to Melanin. The data is baseline corrected in Origin Pro 2018 and plotted in XPSPEAK41.

Ferrous sulphate heptahydrate was made to adsorb on Melanin and heat treated at 90-100 °C. The XPS study of 2p peaks of iron showed characteristic peaks of Fe 2p 3/2 and Fe 2p at 711.1 eV and 725.7 eV respectively. Fe 2p 3/2 have an associated satellite peak which exits as a shoulder in the photoelectron peak and is located ahead by 4.3 eV binding energy as standard in the case of Fe^{2+}. The Fe 2p 3/2 peak corresponding to the binding energy 711.1 eV denotes Fe^{2+} oxidation state of iron as in $FeSO_4$. The peak 2p ½ corresponding to the binding energy 724.5 eV also represents iron in ferric state (Fe(II) (Descostes et al. 2000) (Fig. 4.57 (a).

Investigation of the electronic structure of copper adsorbed onto Melanin using XPS spectra showed the characteristic 2p peak (Fig. 4.57 (b)). Copper exhibited two peaks mainly at 934.58 and 952.92 eV, which corresponds to 2p 3/2 and 2p ½ respectively. Two shoulder satellite peaks are observed at 944.13 and 962.57 eV near to 2p 3/2 and 2p ½. Apart from the 2p 3/2 and 2p ½ peaks at specific binding energies, the shoulder satellite peaks also confirm the presence of copper in +2 oxidation states. The electrons from ligand state are transferred to d orbital to make the satellite peaks in XPS spectra, which is a unique character of Cu^{2+} (Chanquía et al. 2010; Li et al. 2015). As per the XPS spectrum of copper adsorbed melanin in Figure 4.56 (b), copper on adsorption to melanin is reduced to Cu (I) and Cu (0) states. Treatment of copper with $KMnO_4$ have oxidised copper to Copper (II) oxide form and impregnated it on to the surface of melanin (Franklin and Nnodimele 1994).

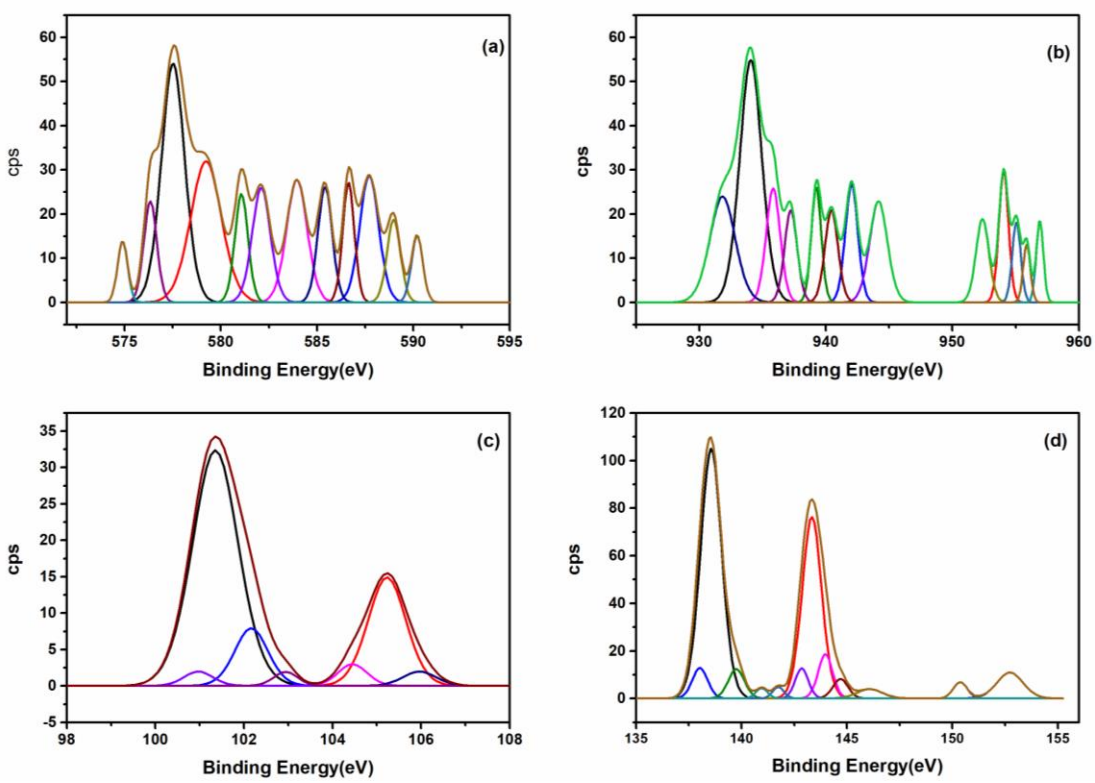

Figure 4.56. XPS elemental analysis of Melanin exposed to 10 mg/L heavy metal solution (a) Cr (VI) (b) Cu (II) (c) Hg (II) (d) Pb (II)

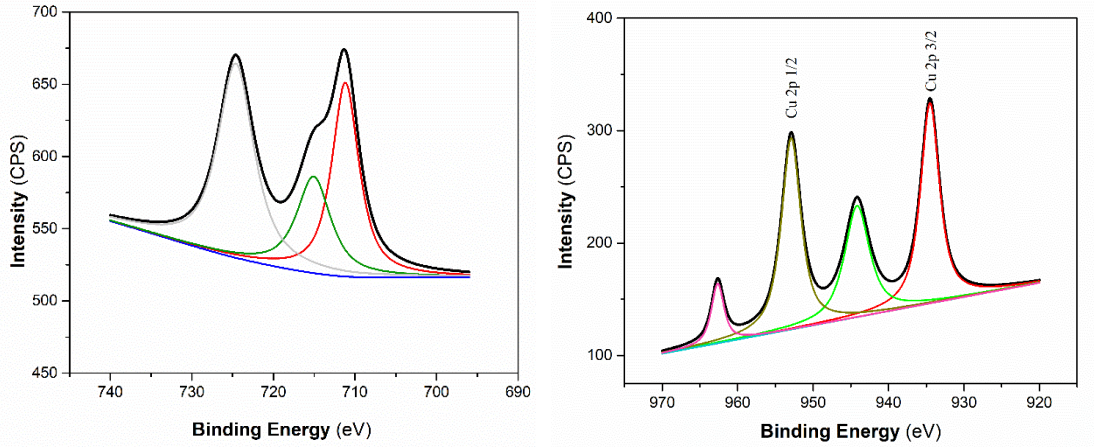

Figure 4.57. XPS spectrum of (a) iron (b) copper

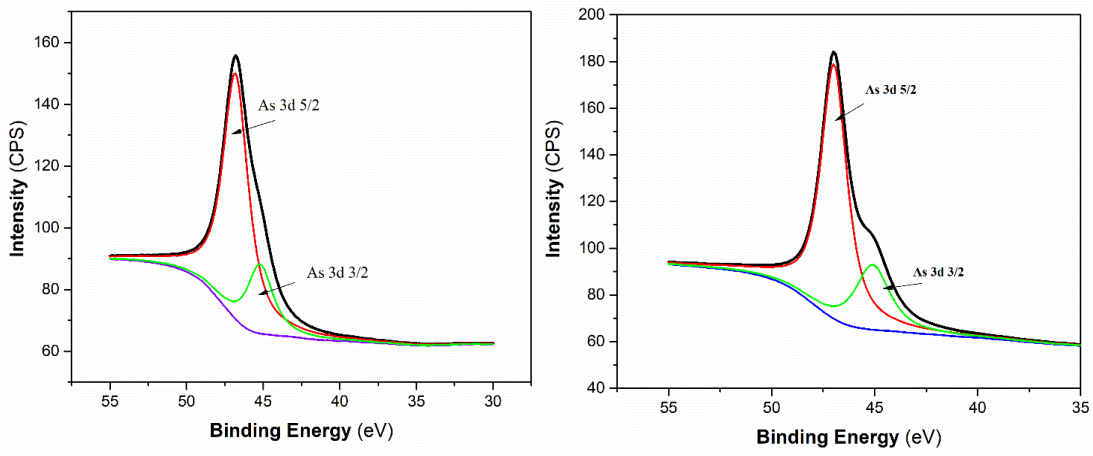

Figure 4.58. XPS spectra of (a) As (V) adsorbed to Fe-Melanin (b) As (III) adsorbed to Fe-Melanin.

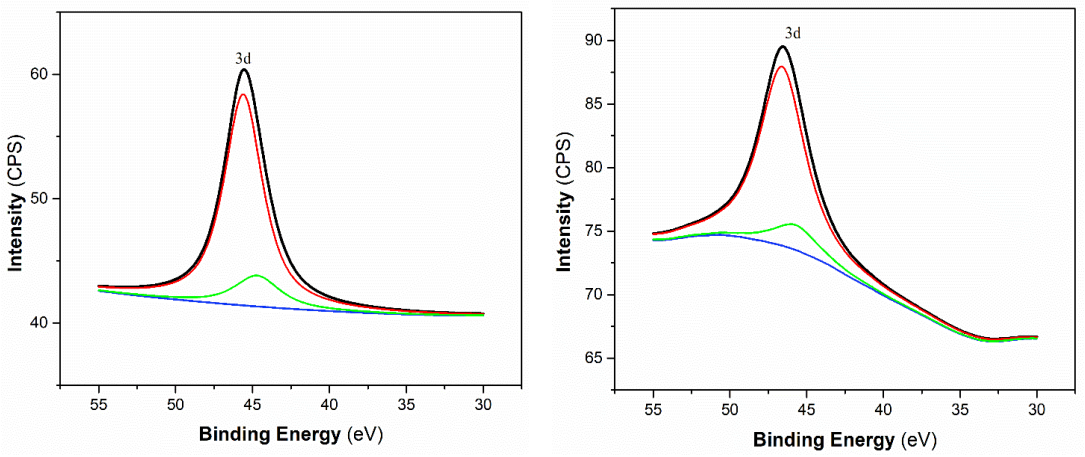

Figure 4.59. XPS spectra of (a) As (V) adsorbed to Fe-Melanin (b) As (III) adsorbed to Cu-Melanin.

The fate of arsenic species after adsorption was understood by analysing the 3d peaks of XPS spectra. The 3d peaks correspond to binding energies 46.99 eV and 46.83 eV for As (III) and As (V) respectively (Fig. 4.58 (a) and (b)). The 3d peaks confirm that arsenic is present as As (V) after adsorption to Fe-Melanin (Bang et al. 2005). As (III) takes a bit more time to attain equilibrium compared to As (V) adsorption, and this is due to the oxidation of As (III) to As (V) during binding to iron in Melanin (Bhowmick et al. 2014). Literatures suggests that the mechanism of adsorption of arsenic to iron is by electrostatic interaction and specific adsorption (Su and Puls 2001).

The XPS spectra of 3d peaks of arsenic bound to Cu-Melanin were analysed to understand the species of arsenic after adsorption (Fig. 4.59 (a) and (b)). The binding energies 46.57 eV and 45.61 eV corresponds to the 3d peaks of As (V) and As (III) bound to copper in Melanin. On further study, it may be evident that As (III) after binding to copper in Melanin got oxidised to As (V) and is bound firmly to copper bound Melanin (Martinson and Reddy 2009).

4.8. Desorption studies

Regeneration by desorption and further reuse makes an adsorbent fit for real-time applications like drinking water purification. Desorption regenerates the adsorption capacity of Melanin, prevents the heavy metals from causing secondary pollution by proper disposal after efficient recovery (Igberase et al. 2019) and also reduces the cost of adsorptive removal. Numerous factors influence the heavy metal desorption rate from the adsorbent such as the binding strength, extent of hydration of metal ions and the Melanin microstructure. For an efficient biosorbent, the adsorbed heavy metals need to be efficiently desorbed and concentrated using acids followed by selective recovery using various solvents by multistage stage precipitation and extraction (Jeon and Ha Park 2005). Different desorbing agents like acids, alkali, organic solvents are employed for removing heavy metals from the adsorbent and depends greatly on the nature of adsorbate, nature of adsorbent and the type of bonding between them. The factors to be considered on choosing a desorbing agent are the efficiency of desorption, non-toxicity, economic aspects and also polluting potential (Chatterjee and Abraham 2019).

Desorption was studied by washing Melanin loaded heavy metals using different desorbing agents, and significant effects were shown by citric acid, and HCl of concentration 0.5 N. 1 N and 3 N. Desorption was conducted for 3 hours, and metal ion concentration was analysed using AAS and ICP-OES. Considering the results in Figure 4.60, 3 N HCl removed more than 98% of Hg (II), Pb (II) and Cu (II) from Melanin while 1N citric acid desorbed around 98% Cr (VI) from Melanin.

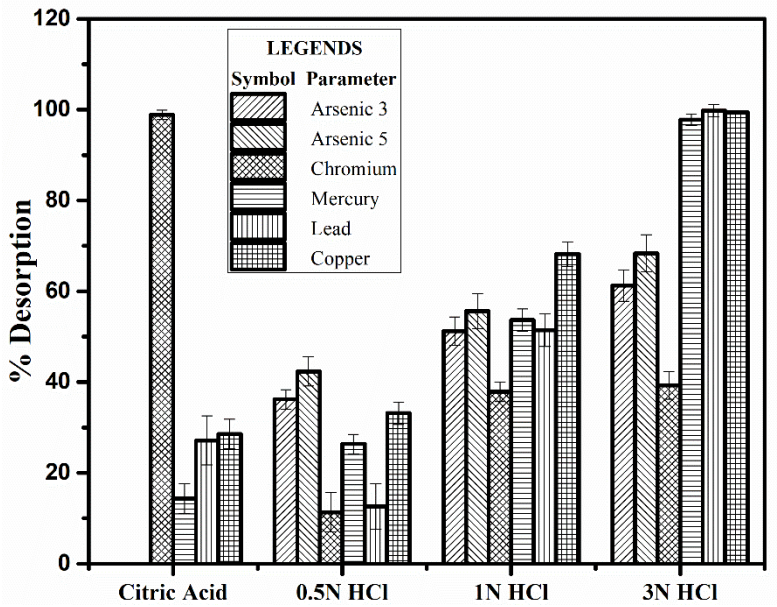

Figure 4.60. Percentage of heavy metals desorbed using various desorbing agents

Table 13. Percentage adsorption and desorption of various heavy metals in four successive cycles

Heavy metal	Cycles⟶	1	2	3	4
Pb (II)	Adsorption	91.02	90.5	88.5	85.36
	Desorption	99.79	98.02	97.36	95.25
Hg (II)	Adsorption	85.47	82.45	81.36	78.25
	Desorption	97.81	96.25	94.58	94.77
Cr (VI)	Adsorption	87.36	83.25	72.35	70.25
	Desorption	98.87	95.58	92.8	89.5
Cu (II)	Adsorption	95.6	95.32	91.58	88.36
	Desorption	99.41	96.78	94.87	90.14
As (V)	Adsorption	99.87	63.36	40.36	24.8
	Desorption	68.36	58.25	48.36	45.2
As (III)	Adsorption	98.97	54.36	33.36	19.25
	Desorption	61.25	64.58	50.3	48.2

Adsorption and desorption were repeated for four cycles to study the extent of Melanin regeneration and reuse. The regeneration study results shown in Table 13 indicates that the efficiency of adsorption decreases at a very low percentage per cycle for all metals except Cr (VI). The adsorption rates showed a considerable decreasing trend in the case of Cr (VI). The desorption studies of As (III) and As (V) from functionalised Melanin did not show significant efficiency of removal. Desorption of efficiency using 3 N HCl showed higher removal efficiency of 68.4% for As (V) and 61.25% for As (III). Acid treatment desorbed the impregnated iron leading to a slow functionality loss, which was recovered by re-functionalisation. Re-functionalised Melanin could remove arsenic from water at more than 99% efficiency for four cycles. The Melanin could hence be recovered and reused efficiently.

5. CONCLUSIONS

5.1. Summary of the work

The marine bacterium *Pseudomonas stutzeri* HMGM-7 was used for the biogenesis of Melanin nanoparticles. Melanin after purification was used for the removal of heavy metals such as divalent mercury, hexavalent chromium, divalent lead and divalent copper. Arsenic being a major groundwater pollutant in the Indian subcontinent was ineffectively binding to Melanin, for which, Melanin was functionalised using copper and iron which facilitated the competent removal of arsenic. Different physio-chemical properties of Melanin were studied using particle size analysis, zeta potential analysis, SEM, TEM, TGA, DSC, FTIR and XRD for Melanin while FT-IR, EDS and XPS analysis were conducted for Melanin before and after adsorption of heavy metals. The kinetic, thermodynamic and equilibrium studies on adsorption of heavy metals to melanin were conducted to optimise different parameters for its efficient batch mode removal. The kinetic studies comprised of the study on the effect of time followed by the modelling of the experimental data using the Lagergren's pseudo-first-order, pseudo-second-order and intra-particle diffusion models to understand the factors affecting adsorption and rate-limiting steps. The equilibrium studies revealed the effect of pH and thereby the mechanism of adsorption of heavy metals to Melanin. Two parameter and three parameter isotherm models were validated with the adsorbate concentration studies. The effect of temperature on adsorption was investigated by conducting the thermodynamic studies from which the thermodynamic parameters and activation energy of adsorption to Melanin were found out. The effect of competitive binding of each heavy metal to Melanin was analysed by performing a ternary system adsorption studies having an equimolar concentration of three metals of interest. The Melanin nanoparticles for the ease of being removed after adsorption was made to bind to different matrices. Melanin was immobilised in N, N-Diethylacrylamide hydrogel and conducted the batch adsorption studies for Cr (VI) removal. Longer equilibrium time, pH and temperature sensitivity were the cons associated with this system. This led to fabricate a precipitative dip coating of Melanin over PVDF membranes. Melanin coated PVDF membranes had only half the efficiency compared to free Melanin nanoparticles and also the cost associated with PVDF membranes was higher. The

hydrogel, as well as PVDF systems, cannot withstand iron and copper treatment of Melanin functionalisation. As the next method, Melanin was impregnated on activated carbon which was cheaply available, non-toxic and non-polluting. Melanin impregnated activated carbon had very close efficiencies in metal removal compared to free Melanin nanoparticles. Melanin had 17 to 19 times more efficacy in Pb (II), Cu (II) and Cr (VI) removal when compared to activated carbon while Hg (II) showed little binding to activated carbon. The batch adsorption studies were conducted with Melanin impregnated activated carbon and were proved to be an efficient system for heavy metal removal. Melanin impregnated activated carbon was then packed in the column as a fixed bed to remove heavy metals from the aqueous medium continuously. The influent liquid flow rate, heavy metal concentration and mass loading of adsorbent were varied to study its effects on continuous metal removal. Continuous adsorption models such as Thomas and Adam-Bohart's model were applied to the experimental data to find out the characteristic of the continuous adsorption system. The desorption studies were conducted to find the regeneration and reuse of Melanin. Different desorbing agents were used for the study, and adsorption-desorption cycles were investigated until four cycles of operation.

Summarising the outcomes of the dissertation, Melanin proved to be very efficient in the removal of Hg (II), As (III), As (V), Pb (II), Cr (VI) and Cu (II). The following conclusions were derived from adsorption studies of heavy metals using Melanin:

- The particle size analysis, as well as TEM studies, revealed that Melanin produced by the bacterium is nanosized in the range of 32 ± 98 nm. The SEM analysis showed Melanin to be aggregated globules of Melanin nanoparticles.
- FTIR analysis confirmed biosynthesised Melanin from *P. stutzeri* as eumelanin with functional groups such as carbonyl, carboxy, amino and hydroxy groups which acted as potent heavy metal binding sites.
- BET surface area analysis showed that the average surface area of Melanin is 26.455 m^2/g, and the average pore diameter is 3.657 nm. The TGA and DSC analysis confirmed that Melanin is chemically stable till 160 ºC.

- Iron impregnation of Melanin by adsorbing iron to Melanin followed by heat treatment at 100 ºC and copper impregnation by adsorbing copper to Melanin followed by $KMnO_4$ treatment resulted in functionalised Melanin for the removal of As (III) and As (V) from the water. The functionalisation procedure did not chemically destabilises Melanin.
- From the batch kinetic studies, it was found to take 90 minutes for Hg (II), Pb (II), Cr (VI) and Cu (II) to attain equilibrium while it took 50 minutes for As (III) and As (V) for Fe-Melanin and 80 minutes for Cu-carbon.
- Maximum adsorption for Hg, Pb and Cu was at pH 5 while it was 3 for Cr. Maximum As (III) and As (V) was adsorbed to Fe-Melanin at pH 4 while for Cu-Melanin the pH was in the range from 4 to 6.
- The Webber and Morris intraparticle diffusion model inferred that intraparticle diffusion is not the only rate limiting step and other phenomena like external diffusion can be adding up to the adsorption process. The Lagergren's pseudo-second-order model fitted well with the experimental data for all metals, indicating the process to be chemisorption.
- Maximum adsorption was shown at 328 K, and the thermodynamic parameters concluded that the adsorption of all heavy metals onto Melanin and functionalised Melanin are thermodynamically feasible and spontaneous. The adsorption process was found to be endothermic, and the entropy study inferred increased randomness at solids liquid interface. The activation energies of all metals binding to Melanin were below 40 kJ/mol, and hence the process was confirmed to be physical adsorption.
- The distribution coefficient from the adsorbate concentration studies showed a very high K_D value indicating that Melanin is efficient to remove heavy metals in water even at lower concentrations.
- Langmuir isotherm fitted well in case of two-parameter system affirming monolayer adsorption of heavy metals to Melanin. The maximum adsorption capacity obtained is 82.37, 147.49, 126.90 and 167.78 for Hg (II), Pb (II), Cr (VI), Cu (II) while 50.12, 39.98, 20.387 and 19.519 mg/g for As (V) and As (III) using Fe-Melanin and Cu-Melanin respectively in the adsorbate concentration range of 5

to 25 mg/L. The R-P isotherm model fitted well for all metals and substantiated that the adsorption process behaves akin to the Langmuir isotherm model.

- The competitive adsorption studies using ternary system demonstrated that Pb (II), Cu (II) and Cr (VI) have a higher affinity towards Melanin in the order specified.
- Hydrogel immobilised Melanin showed maximum adsorption of Cr (VI) at pH 7, equilibrium time of 30 hours and 318 K.
- Equilibrium was attained in the case of Melanin coated PVDF after 3.3 hours. The efficiency of heavy metal adsorption was about half than that of free Melanin.
- Except for a 1.5 to 2% decrease in efficiency, Melanin impregnated activated carbon showed comparable results of kinetic, equilibrium and thermodynamic adsorption of heavy metals.
- Continuous studies with Melanin impregnated activated carbon as the fixed bed in a column showed maximum breakthrough at a flow rate of 0.5 mL/min, the heavy metal influent concentration of 1 mg/L and adsorbent loading of 100 mg.
- Experimental data fitted with isotherm models showed the best fit with the Thomas model having the assumption that the column follows plug flow pattern and Langmuir adsorption model.
- The EDS confirmed the adsorption of heavy metals by quantifying the concentration of heavy metals in Melanin after adsorption. FTIR analysis examined the chemical characteristics of Melanin after adsorption and found that the heavy metal is bound to different functional groups in melanin.
- The XPS study showed the state of heavy metals after adsorption. As (III) was oxidised to As (V) during adsorption while Cr (VI) got reduced to Cr (III). Cu (II) changed to Cu (I) and Cu (0) after adsorption. Mercury got adsorbed in Hg (II) state itself.
- The desorption studies illustrated that 3 N HCl would remove more than 98 % of adsorbed Hg, Pb and Cu from Melanin while 1 N citric acid removed more than 98 % Cr (VI) from Melanin. 3 N HCl could remove the impregnated iron in Fe-Melanin, reducing the desorption as well as the next adsorption cycle. The functionalisation procedure was hence repeated to get better adsorption after dissolving the impregnated iron in 5 N HCl for desorbing the arsenic from melanin and to reuse melanin.

- Significant adsorption-desorption ability was shown by Melanin until four cycles of study.

5.2. Future scope of the study

Synthesis of Melanin in bioreactors to obtain large quantities of Melanin to be packed in a cartridge for standard household water purifier. This large scale kinetic and equilibrium studies can render Melanin for commercial applications. Melanin which is an efficient adsorbent for cation removal can also be used for the removal of anions like fluorine and even ionic and non-ionic surfactants from the water. Melanin being natural in origin without any toxic effects can be used for the recovery of many useful substances like acetic acid.

Recovery of heavy metals for reuse is one of the most important aspect of water treatment which prevents the heavy metals from returning to environment. The desorbing agents being highly acidic in nature imparts a devastating effect on different process envisaged for metal recovery. Heavy metals in groundwater are majorly in the concentration less than 10 mg/L. Melanin could remove heavy metals of very low concentration with very low dosage. The desorbing agents in the range of millilitres will be sufficient for treating grams of melanin. When the desorbed heavy metal concentration reaches around 1000 mg/L, chemical precipitation can be employed for precipitating out the metals from the desorbing agents. Different methods of chemical precipitation can be practised based on the type of heavy metals which all are ultimately dependent on the reduction of pH to the range of 5 to 9, One of the most common and conventional method is the use of lime or limestone. The metals may be precipitated out on its activity which on further purification can be reused (Barakat 2011). Even though there are various methods for heavy metal recovery from desorbing agents chemical precipitation can be efficient, economical, convenient and safe option and also the concentrated desorbing agents can be neutralised and made safe to the ecology. The exhausted melanin after heavy metal desorption can be send to landfills for disposal. Melanin being biological in origin can be degraded by microbial action.

LIST OF PUBLICATIONS AND CONFERENCES

Patents Filed

1. Removal of heavy metals from contaminated water by adsorption using Melanin bound activated carbon.
   Inventors: Keyur Raval, Vishnu M, Raj Mohan B.
   Application no: 201841000695, Reference Number: TEMP/E1/48394/2017- CHE.

2. Title: Method, system and apparatus for arsenic removal from water using functionalized Melanin.
   Application number: 201841047554, Reference No: TEMP/E-1/51794/2018-CHE
   Inventors: Raj Mohan Balakrishnan, Keyur Raval and Vishnu M

Research article

1. Manirethan, V., Raval, K., Rajan, R., Thaira, H., and Balakrishnan, R. M. (2018). "Kinetic and thermodynamic studies on the adsorption of heavy metals from aqueous solution by Melanin nanopigment obtained from marine source: Pseudomonas stutzeri." *Journal of Environmental Management*, 214, 315–324.

2. Thaira, H., Raval, K., Manirethan, V., and Balakrishnan, R. M. (2018). "Melanin nano-pigments for heavy metal remediation from water." *Separation Science and Technology*., 1–10.

3. Manirethan, V., Raval, K., Rajan, R., Thaira, H., and Balakrishnan, R. M. (2018). "Data supporting the adsorption studies of heavy metals from aqueous solution by Melanin nanopigment obtained from marine source: Pseudomonas stutzeri." *Data – in – Brief*, 20,178–189.

4. Manirethan, V., Gupta, N., Raval, K., and Balakrishnan, R. M. (2019). "Batch and continuous studies on the removal of heavy metals from aqueous solution using melanin coated PVDF membranes." *Environmental Science And Pollution Research*, (Accepted, In Press).

Conferences

1. Vishnu Manirethan, Keyur Raval and Raj Mohan B "Tetravalent selenium removal from aqueous solutions using biosynthesised Melanin coated PVDF membrane", G16-Asian: 5th International Conference on Research Frontiers in Chalcogen Cycle Science and Technology organised by UNESCO-IHE and NITK on December 19 -21, 2016, pp 18.

2. Vishnu Manirethan, Harsha Thaira, Keyur Raval and Raj Mohan Balakrishnan "Optimizing the Biosynthesis of Melanin Nano Particles and their Application in Heavy Metal Contaminated Ground Water Remediation". International Conference on 'Nanotechnology Applications: Chemical, Energy and Environment' Organised by SVNIT Surat on March 22-23, 2017.

3. Vishnu M, Reju Rajan, Raj Mohan Balakrishnan and Keyur Raval. "Heavy metal remediation from groundwater using bacterial Melanin", International Conference on Crystal Ball Vision on Science and Engineering for Societal Upliftment organised by Indian JSPS Alumni Association and CSIR-NIO Goa on 7th and 8th August 2017

4. Raj Mohan B, Vishnu Manirethan, Niharika Gupta and Keyur Raval. "Batch and continuous studies on the removal of heavy metals from aqueous solution using Melanin coated PVDF discs**"** was presented for "11th CESE conference, International Conference in Challenges in Environmental Science and Engineering" which was conducted from Bangkok, Thailand, 4th -8th November 2018.

Achievements

Represented the institute and presented our research work in the **"Festival of Innovation and Entrepreneurship (FINE) – 2018"** organised by the National Innovation Foundation – India (DST) at the **Rashtrapati Bhavan,** New Delhi on 19th March 2018.

REFERENCES

Abdel-Raouf, M. S., and Abdul-Raheim, A. R. M. (2017). "Removal of Heavy Metals from Industrial Waste Water by Biomass-Based Materials: A Review." *J Pollut Eff Cont*, 5, 180.

Abdel-Shafy, H. I., Abdel-Sabour, M. F., and Aly, R. O. (1998). "Adsorption of nickel and mercury from drinking water simulant by activated carbon." *Environ. Manag. Heal.*, 9(4), 170–175.

Abid, M., Niazi, N. K., Bibi, I., Farooqi, A., Ok, Y. S., Kunhikrishnan, A., Ali, F., Ali, S., Igalavithana, A. D., and Arshad, M. (2016). "Arsenic (V) biosorption by charred orange peel in aqueous environments." *Int. J. Phytoremediation*, 18(5), 442–449.

Acharya, J., Sahu, J. N., Sahoo, B. K., Mohanty, C. R., and Meikap, B. C. (2009). "Removal of chromium (VI) from wastewater by activated carbon developed from Tamarind wood activated with zinc chloride." *Chem. Eng. J.*, 150(1), 25–39.

Akpomie, K. G., Dawodu, F. A., and Adebowale, K. O. (2015). "Mechanism on the sorption of heavy metals from binary-solution by a low cost montmorillonite and its desorption potential." *Alexandria Eng. J.*, 54(3), 757–767.

AL-Othman, Z. A., Ali, R., and Naushad, M. (2012). "Hexavalent chromium removal from aqueous medium by activated carbon prepared from peanut shell: Adsorption kinetics, equilibrium and thermodynamic studies." *Chem. Eng. J.*, 184, 238-247.

Albadarin, A. B., Al-lagtah, N., Salameh, Y., Ahmad, M. N. M., Allen, S. J., and Walker, G. M. (2011). "Biosorption of toxic chromium from aqueous phase by lignin: mechanism, effect of other metal ions and salts." *Chem. Eng. J.*, 169, 1-3.

Ali, R. M., Hamad, H. A., Hussein, M. M., and Malash, G. F. (2016). "Potential of using green adsorbent of heavy metal removal from aqueous solutions: Adsorption kinetics, isotherm, thermodynamic, mechanism and economic analysis." *Ecol. Eng.*, 91, 317–332.

Allen, S. J., and Brown, P. A. (1995). "Isotherm analyses for single component and multi-component metal sorption onto lignite." *J. Chem. Technol. Biotechnol.*, 62(1), 17–24.

Alswat, A. A., Ahmad, M. Bin, and Saleh, T. A. (2016). “Zeolite modified with copper oxide and iron oxide for lead and arsenic adsorption from aqueous solutions.” *J. Water Supply Res. Technol.*, 65(6), 465–479.

Aly, Z., Graulet, A., Scales, N., and Hanley, T. (2014). “Removal of aluminium from aqueous solutions using PAN-based adsorbents: characterisation, kinetics, equilibrium and thermodynamic studies.” *Environ. Sci. Pollut. Res.*, 21(5), 3972–3986.

Anagnostopoulos, V. A., Manariotis, I. D., Karapanagioti, H. K., and Chrysikopoulos, C. V. (2012). “Removal of mercury from aqueous solutions by malt spent rootlets.” *Chem. Eng. J.*, 213, 135–141.

Anastopoulos, I., and Kyzas, G. Z. (2016). “Are the thermodynamic parameters correctly estimated in liquid-phase adsorption phenomena?” *J. Mol. Liq.*, 218, 174–185.

Arias, F. E. A., Beneduci, A., Chidichimo, F., Furia, E., and Straface, S. (2017). “Study of the adsorption of mercury (II) on lignocellulosic materials under static and dynamic conditions.” *Chemosphere*, 180, 11–23.

Aryal, M., Ziagova, M., and Liakopoulou-Kyriakides, M. (2010). “Study on arsenic biosorption using Fe(III)-treated biomass of Staphylococcus xylosus.” *Chem. Eng. J.*, 162(1), 178–185.

Aydın, H., Bulut, Y., and Yerlikaya, Ç. (2008). “Removal of copper (II) from aqueous solution by adsorption onto low-cost adsorbents.” *J. Environ. Manage.*, 87(1), 37–45.

Babaee, Y., Mulligan, C. N., and Rahaman, M. S. (2017). “Removal of arsenic (III) and arsenic (V) from aqueous solutions through adsorption by Fe/Cu nanoparticles.” *J. Chem. Technol. Biotechnol.*, 93(1), 63–71.

Bang, S., Johnson, M. D., Korfiatis, G. P., and Meng, X. (2005). “Chemical reactions between arsenic and zero-valent iron in water.” *Water Res.*, 39(5), 763–770.

Barakat, M. A. (2011). “New trends in removing heavy metals from industrial wastewater.” *Arab. J. Chem.*, 4(4), 361–377.

Baruthio, F. (1992). “Toxic effects of chromium and its compounds.” *Biol. Trace Elem. Res.* 32(1-3), 145-153.

Benramdane, L., Accominotti, M., Fanton, L., Malicier, D., and Vallon, J. J. (1999). "Arsenic speciation in human organs following fatal arsenic trioxide poisoning - A case report." *Clin. Chem.* 45(2), 301-306.

Bernhoft, R. A. (2012). "Mercury toxicity and treatment: A review of the literature." *J. Environ. Public Health*. 2012.

Bertrand, P. A., and Fleischauer, P. D. (1980). "X-ray photoelectron spectroscopy study of the surface adsorption of lead naphthenate." *J. Vac. Sci. Technol.*, 17(6), 1309–1314.

Bhainsa, K. C., and D'Souza, S. F. (2009). "Thorium biosorption by Aspergillus fumigatus, a filamentous fungal biomass." *J. Hazard. Mater.*, 165(1–3), 670–676.

Bhowmick, S., Chakraborty, S., Mondal, P., Renterghem, W. Van, Berghe, S. Van den, Roman-Ross, G., Chatterjee, D., and Iglesias, M. (2014). "Montmorillonite-supported nanoscale zero-valent iron for removal of arsenic from aqueous solution: Kinetics and mechanism." *Chem. Eng. J.*, 243, 14–23.

Bradl, H. B. (2004). "Adsorption of heavy metal ions on soils and soils constituents." *J. Colloid Interface Sci.*, 277(1), 1–18.

Butler, M. J., and Day, A. W. (1998). "Fungal melanins: a review." *Can. J. Microbiol.*, 44(12), 1115–1136.

Campbell, J. P., and Alvarez, J. A. (1989). "Acute arsenic intoxication." *Am. Fam. Physician*. 40(6), 93-98.

Can, N., Ömür, B. C., and Altındal, A. (2016). "Modeling of heavy metal ion adsorption isotherms onto metallophthalocyanine film." *Sensors Actuators B Chem.*, 237(Supplement C), 953–961.

Carocci, A., Rovito, N., Sinicropi, M. S., and Genchi, G. (2014). "Mercury toxicity and neurodegenerative effects." *Rev. Environ. Contam. Toxicol.*, 1-18, Springer, Cham.

Castro, L., Blázquez, M. L., González, F., Muñoz, J. A., and Ballester, A. (2018). "Heavy metal adsorption using biogenic iron compounds." *Hydrometallurgy*, 179, 44–51.

Chanquía, C. M., Sapag, K., Rodríguez-Castellón, E., Herrero, E. R., and Eimer, G. A.

(2010). “Nature and location of copper nanospecies in mesoporous molecular sieves.” *J. Phys. Chem. C*, 114(3), 1481–1490.

Chaouch, N., Ouahrani, M. R., and Laouini, S. E. (2014). “Adsorption of lead (II) from aqueous solutions onto activated carbon prepared from Algerian dates stones of phoenix dactylifera L (Ghars variety) by H3PO4 activation.” *Orient. J. Chem.*, 30(3), 1317–1322.

Chatterjee, A., and Abraham, J. (2019). “Desorption of heavy metals from metal loaded sorbents and e-wastes: A review.” *Biotechnol. Lett.* 41(3), 319-333

Chaturvedi, A., Bhattacharjee, S., Singh, A. K., and Kumar, V. (2018). “A new approach for indexing groundwater heavy metal pollution.” *Ecol. Indic.*, 87, 323–331.

Chen, P., Zhai, J., Sun, W., Hu, Y., Yin, Z., and Lai, X. (2017). “Adsorption mechanism of lead ions at ilmenite/water interface and its influence on ilmenite flotability.” *J. Ind. Eng. Chem.*, 53(Supplement C), 285–293.

Chen, S., Xue, C., Wang, J., Feng, H., Wang, Y., Ma, Q., and Wang, D. (2009). “Adsorption of Pb (II) and Cd (II) by squid Ommastrephes bartrami melanin.” *Bioinorg. Chem. Appl.*, 2009.

Chen, S., Xue, C., Wang, J., Feng, H., Wang, Y., Ma, Q., and Wang, D. (2010). “Adsorption of Pb (II) and Cd (II) by squid Ommastrephes bartrami melanin.” *Bioinorg. Chem. Appl.*, 2009.

Chen, S., Yue, Q., Gao, B., Li, Q., Xu, X., and Fu, K. (2012). “Adsorption of hexavalent chromium from aqueous solution by modified corn stalk: A fixed-bed column study.” *Bioresour. Technol.*, 113, 114–120.

Cobo, J. M., and Castiñeira, M. (1997). “Oxidative stress, mitochondrial respiration, and glycemic control: Clues from chronic supplementation with Cr3+ or As3+ to male Wistar rats.” *Nutrition*. 13(11-12), 965-970.

Cornell, R. M., and Schwertmann, U. (1996). “The Iron Oxides: Structure, Properties, Reactions, Occurrence and Uses.” VCH Verlagsgesellshaft GMBH Weinheim, Germany.

Dai, M. (1994). “The Effect of Zeta Potential of Activated Carbon on the Adsorption

of Dyes from Aqueous Solution: I. The Adsorption of Cationic Dyes: Methyl Green and Methyl Violet." *J. Colloid Interface Sci.*, 164(1), 223–228.

Demiral, H., and Güngör, C. (2016). "Adsorption of copper(II) from aqueous solutions on activated carbon prepared from grape bagasse." *J. Clean. Prod.* 124, 103-113

Demirezen, D. A., Yıldız, Y. Ş., and Yılmaz, D. D. (2019). "Amoxicillin degradation using green synthesized iron oxide nanoparticles: Kinetics and mechanism analysis." *Environ. Nanotechnology, Monit. Manag.*, 11, 100219.

Descostes, M., Mercier, F., Thromat, N., Beaucaire, C., and Gautier-Soyer, M. (2000). "Use of XPS in the determination of chemical environment and oxidation state of iron and sulfur samples: constitution of a data basis in binding energies for Fe and S reference compounds and applications to the evidence of surface species of an oxidized py." *Appl. Surf. Sci.*, 165(4), 288–302.

Doke, K. M., and Khan, E. M. (2017). "Equilibrium, kinetic and diffusion mechanism of Cr(VI) adsorption onto activated carbon derived from wood apple shell." *Arab. J. Chem.*, 10 (Supplement 1), S252–S260.

Dong, C., Zhang, F., Pang, Z., and Yang, G. (2016). "Efficient and selective adsorption of multi-metal ions using sulfonated cellulose as adsorbent." *Carbohydr. Polym.*, 151, 230–236.

Dunn, R. O., Bantchev, G. B., Doll, K. M., Ascherl, K. L., Lansing, J. C., and Murray, R. E. (2018). "Thioether-Functionalized Corn Oil Biosorbents for the Removal of Mercury and Silver Ions from Aqueous Solutions." *J. Am. Oil Chem. Soc.*, 95(9), 1189–1200.

Dupont, L., and Guillon, E. (2003). "Removal of hexavalent chromium with a lignocellulosic substrate extracted from wheat bran." *Environ. Sci. Technol. 37*(18), 4235-4241.

Duranoğlu, D., Trochimczuk, A. W., and Beker, U. (2012). "Kinetics and thermodynamics of hexavalent chromium adsorption onto activated carbon derived from acrylonitrile-divinylbenzene copolymer." *Chem. Eng. J.*, 187 (Supplement C), 193–202.

Erdemoğlu, M., and Sarıkaya, M. (2006). “Effects of heavy metals and oxalate on the zeta potential of magnetite.” *J. Colloid Interface Sci.*, 300(2), 795–804.

Fierro, V., Torné-Fernández, V., Montané, D., and Celzard, A. (2008). “Adsorption of phenol onto activated carbons having different textural and surface properties.” *Microporous Mesoporous Mater.*, 111(1–3), 276–284.

Franklin, T. C., and Nnodimele, R. A. (1994). “The amperometric titration of copper(II) sulfate with potassium permanganate in surfactant suspensions.” *Electroanalysis*, 6(11-12), 1103–1106.

Freundlich, H. M. . (1906). “Over the adsorption in solution.” *J. Phys. Chem*, 57, 385–470.

Fu, F., and Wang, Q. (2011). “Removal of heavy metal ions from wastewaters: A review.” *J. Environ. Manage.*, 92(3), 407–418.

Gan, M., Li, J., Sun, S., Cao, Y., Zheng, Z., Zhu, J., Liu, X., Wang, J., and Qiu, G. (2018). “The enhanced effect of Acidithiobacillus ferrooxidans on pyrite based Cr(VI) reduction.” *Chem. Eng. J.*

Ganesh Kumar, C., Sahu, N., Narender Reddy, G., Prasad, R. B. N., Nagesh, N., and Kamal, A. (2013). “Production of melanin pigment from Pseudomonas stutzeri isolated from red seaweed Hypnea musciformis.” *Lett. Appl. Microbiol.*, 57(4), 295–302.

Gerçel, Ö., and Gerçel, H. F. (2007). “Adsorption of lead(II) ions from aqueous solutions by activated carbon prepared from biomass plant material of Euphorbia rigida.” *Chem. Eng. J.*, 132(1–3), 289–297.

Ghasemabadi, S. M., Baghdadi, M., Safari, E., and Ghazban, F. (2018). “Investigation of continuous adsorption of Pb(II), As(III), Cd(II), and Cr(VI) using a mixture of magnetic graphite oxide and sand as a medium in a fixed-bed column.” *J. Environ. Chem. Eng.*, 6(4), 4840–4849.

Giagnorio, M., Ruffino, B., Grinic, D., Steffenino, S., Meucci, L., Zanetti, M. C., and Tiraferri, A. (2018). “Achieving low concentrations of chromium in drinking water by nanofiltration: membrane performance and selection.” *Environ. Sci. Pollut. Res.*, 25(25), 25294–25305.

Giles, D. E., Mohapatra, M., Issa, T. B., Anand, S., and Singh, P. (2011). "Iron and aluminium based adsorption strategies for removing arsenic from water." *J. Environ. Manage.* 92(12), 3011-3022.

Goel, J., Kadirvelu, K., Rajagopal, C., and Garg, V. K. (2005). "Removal of lead(II) by adsorption using treated granular activated carbon: Batch and column studies." *J. Hazard. Mater. 125*(1-3), 211-220.

Goswami, A., Raul, P. K., and Purkait, M. K. (2012). "Arsenic adsorption using copper (II) oxide nanoparticles." *Chem. Eng. Res. Des.* 90(9), 1387-1396.

González-Fernández, B., Menéndez-Casares, E., Meléndez-Asensio, M., Fernández-Menéndez, S., Ramos-Muñiz, F., Cruz-Hernández, P., and González-Quirós, A. (2014). "Sources of mercury in groundwater and soils of west Gijón (Asturias, NW Spain)." *Sci. Total Environ.*, 481, 217–231.

Greenberg, C., Davies, S., McGowan, T., Schorer, A., and Drage, C. (1979). "Acute respiratory failure following severe arsenic poisoning." *Chest. 76*(5), 596-598.

Guedes, M., Ferreira, J. M. F., and Ferro, A. C. (2009). "A study on the aqueous dispersion mechanism of CuO powders using Tiron." *J. Colloid Interface Sci.*, 330(1), 119–124.

Guertin, J. (2005). "Toxicity and Health Effects of Chromium (All Oxidation States)." *Chromium Handb.* 215-230.

Gupta, V. K., Rastogi, A., and Nayak, A. (2010). "Adsorption studies on the removal of hexavalent chromium from aqueous solution using a low cost fertilizer industry waste material." *J. Colloid Interface Sci.*, 342(1), 135–141.

Hadi, P., To, M.-H., Hui, C.-W., Lin, C. S. K., and McKay, G. (2015). "Aqueous mercury adsorption by activated carbons." *Water Res.*, 73, 37–55.

Hayati, B., Maleki, A., Najafi, F., Gharibi, F., McKay, G., Gupta, V. K., Harikaranahalli Puttaiah, S., and Marzban, N. (2018). "Heavy metal adsorption using PAMAM/CNT nanocomposite from aqueous solution in batch and continuous fixed bed systems." *Chem. Eng. J.*, 346, 258–270.

Ho, Y. S. (2004). "Citation review of Lagergren kinetic rate equation on adsorption

reactions." *Scientometrics*. 59(1), 171-177.

Ho, Y. S., and McKay, G. (1999). "Pseudo-second order model for sorption processes." *Process Biochem.*, 34(5), 451–465.

Hossain, M. A., Ngo, H. H., Guo, W. S., and Nguyen, T. V. (2012). "Removal of copper from water by adsorption onto banana peel as bioadsorbent." *Int. J. Geomate*, 2(2), 227–234.

Hu, X., Ding, Z., Zimmerman, A. R., Wang, S., and Gao, B. (2015). "Batch and column sorption of arsenic onto iron-impregnated biochar synthesized through hydrolysis." *Water Res.* 68, 206-216.

Hugli, T. (2012). *Techniques in protein chemistry*. Elsevier.

Hung, Y. C., Sava, V. M., Blagodarsky, V. A., Hong, M. Y., and Huang, G. S. (2003). "Protection of tea melanin on hydrazine-induced liver injury." *Life Sci. 72*(9), 1061-1071.

Hutson, N. D., Attwood, B. C., and Scheckel, K. G. (2007). "XAS and XPS characterization of mercury binding on brominated activated carbon." *Environ. Sci. Technol.*, 41(5), 1747–1752.

Hyder, A. H. M. G., Begum, S. A., and Egiebor, N. O. (2015). "Adsorption isotherm and kinetic studies of hexavalent chromium removal from aqueous solution onto bone char." *J. Environ. Chem. Eng.*, 3(2), 1329–1336.

Igberase, E., Ofomaja, A., and Osifo, P. O. (2019). "Enhanced heavy metal ions adsorption by 4-aminobenzoic acid grafted on chitosan/epichlorohydrin composite: Kinetics, isotherms, thermodynamics and desorption studies." *Int. J. Biol. Macromol.*, 123, 664–676.

Issa, N. Ben, Rajaković-Ognjanović, V. N., Jovanović, B. M., and Rajaković, L. V. (2010). "Determination of inorganic arsenic species in natural waters—Benefits of separation and preconcentration on ion exchange and hybrid resins." *Anal. Chim. Acta*, 673(2), 185–193.

Ithurbide, A., Frateur, I., Galtayries, A., and Marcus, P. (2007). "XPS and flow-cell EQCM study of albumin adsorption on passivated chromium surfaces: Influence of

potential and pH." *Electrochim. Acta*, 53(3), 1336–1345.

Janyasuthiwong, S., Phiri, S. M., Kijjanapanich, P., Rene, E. R., Esposito, G., and Lens, P. N. L. (2015). "Copper, lead and zinc removal from metal-contaminated wastewater by adsorption onto agricultural wastes." *Environ. Technol.*, 36(24), 3071–3083.

Jeon, C., and Ha Park, K. (2005). "Adsorption and desorption characteristics of mercury(II) ions using aminated chitosan bead." *Water Res.*, 39(16), 3938–3944.

Karthikeyan, T., Rajgopal, S., and Miranda, L. R. (2005). "Chromium (VI) adsorption from aqueous solution by Hevea Brasilinesis sawdust activated carbon." *J. Hazard. Mater.*, 124(1), 192–199.

Khatamian, M., Khodakarampoor, N., and Saket-Oskoui, M. (2017). "Efficient removal of arsenic using graphene-zeolite based composites." *J. Colloid Interface Sci.*, 498, 433–441.

Kobielska, P. A., Howarth, A. J., Farha, O. K., and Nayak, S. (2018). "Metal–organic frameworks for heavy metal removal from water." *Coord. Chem. Rev*. 358, 92-107.

Lagergren, S. (1898). "About the theory of so-called adsorption of soluble substances."

Langmuir, I. (1918). "The adsorption of gases on plane surfaces of glass, mica and platinum." *J. Am. Chem. Soc.*, 40(9), 1361–1403.

Lenoble, V., Laclautre, C., Deluchat, V., Serpaud, B., and Bollinger, J.-C. (2005). "Arsenic removal by adsorption on iron(III) phosphate." *J. Hazard. Mater.*, 123(1), 262–268.

Lezehari, M., Baudu, M., Bouras, O., and Basly, J.-P. (2012). "Fixed-bed column studies of pentachlorophenol removal by use of alginate-encapsulated pillared clay microbeads." *J. Colloid Interface Sci.*, 379(1), 101–106.

Li, B., Luo, X., Zhu, Y., and Wang, X. (2015). "Immobilization of Cu(II) in KIT-6 supported Co3O4 and catalytic performance for epoxidation of styrene." *Appl. Surf. Sci.*, 359, 609–620.

Li, J., Xing, X., Li, J., Shi, M., Lin, A., Xu, C., Zheng, J., and Li, R. (2018). "Preparation of thiol-functionalized activated carbon from sewage sludge with coal blending for

heavy metal removal from contaminated water." *Environ. Pollut.*, 234, 677–683.

Li, Y., Li, W., Liu, Q., Meng, H., Lu, Y., and Li, C. (2017). "Alkynyl carbon materials as novel and efficient sorbents for the adsorption of mercury (II) from wastewater." *J. Environ. Sci.* 68, 169-176

Liao, L.-F., Lien, C.-F., Shieh, D.-L., Chen, M.-T., and Lin, J.-L. (2002). "FTIR study of adsorption and photoassisted oxygen isotopic exchange of carbon monoxide, carbon dioxide, carbonate, and formate on TiO2." *J. Phys. Chem. B*, 106(43), 11240–11245.

Lien, H. C., Tsai, T. F., Yu Yun Lee, and Hsiao, C. H. (1999). "Merkel cell carcinoma and chronic arsenicism." *J. Am. Acad. Dermatol.* 41(4), 641-643.

Liu, F., Cristofaro, A. De, and Violante, A. (2001). "Effect of pH, phosphate and oxalate on the adsorption/desorption of arsenate on/from goethite." *Soil Sci.*, 166(3), 197–208.

Lin, W. P., Lai, H. L., Liu, Y. L., Chiung, Y. M., Shiau, C. Y., Han, J. M., ... & Liu, Y. T. (2005). "Effect of melanin produced by a recombinant Escherichia coli on antibacterial activity of antibiotics." *J Microbiol Immunol Infect*. 38(5), 320-326.

Long, Z., and Hiroshi, M. (2008). "Adsorption of heavy metal ions from aqueous solution onto chitosan entrapped CM-cellulose hydrogels synthesized by irradiation." *J. Appl. Polym. Sci.*, 110(3), 1388–1395.

Ma, X., Subramanian, K. S., Chakrabarti, C. L., Guo, R., Cheng, J., Lu, Y., and Pickering, W. F. (1992). "Removal of trace mercury (II) from drinking water: sorption by granular activated carbon." *J. Environ. Sci. Heal. Part A*, 27(6), 1389–1404.

Mahdi, Z., Yu, Q. J., and Hanandeh, A. El. (2018). "Investigation of the kinetics and mechanisms of nickel and copper ions adsorption from aqueous solutions by date seed derived biochar." *J. Environ. Chem. Eng.*, 6(1), 1171–1181.

Maji, S., Ghosh, A., Gupta, K., Ghosh, A., Ghorai, U., Santra, A., Sasikumar, P., and Ghosh, U. C. (2018). "Efficiency evaluation of arsenic(III) adsorption of novel graphene oxide@iron-aluminium oxide composite for the contaminated water purification." *Sep. Purif. Technol.*, 197, 388–400.

Martinson, C. A., and Reddy, K. J. (2009). "Adsorption of arsenic(III) and arsenic(V)

by cupric oxide nanoparticles." *J. Colloid Interface Sci.*, 336(2), 406–411.

Matouq, M., Jildeh, N., Qtaishat, M., Hindiyeh, M., and Syouf, M. Q. Al. (2015). "The adsorption kinetics and modeling for heavy metals removal from wastewater by Moringa pods." *J. Environ. Chem. Eng.*, 3(2), 775–784.

McDevitt, N. T., and Baun, W. L. (1964). "Infrared absorption study of metal oxides in the low frequency region (700-240 cm− 1)." *Spectrochim. Acta*, 20(5), 799–808.

Mende, M., Schwarz, D., Steinbach, C., Boldt, R., and Schwarz, S. (2016). "Simultaneous adsorption of heavy metal ions and anions from aqueous solutions on chitosan—Investigated by spectrophotometry and SEM-EDX analysis." *Colloids Surfaces A Physicochem. Eng. Asp.*, 510(Supplement C), 275–282.

Milonjić, S. K. (2007). "A consideration of the correct calculation of thermodynamic parameters of adsorption." *J. Serbian Chem. Soc.*, 72(12).

Momčilović, M., Purenović, M., Bojić, A., Zarubica, A., and Randelovid, M. (2011). "Removal of lead(II) ions from aqueous solutions by adsorption onto pine cone activated carbon." *Desalination*, 276(1–3), 53–59.

Mora Alvarez, N. M., Pastrana, J. M., Lagos, Y., and Lozada, J. J. (2018). "Evaluation of mercury (Hg^{2+}) adsorption capacity using exhausted coffee waste." *Sustain. Chem. Pharm.* 10, 60-70.

Mthombeni, N. H., Mbakop, S., Ray, S. C., Leswifi, T., Ochieng, A., and Onyango, M. S. (2018). "Highly efficient removal of chromium (VI) through adsorption and reduction: A column dynamic study using magnetized natural zeolite-polypyrrole composite." *J. Environ. Chem. Eng.*, 6(4), 4008–4017.

Mueller, P. D., and Benowitz, N. L. (1989). "Toxicologic causes of acute abdominal disorders." *Emerg. Med. Clin. North Am.* 7(3), 667-682.

Nacke, H., Gonçalves, A. C., Campagnolo, M. A., Coelho, G. F., Schwantes, D., Santos, M. G. Dos, Briesch, D. L., and Zimmermann, J. (2016). "Adsorption of Cu (II) and Zn (II) from Water by Jatropha curcas L. as Biosorbent." *Open Chem.*, 14(1), 103–117.

Nath, B. K., Chaliha, C., Bhuyan, B., Kalita, E., Baruah, D. C., and Bhagabati, A. K.

(2018). “GIS mapping-based impact assessment of groundwater contamination by arsenic and other heavy metal contaminants in the Brahmaputra River valley: A water quality assessment study.” *J. Clean. Prod.*, 201, 1001–1011.

Netzer, A., and Hughes, D. E. (1984). “Adsorption of copper, lead and cobalt by activated carbon.” *Water Res*. 18(8), 927-933.

Nikić, J., Watson, M., Tubić, A., Isakovski, M. K., Maletić, S., Mohora, E., and Agbaba, J. (2018). “Arsenic removal from water using a one-pot synthesized low cost mesoporous Fe-Mn modified biosorbent.” *J. Serb. Chem. Soc.* 84(3)

Nordlund, J. J., Boissy, R. E., Hearing, V. J., King, R. A., Oetting, W. S., and Ortonne, J.-P. (1998). *The pigmentary system: physiology and pathophysiology*. Oxford University Press New York.

Ociński, D., Jacukowicz-Sobala, I., Raczyk, J., and Kociołek-Balawejder, E. (2014). “Evaluation of hybrid polymer containing iron oxides as As(III) and As(V) sorbent for drinking water purification.” *React. Funct. Polym. 83*, 24-32.

Ouma, I. L. A., Naidoo, E. B., and Ofomaja, A. E. (2018). “Thermodynamic, kinetic and spectroscopic investigation of arsenite adsorption mechanism on pine cone-magnetite composite.” *J. Environ. Chem. Eng*. 6(4), 5409-5419.

Park, D., Yun, Y. S., Kim, J. Y., and Park, J. M. (2008). “How to study Cr(VI) biosorption: Use of fermentation waste for detoxifying Cr(VI) in aqueous solution.” *Chem. Eng. J.* 136(2-3), 173-179.

Pathirana, C., Ziyath, A. M., Jinadasa, K. B. S. N., Egodawatta, P., Sarina, S., and Goonetilleke, A. (2019). “Quantifying the influence of surface physico-chemical properties of biosorbents on heavy metal adsorption.” *Chemosphere*, 234, 488–495.

Pehlivan, E., Tran, T. H., Ouédraogo, W. K. I., Schmidt, C., Zachmann, D., and Bahadir, M. (2013). “Removal of As(V) from aqueous solutions by iron coated rice husk.” *Fuel Process. Technol.* 106, 511-517.

Pillewan, P., Mukherjee, S., Meher, A. K., Rayalu, S., and Bansiwal, A. (2014). “Removal of arsenic (III) and arsenic (V) using copper exchange zeolite-a.” *Environ. Prog. Sustain. Energy*, 33(4), 1274–1282.

Pongpiachan, S. (2014). “FTIR spectra of organic functional group compositions in PM2. 5 collected at Chiang-Mai City, Thailand during the haze episode in March 2012.” *J. Appl. Sci*, 14(22), 2967–2977.

Powell, K. J., Brown, P. L., Byrne, R. H., Gajda, T., Hefter, G., Sjöberg, S., and Wanner, H. (2007). “Chemical speciation of environmentally significant metals with inorganic ligands Part 2: The Cu2+-OH-, Cl-, CO32-, SO42-, and PO43-systems (IUPAC Technical Report).” *Pure Appl. Chem.*, 79(5), 895–950.

Prasad, B., Ghosh, C., Chakraborty, A., Bandyopadhyay, N., and Ray, R. K. (2011). “Adsorption of arsenite (As3+) on nano-sized Fe2O3 waste powder from the steel industry.” *Desalination*. 274(1-3), 105-112.

Ramos Guivar, J. A., Bustamante D., A., Gonzalez, J. C., Sanches, E. A., Morales, M. A., Raez, J. M., López-Muñoz, M. J., and Arencibia, A. (2018). “Adsorption of arsenite and arsenate on binary and ternary magnetic nanocomposites with high iron oxide content.” *Appl. Surf. Sci.* 454, 87-100.

Ratnaike, R. N. (2003). “Acute and chronic arsenic toxicity.” *Postgrad. Med. J.* 79(933), 391-396.

Raza, M. H., Sadiq, A., Farooq, U., Athar, M., Hussain, T., Mujahid, A., and Salman, M. (2015). “Phragmites karka as a biosorbent for the removal of mercury metal ions from aqueous solution: effect of modification.” *J. Chem.*, 2015.

Saini, A. S., and Melo, J. S. (2013). “Biosorption of uranium by melanin: Kinetic, equilibrium and thermodynamic studies.” *Bioresour. Technol.*, 149, 155–162.

Sajjan, S. S., Anjaneya, O., Kulkarni, G. B., Nayak, A. S., Mashetty, S. B., and Karegoudar, T. B. (2013). “Properties and functions of melanin pigment from Klebsiella sp. GSK.” *Korean J. Microbiol. Biotechnol.*, 41(1), 60–69.

Saleh, T. A. (2016). “Nanocomposite of carbon nanotubes/silica nanoparticles and their use for adsorption of Pb(II): from surface properties to sorption mechanism.” *Desalin. Water Treat.*, 57(23), 10730–10744.

Schneider, R. M., Cavalin, C. F., Barros, M. A. S. D., and Tavares, C. R. G. (2007). “Adsorption of chromium ions in activated carbon.” *Chem. Eng. J.*, 132(1–3), 355–362.

Sehaqui, H., Larraya, U. P. de, Liu, P., Pfenninger, N., Mathew, A. P., Zimmermann, T., and Tingaut, P. (2014). “Enhancing adsorption of heavy metal ions onto biobased nanofibers from waste pulp residues for application in wastewater treatment.” *Cellulose*, 21(4), 2831–2844.

Sen, R., and Sarkar, S. (2019). “Arsenic Contamination of Groundwater in West Bengal: A Report BT - Waste Management and Resource Efficiency.” S. K. Ghosh, ed., Singapore: Springer Singapore, 249–259.

Services, U. S. D. of H. and H. (1999). “Agency for Toxic Substances and Disease Registry: Toxicological profile for Lead (update) PB/99/166704.” *Atlanta US Dep. Heal. Hum. Serv.*

Shahbazi, A., Younesi, H., and Badiei, A. (2013). “Batch and fixed-bed column adsorption of Cu (II), Pb (II) and Cd (II) from aqueous solution onto functionalised SBA-15 mesoporous silica.” *Can. J. Chem. Eng.*, 91(4), 739–750.

Shekinah, P., Kadirvelu, K., Kanmani, P., Senthilkumar, P., and Subburam, V. (2002). “Adsorption of lead(II) from aqueous solution by activated carbon prepared from Eichhornia.” *J. Chem. Technol. Biotechnol.*, 77(4), 458–464.

Shuibo, X., Chun, Z., Xinghuo, Z., Jing, Y., Xiaojian, Z., and Jingsong, W. (2009). “Removal of uranium (VI) from aqueous solution by adsorption of hematite.” *J. Environ. Radioact.* 100(2), 162-166.

Silva, F., Ume, I., and Scamni, W. (1996). “Effects of surface chemistry of activated carbon on the adsorption of aromatics containing electron-withdrawing and electron-donating functional groups.” *spectroscopy*, 1, 1.

Silverstein, R. M., and Bassler, G. C. (1962). “Spectrometric identification of organic compounds.” *J. Chem. Educ.*, 39(11), 546.

Sing, C., and Yu, J. (1998). “Copper adsorption and removal from water by living mycelium of white-rot fungus Phanerochaete chrysosporium.” *Water Res.* 32(9), 2746-2752.

Singh, T. S., and Pant, K. K. (2006). “Experimental and modelling studies on fixed bed adsorption of As(III) ions from aqueous solution.” *Sep. Purif. Technol.*, 48(3), 288–

296.

Solano, F. (2014). “Melanins: Skin Pigments and Much More—Types, Structural Models, Biological Functions, and Formation Routes.” *New J. Sci.*, 2014, 1–28.

Solisio, C., Arni, S. Al, and Converti, A. (2019). “Adsorption of inorganic mercury from aqueous solutions onto dry biomass of Chlorella vulgaris: kinetic and isotherm study.” *Environ. Technol.*, 40(5), 664–672.

Soltani, R., Marjani, A., and Shirazian, S. (2019). “Shell-in-shell monodispersed triamine-functionalized SiO2 hollow microspheres with micro-mesostructured shells for highly efficient removal of heavy metals from aqueous solutions.” *J. Environ. Chem. Eng.*, 7(1), 102832.

Sono, K., Lye, D., Moore, C. A., Boyd, W. C., Gorlin, T. A., and Belitsky, J. M. (2012). “Melanin-based coatings as lead-binding agents.” *Bioinorg. Chem. Appl.*, 2012.

Su, C., and Puls, R. W. (2001). “Arsenate and Arsenite Removal by Zerovalent Iron: Kinetics, Redox Transformation, and Implications for in Situ Groundwater Remediation.” *Environ. Sci. Technol.*, 35(7), 1487–1492.

Sun, S., Zhu, J., Zheng, Z., Li, J., and Gan, M. (2019). “Biosynthesis of β-cyclodextrin modified Schwertmannite and the application in heavy metals adsorption.” *Powder Technol.* 342, 181-192.

Thaira, H., Bhosle, S. S., Balakrishnan, R., and Raval, K. (2016). “Selection of Medium and Optimization of Process Parameters for Melanin Biosynthesis from Pseudomonas stutzeri HMGM-7 BT - Biotechnology and Biochemical Engineering: Select Proceedings of ICACE 2015.” P. B. D., S. N. Gummadi, and P. V Vadlani, eds., Singapore: Springer Singapore, 1–10.

Tiwari, D. P., Singh, D. K., and Saksena, D. N. (1995). “Hg (II) adsorption from aqueous solutions using rice-husk ash.” *J. Environ. Eng.*, 121(6), 479–481.

Tsunashima, A., Br1ndley, G. W., and Bastovanov, M. (1981). “Adsorption of uranium from solutions by montmorillonite; compositions and properties of uranyl montmorillonites.” *Clays Clay Miner.* 29(1), 10-16.

Tumin, N. D., Chuah, A. L., Zawani, Z., and Rashid, S. A. (2008). “Adsorption of

copper from aqueous solution by Elais Guineensis kernel activated carbon." *J. Eng. Sci. Technol.*, 3(2), 180–189.

Udeye, S. T. and N. I. and J. T. and V. (2009). "Adsorption of Lead(II) and Cadmium(II) Ions from Aqueous Solutions by Adsorption on Activated Carbon Prepared from Cashew Nut Shells." *Int. J. Chem. Mol. Nucl. Mater. Metall. Eng.* 52, 110-116.

Vakili, M., Deng, S., Li, T., Wang, W., Wang, W., and Yu, G. (2018). "Novel crosslinked chitosan for enhanced adsorption of hexavalent chromium in acidic solution." *Chem. Eng. J.*, 347, 782–790.

Vieira, R. S., and Beppu, M. M. (2006). "Dynamic and static adsorption and desorption of Hg(II) ions on chitosan membranes and spheres." *Water Res.*, 40(8), 1726–1734.

Vold, I. M. N., Vårum, K. M., Guibal, E., and Smidsrød, O. (2003). "Binding of ions to chitosan—selectivity studies." *Carbohydr. Polym.*, 54(4), 471–477.

Wang, X. Q., Wang, P., Ning, P., Ma, Y. X., Wang, F., Guo, X. L., and Lan, Y. (2015a). "Adsorption of gaseous elemental mercury with activated carbon impregnated with ferric chloride." *RSC Adv.*, 5(32), 24899–24907.

Wang, Y., Liu, D., Lu, J., and Huang, J. (2015b). "Enhanced adsorption of hexavalent chromium from aqueous solutions on facilely synthesized mesoporous iron-zirconium bimetal oxide." *Colloids Surfaces A Physicochem. Eng. Asp.*, 481, 133–142.

Wilbur, S., Abadin, H., Fay, M., Yu, D., Tencza, B., Ingerman, L., Klotzbach, J., and James, S. (2012). "Health effects."

Wu, F.-C., Liu, B.-L., Wu, K.-T., and Tseng, R.-L. (2010). "A new linear form analysis of Redlich–Peterson isotherm equation for the adsorptions of dyes." *Chem. Eng. J.*, 162(1), 21–27.

Xiong, Y., Tong, Q., Shan, W., Xing, Z., Wang, Y., Wen, S., and Lou, Z. (2017). "Arsenic transformation and adsorption by iron hydroxide/manganese dioxide doped straw activated carbon." *Appl. Surf. Sci.*, 416, 618–627.

Yan, G., and Viraraghavan, T. (2000). "Effect of pretreatment on the bioadsorption of heavy metals on Mucor rouxii." *Water SA*, 26(1), 119–123.

Yang, J., Yu, M., and Chen, W. (2015). “Adsorption of hexavalent chromium from aqueous solution by activated carbon prepared from longan seed: Kinetics, equilibrium and thermodynamics.” *J. Ind. Eng. Chem.*, 21, 414–422.

Yildiz, U., Kemik, Ö. F., and Hazer, B. (2010). “The removal of heavy metal ions from aqueous solutions by novel pH-sensitive hydrogels.” *J. Hazard. Mater.*, 183(1), 521–532.

Yu, B., Zhang, Y., Shukla, A, Shukla, S. S., and Dorris, K. L. (2001). “The removal of heavy metals from aqueous solutions by sawdust adsorption--removal of lead and comparison of its adsorption with copper.” *J. Hazard. Mater.*, 84(1), 83–94.

Zhang, Q., Liu, N., Cao, Y., Zhang, W., Wei, Y., Feng, L., and Jiang, L. (2018). “A facile method to prepare dual-functional membrane for efficient oil removal and in situ reversible mercury ions adsorption from wastewater.” *Appl. Surf. Sci.*, 434 (Supplement C), 57–62.

Zhang, Y.-J., Ou, J.-L., Duan, Z.-K., Xing, Z.-J., and Wang, Y. (2015). “Adsorption of Cr (VI) on bamboo bark-based activated carbon in the absence and presence of humic acid.” *Colloids Surfaces A Physicochem. Eng. Asp.*, 481, 108–116.

Zhou, X., and Zhou, X. (2014). “The unit problem in the thermodynamic calculation of adsorption using the Langmuir equation.” *Chem. Eng. Commun.*, 201(11), 1459–1467.

APPENDIX

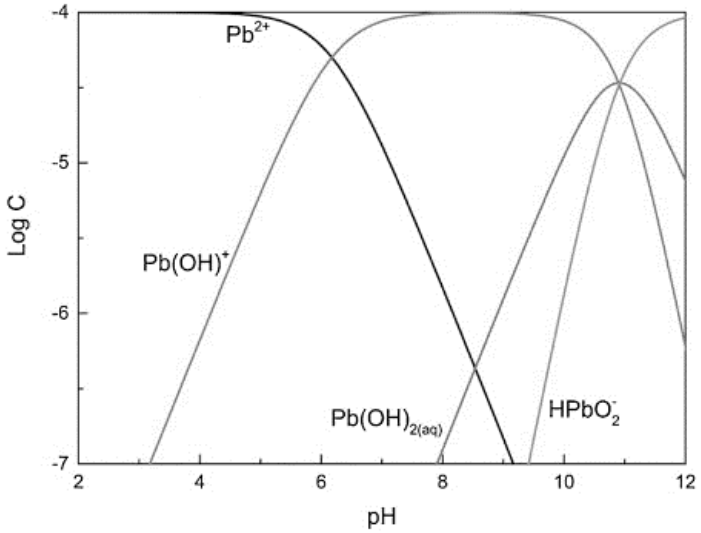

Figure 1. Speciation of lead in aqueous medium (Chen et al. 2017)

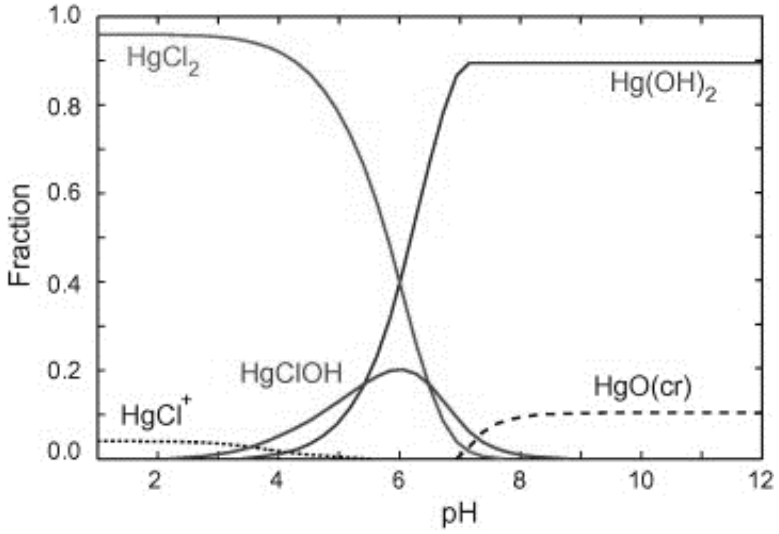

Figure 2. Speciation of mercury in distilled water (C_o = 25 mg/L)(Anagnostopoulos et al. 2012)

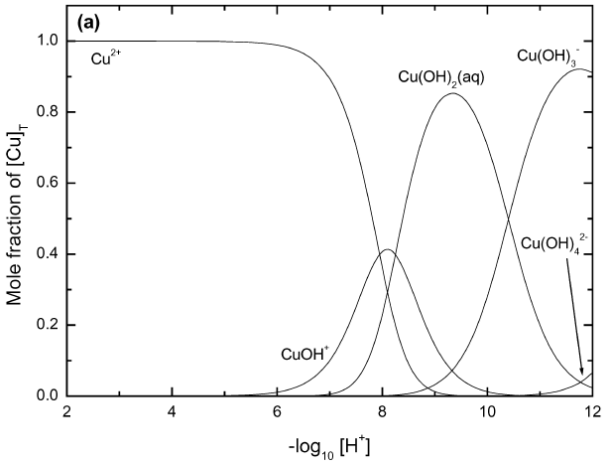

Figure 3. Speciation diagram for the binary Cu^{2+}-hydroxide system at 25 °C at copper concentration of 10^{-5} mol/L (Powell et al. 2007)

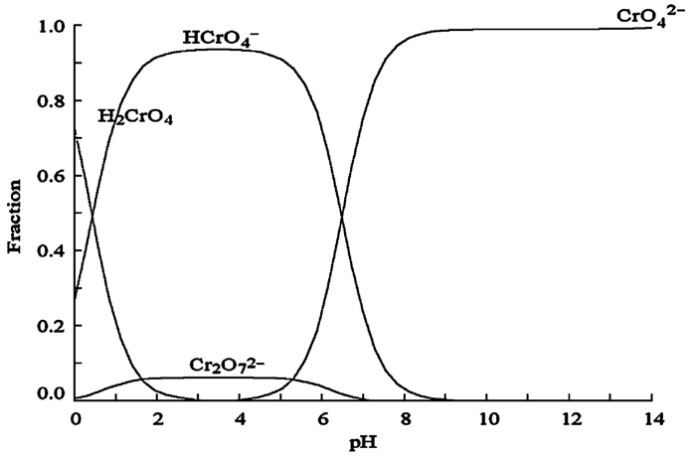

Figure 4. Hexavalent chromium speciation at 5 mmol/L

Table 1. Ionic properties of lead, copper, mercury and chromium

Heavy metal	Atomic radius (A°)	Electronegativity (Pauling's)	Ionisation energy (KJ/mol)
Pb	1.75	1.8	715.6
Cu	1.28	1.9	754.5
Hg	1.5	2	1007.1
Cr	1.28	1.66	652.9
As	1.21	2.18	947

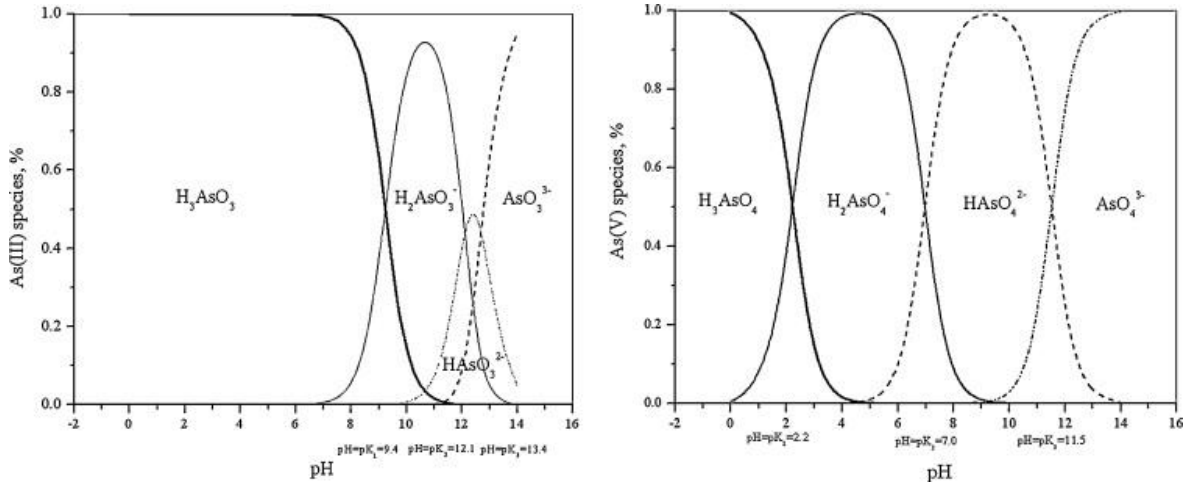

Figure 5: Arsenic III and V speciation at different pH (Issa et al. 2010)

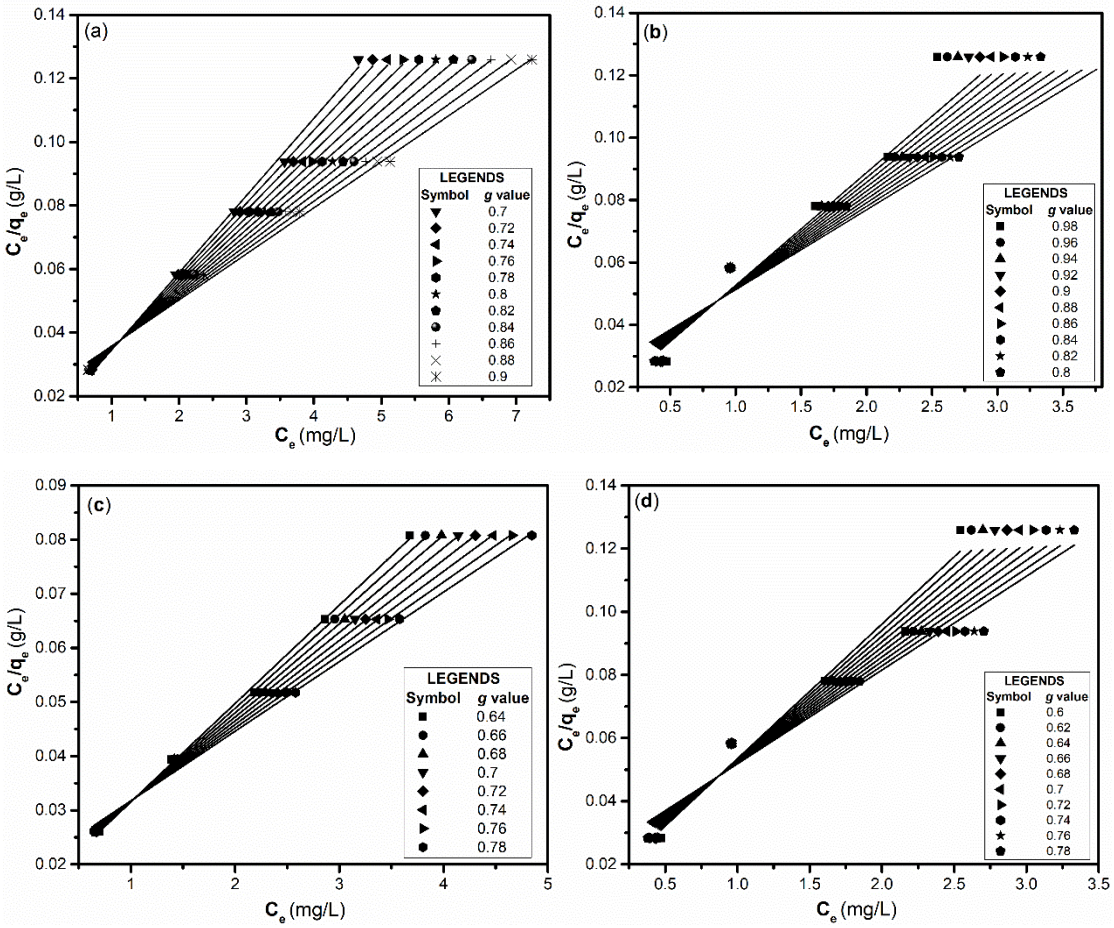

Figure 6. Adsorption of (a) Hg (II) (b) Pb (II) (c) Cr (VI) (d) Cu (II) on to Melanin fitted with linear form of Redlich–Peterson isotherm equation

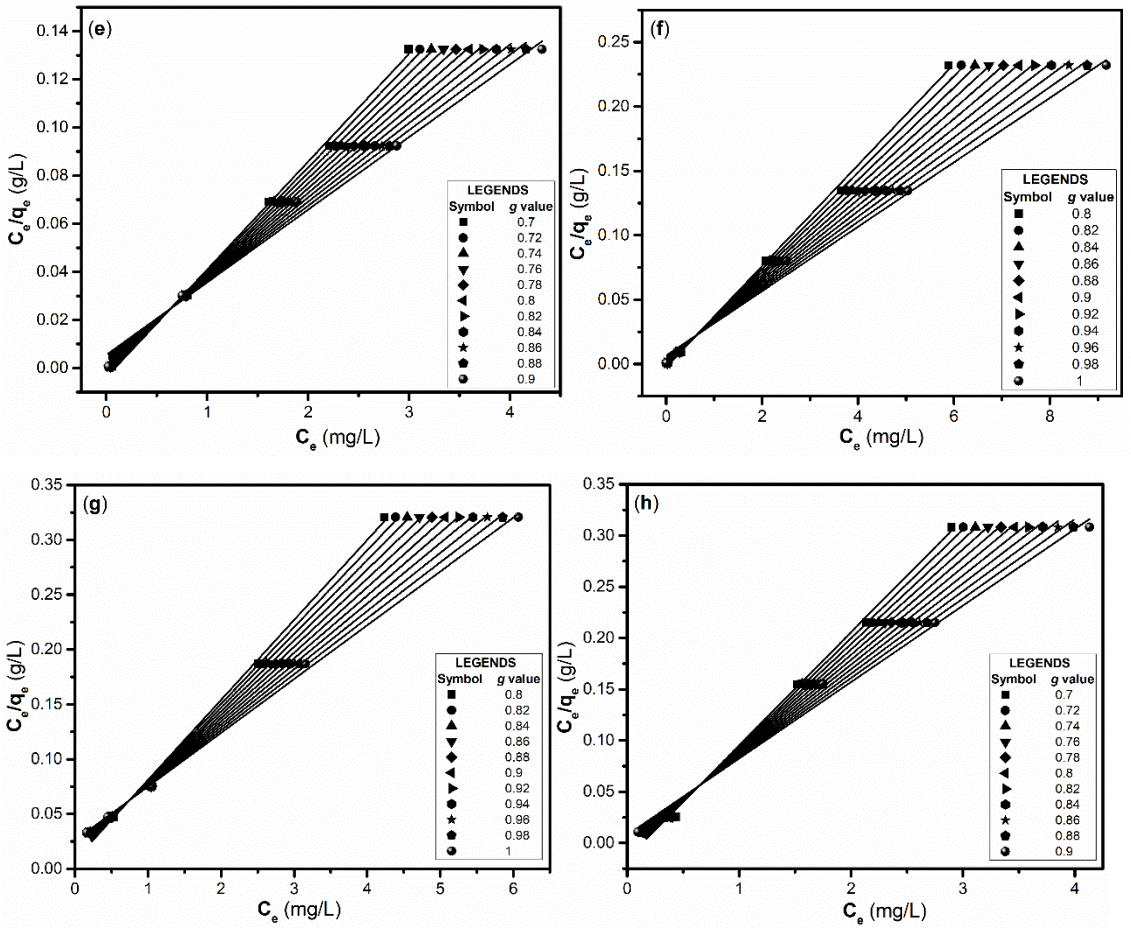

Figure 7. Adsorption of (e) As (V) on Fe-Melanin (f) As (III) on Fe-Melanin (g) As (V) on Cu-Melanin (h) As (III) on Cu-Melanin fitted with linear form of Redlich–Peterson isotherm equation.

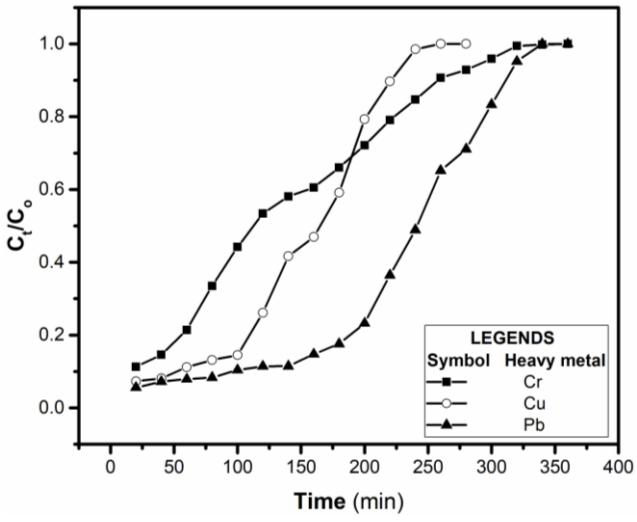

Figure 8. Continuous adsorption of heavy metals using 25 mg activated carbon [C_0= 1 mg/L, v=0.5mL/min]

BIODATA

Vishnu Manirethan

Thekkemangalath Veedu

Thattamala PO, Kollam, Kerala – 691020

Contact Number: +919496328806

E-Mail ID: vishnumvishnu@gmail.com

Educational Profile

- ***Doctor of Philosophy***
  Chemical Engineering | CGPA: 7.33
  NITK Surathkal | Dakshina Kannada, India
  01/2016 – Present

Thesis title: Studies on removal of heavy metals from aqueous solution using melanin coated matrix

- ***Master of Technology***
  Industrial Pollution Control (Chemical Engineering) |CGPA: 7.11
  NITK Surathkal | Dakshina Kannada, India
  08/2013 – 07/2015

Thesis title: Heavy metal removal studies from aqueous solutions using NIPAm/PVP hydrogel.

- ***Bachelor of Technology***
  Biotechnology and Biochemical Engineering |CGPA: 7.05
  University of Kerala | Thiruvananthapuram, Kerala, India
  08/2008 – 08/2012

Thesis title: Antimicrobial activity of selected medicinal plants for the preparation of *Pippalyasavam*.

Professional profile

- ***Senior Research Fellow | NITK Surathkal***

  Project: Melanin coated polymer matrix for heavy metal removal from aqueous solution [DST/TSG/WP/2014/58].
  08/2017 – 12/2017

- ***Junior Research Fellow | NITK Surathkal***
  Promoted to SRF on 6 August 2017

Achievements

- Represented the institute and presented our research work in the *Festival of Innovation and Entrepreneurship (FINE) 2018* organised by the National Innovation Foundation – India and DST at the ***Rashtrapati Bhavan*** on 19th March 2018.
- Secured all India rank 1626 for Graduate Aptitude Test in Engineering (GATE Biotechnology, 2013)
- Second best award at the International conference on recent trends in molecular medicine for the poster titled "Antimicrobial activity of selected medicinal plants" held at Sree Buddha College of Engineering, Alappuzha, Kerala, organized by the Kerala State Council for Science Technology and Environment (KSCSTE), Government of Kerala.

Extracurricular activities

- Department Representative (Ph.D.) and Student 's Council member (2017-18).
- Member, Hostel Council, NITK Student Hostels (2016-17).

Declaration

I hereby declare that all the details furnished above are true to the best of my knowledge and belief.

30 August 2019 **Vishnu Manirethan**